

Chapter 22

Self-healing thermosets

Larysa Kutuzova and Andreas Kandelbauer

School of Applied Chemistry, Reutlingen University, Reutlingen, Germany

Chapter outline

Introduction	953	Improving commercial systems by healing additives	976
Basic strategies in self-healing	954	Influence of the matrix on self-healing performance of the self-healing additive	984
Extrinsic self-healing approach	954	Dual versus single-capsule strategy	985
Intrinsic self-healing approach	956	Complex containers and design of microcapsule walls	986
Toward long-lasting smart materials: combining extrinsic and intrinsic strategies	956	Microvascular strategies	989
Selected analytical techniques to evaluate self-healing efficiency	958	Intrinsic self-healing of thermoset systems: the “chemical design” approach	995
General aspects	958	Covalent reaction mechanisms	995
Electrochemical methods for coating thermosets	959	Noncovalent network formation	995
Mechanical methods for bulk thermosets	965	Intrinsically self-healing polyurethanes	997
Optical spectroscopy	971	Intrinsically self-healing epoxies	1000
Comments on self-healing efficiency	975	Other intrinsically self-healing thermosets	1004
Extrinsic self-healing of thermoset systems: the “additive” approach	976	Summary	1006
		References	1008

Introduction

A fundamental problem in the use of materials in general is the loss of their functionality during practical application. This loss of functionality may be due to continuous wear and tear of the materials during their use or to abrupt damage caused by the sudden impact of harmful events such as impact, shock, or pull. This material failure leads to an undesirable collapse in mechanical strength and can cause further consequential damage. The defective component must be replaced. In case of composite materials additional problems arise due to the absence of appropriate recycling strategies. Extending the service life of materials, improving durability, and maintaining functionality for as long a period as possible, even under harsh environmental conditions, are important objectives in the design of materials both, from an economical and an environmental point of view.

An essential strategy to improve the long-term stability of materials under application conditions is the implementation of self-healing properties in the material. When properly designed, a material can react to an external

damage influence and repair itself to a certain extent. For example, cracks that have formed after mechanical impact can be amended before they can lead to functional component failure. Ideally, the original material characteristics that existed before the damage occurred are restored. A variety of strategies to realize self-healing properties in materials have been described in the literature [1–5].

When aiming at self-healing properties, engineers are faced with particular challenges when thermosetting polymers and polymer composites based on fiber-reinforced thermoset matrix systems are concerned [6]. Thermosetting polymers are characterized by high hardness and chemical resistance. They consist of highly cross-linked polymer chains, which have an already high durability compared to thermoplastic polymer systems. Therefore, they show some advantageous characteristics compared to thermoplastics in terms of application properties. However, the high degree of crosslinking also results in a very limited mobility of the individual network segments. Thermosets are brittle and, unlike thermoplastics, the rigid networks cannot usually be softened nondestructively by increasing the temperature. Hence, while minor mechanical damage

to thermoplastics can often be healed again by local temperature exposure (flow of the thermoplastic matrix during so-called “tempering” with concomitant sealing of the crack), this is typically not possible with thermoset systems.

Thermosets, which are able to maintain their mechanical properties over the long term and counteract rapid wear intelligently, are in great demand in various areas of industry, engineering, and electronics. The development of formulations for intelligent self-healing composite matrix systems and coatings based on thermosets has remained a highly topical research topic over the last 20 years. In recent years, research has focused on a rather comprehensive approach in property design to extending the service life of thermoset materials for very specific applications [3,5,7–38]. This means that, as a rule, several complementary self-healing strategies are pursued simultaneously in order to avoid the loss of functionality at different performance levels at the same time in the sense of multifunctional material optimization.

For example, in the development of thermosetting coatings for metal surfaces of underwater structures, the aim is to use self-healing systems that not only restore mechanical integrity in the event of mechanical damage but also ensure stability against corrosion processes and biofouling (i.e., the decomposing attack of microorganisms). Self-healing additives thus include catalysts for the regeneration of the polymer network as well as corrosion inhibitors, bacterial agents, and antifouling agents [8,39]. In the automotive and aircraft industries on the other hand, development attempts are aimed at anticorrosive, UV-curing and at the same time antiyellowing and mechanically reinforced coating systems (e.g., by incorporation of inorganic hard materials) that are, in addition, based on renewable raw materials (“green” high-performance coating systems). If it were possible to furthermore incorporate also a very high self-healing potential, such systems would have a very large application potential in automotive and aircraft applications [15,27,35].

Thus, an important trend in the development of self-healing materials is therefore the regeneration of the entire property profile required for a specific application. Very high demands are therefore placed on the corresponding self-healing systems and there are a large number of specialized approaches for specific fields of application. Under no circumstances should the overall property profile of the material be adversely affected by the additional modifications required to impart self-healing properties.

In the recent literature one can find many examples where the concept of self-healing is combined with the optimization of other high-performance characteristics. In this sense, modern thermosets are therefore no longer just

about developing polymer networks capable of self-healing, but rather highly developed high-performance materials with pronounced multifunctionality, whose property profile is holistically optimized for special applications. A number of properties that have been realized together with the ability to self-heal in thermoset systems in recent years are summarized in Fig. 22.1.

For example, the combination of the self-healing ability with (a) a pronounced corrosion protection effect [25,26,40–43], with high mechanical reinforcement [44–50], with self-monitoring [51], self-cleaning [7,8,11,39,52–55], self-lubricating [56–59], and/or antibacterial [60–62] properties as well as shape-memory properties has been realized [63–66].

Multifunctionality, high performance and a property profile tailored to a defined field of application extend the wide range of applications of modern thermosetting materials and allow their practical use also from the point of view of process economy and sustainability (Fig. 22.1). Of great interest in this context is the special consideration of the possibility of recycling and reusing thermoset-based materials. Thermoset materials are generally difficult to recycle. Composite materials based on thermosets in particular present a serious challenge. The use of complex mixtures of different types of materials seems to be largely incompatible with intelligent recycling of the products made from them. With the introduction of intrinsic concepts for self-healing (see next section), where no complicated material mixtures are used, it seems that the solution of recycling problems has come closer and more sustainable high-performance thermoset-based materials will be possible in the near future. [21,63,67,69–71].

Basic strategies in self-healing

In principle, self-healing properties can be incorporated into a thermoset material according to two basic strategies: on the one hand, the potential for self-healing can be anchored in the structural framework of the thermoset by selecting suitable monomers and comonomers. In this case one speaks of structural or “intrinsic” self-healing properties. On the other hand, the ability to self-heal can be mediated by suitable additives (i.e., chemical compounds or fillers such as microparticles or hierarchical structures). One then speaks of “extrinsic” self-healing properties (Fig. 22.2).

Extrinsic self-healing approach

The best known and most widely used approach to realize an extrinsic self-healing strategy is the addition of microcapsules. In this process, the self-healing hollow spheres are added to the bulk thermoset material in as even a

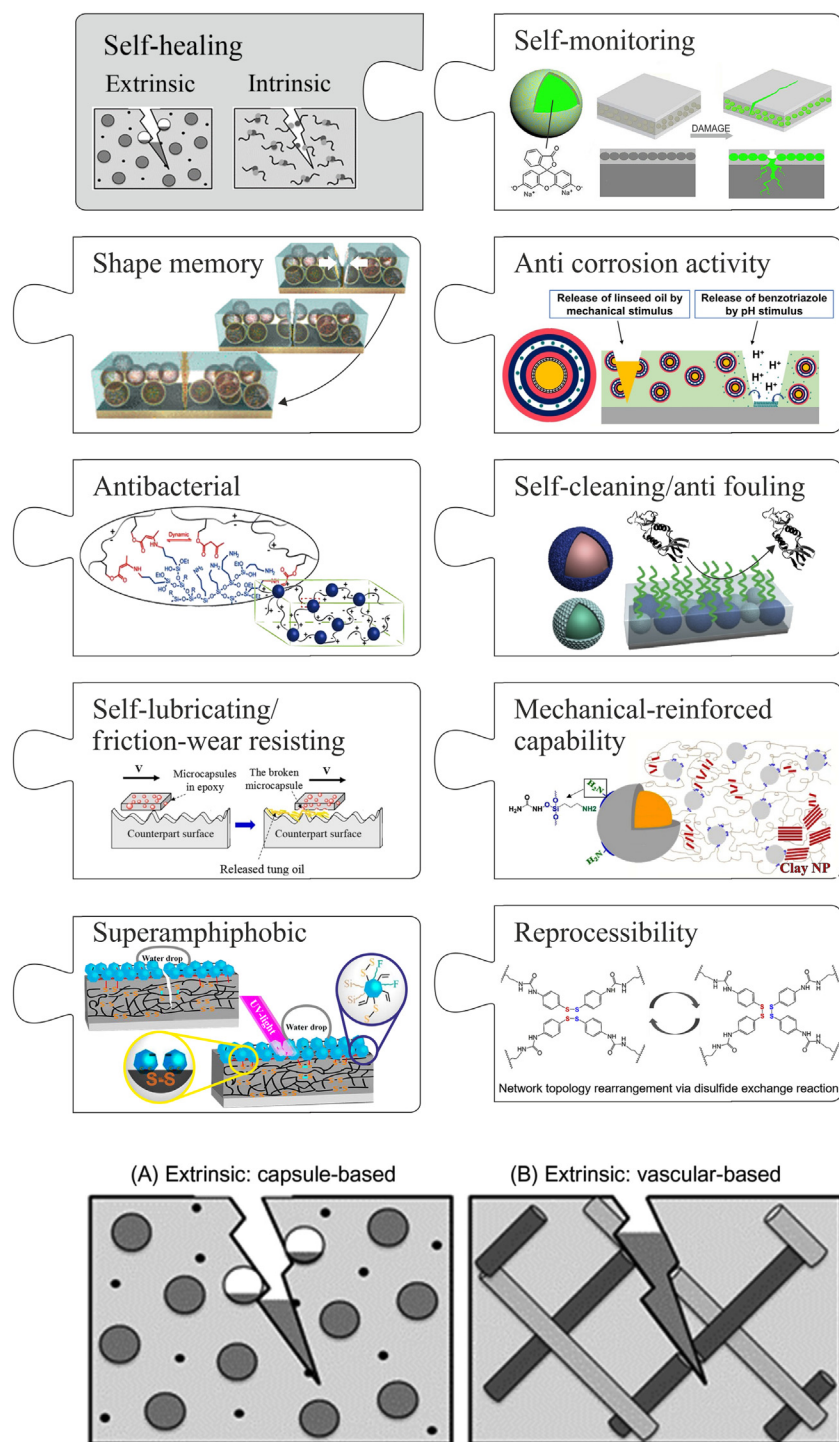


FIGURE 22.2 Self-healing-approaches (A) capsule-based extrinsic, (B) vascular-based extrinsic methodology (C) intrinsic reorganization of the matrix functionalities via an external trigger. Taken from Urdl K, Kandelbauer A, Kern W, Muller U, Thebault M, Zikulnig-Rusch E. *Self-healing of densely cross-linked thermoset polymers—a critical review*. *Prog Org Coat* 2017;104:232–49. Available from: <https://doi.org/10.1016/j.porgcoat.2016.11.010> [6].

distribution as possible. Repairing is usually achieved via a two-component curing/healing system. For this, one part of the hollow spheres is filled with a reactive, not yet polymerized reaction mass, another part of the hollow particles is filled with catalyst, which causes or

accelerates the curing of this reaction mass. Self-healing is based on the fact that a crack damages the hollow spheres simultaneously with the matrix. If mechanical damage occurs, the hollow spheres located in the damage zone are destroyed, their contents are liberated and can

FIGURE 22.1 Multifunctional self-healing thermoset systems in composite coating and matrix composite applications [6]: self-healing ability in combination with corrosion protection [40], mechanical reinforcement [50], self-monitoring [51], self-cleaning and superamphiphobic [39,53], self-lubricating [72], antibacterial [73] properties, shape memory [64], and reprocessability [68]. Modified after Zhang Y, Yuan L, Guan Q, Liang G, Gu A. *Developing self-healable and antibacterial polyacrylate coatings with high mechanical strength through crosslinking by multi-amine hyperbranched polysiloxane viadynamic vinyllogous urethane*. *J Mater Chem A* 2017;5(32):16889–97. Available from: <https://doi.org/10.1039/C7TA04141A>; Huang Y, Deng L, Ju P, Huang L, Qian H, Zhang D, et al. *Tripleaction self-healing protective coatings based on shape memory polymers containing dual-function microspheres*. *ACS Appl Mater Interfaces* 2018;10(27):23369–79. Available from: <https://doi.org/10.1021/acsami.8b06985>; Zhao D, Du Z, Liu S, Wu Y, Guan T, Sun Q, et al. *UV light curable self-healing superamphiphobic coatings by photopromoted disulfide exchange reaction*. *ACS Appl Polym Mater* 2019;1(11):2951–60. Available from: <https://doi.org/10.1021/acsapm.9b00656>; Chen J-H, Hu D-D, Li Y-D, Meng F, Zhu J, Zeng J-B. *Castor oil derived poly(urethane urea) networks with reprocessability and enhanced mechanical properties*. *Polymer* 2018;143:79–86. Available from: <https://doi.org/10.1016/j.polymer.2018.04.013> [68].

fill the crack again with reactive material. At the same time the reactive reaction mass (loading of the microsphere of type 1) comes into contact with the catalyst molecules (loading of the microspheres of type 2), the liberated reaction mass hardens and the crack is repaired.

In the extrinsic strategy, the original mechanical properties of the thermoset can be automatically improved by introducing particularly hard “healing” capsules based on several layers of different thermosets as the shell material of the microsphere or by hardening a single-layer shell with carbide and/or ceramic additives [46,48,49,74]. Such additives additionally act as membranes and contribute to a uniform (controlled) release of reactive monomer from the core and its more effective polymerization [27,56,75].

The success of self-healing when using functional microparticles depends very much on the even distribution over the thermoset volume and the degree of filling of the thermoset with microspheres. The more homogeneous the distribution and the higher the degree of filling, the greater the probability that a crack will actually lead to the destruction of microparticles and thus to the release of the chemical repair system. Once the repair material has been released at one location, a new damage at the same location cannot be repaired a second time. Since the content of the microparticle is used up, the self-healing properties are exhausted.

In order to partially circumvent this disadvantage, a further development of the microparticle strategy is based on repair systems that resemble those found in living organisms. It consists the incorporation of microvascular structures in which the repair systems can be stored and transported across the bulk thermoset. Microvascular network systems, for example, made of porous ceramics [48] or carbon fibers [76–78] as a depot for reactants in the extrinsic approach, also improve the mechanical strength of the thermoset matrix by acting as additional reinforcing materials. Extrinsic strategies based on the capsule and vessel structures often do not require an external stimulus to trigger the self-healing process such as an increase in temperature to initiate thermal polymerization of the repair matrix or an exposure to light for photopolymerization. They are usually independent of the environment and therefore, they are also called autonomous healing techniques.

Intrinsic self-healing approach

In contrast, the intrinsic strategy of self-healing aims at structural modifications of the chemical structure in the thermoset network: by suitable selection of monomers and/or comonomers, additional functional groups are incorporated into the network, which upon damage are capable of creating additional chemical bonds in the polymer matrix if one or more of a variety of different

external stimuli are applied to initiate the self-healing process [1,79,80]. However, the implementation of this strategy is difficult to apply to very rigid thermoset matrix systems with very high crosslinking densities, as it requires a minimum of flexibility of the chains and network segments carrying the self-healing functionality in order for them to rearrange their relative positions. The reactive functionalities must be able to align themselves toward each other after the damage has occurred so that the reaction can take place. This is only possible to a very limited extent with overly rigid networks. Therefore, the network density in such thermosets must not be too high, which, however, leads to a corresponding decrease in glass transition temperature, deterioration of thermal stability, and inferior mechanical strength. The mechanical strength of such intrinsically self-healing thermosets can usually only be improved by the formation of multiple bonds, including covalent, intramolecular coordination (chelation), and hydrogen bonds [47,81,82]. The additional introduction of ceramic nanoparticles or carbon nanotubes with a functionalized surface for click reactions can cause an additional significant hardening in the thermoset matrix, similar to composite rubbers matrix [20,44,45,83,84]. It should be noted that the successful practical application of thermosets modified with intrinsic self-healing properties can be supported by introducing the ability of shape-memory effects, especially in composite coatings [65,85].

Toward long-lasting smart materials: combining extrinsic and intrinsic strategies

The main motivation behind the introduction of self-healing properties in thermosetting polymer systems is to extend their useful lifespan. Fig. 22.3 shows schematically the increase in service life of various thermoset systems based on the temporal progression of mechanical strength over the service life, as has been achieved so far by introducing self-healing properties of matrix or coating materials based on thermosetting polymers.

The dashed curve “a” shows the typical time course of mechanical strength of a standard thermoset without self-healing properties. Although this thermoset may well be filled with reinforcing fillers such as fibers or hard particles to increase the original material strength, the filler does not have any self-amending or self-repairing properties and is chemically inactive in this respect. Once mechanical damage has occurred, the mechanical stability of the material decreases rapidly, the material properties collapse, and the component has reached the end of its service life and must be replaced.

Curve “b” shows the typical course over time of the strength properties for an extrinsically self-healing

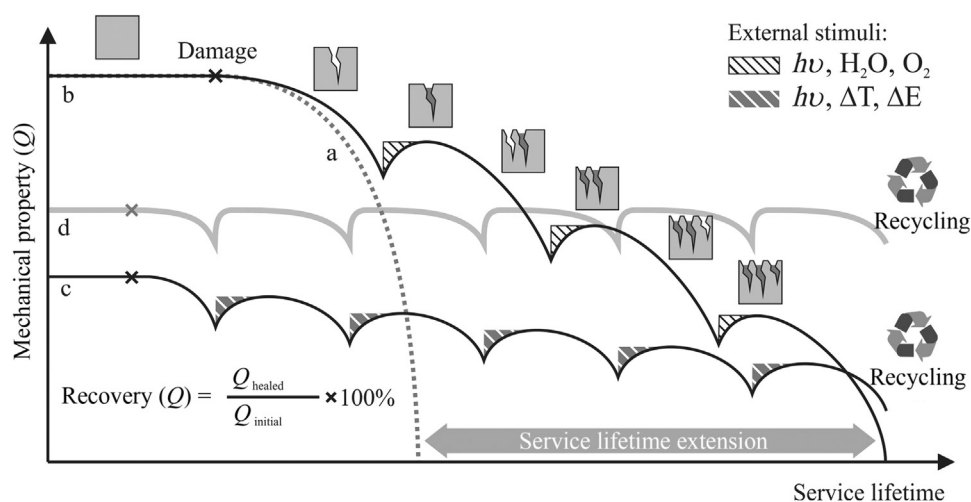


FIGURE 22.3 Idealized healing efficiency (recovery) of material performance and schematic representation of the extension of service life of self-healing thermoset materials: (a) thermoset without self-healing ability, (b) thermoset enhanced by extrinsic healing strategy, (c) thermoset enhanced with intrinsic healing strategy, and (d) ideal self-healing thermoset combining extrinsic and intrinsic healing strategies.

thermoset composite material reinforced with embedded hard microcapsules that are filled with some reactive reaction mass. Due to the polymerizable additives contained in the hollow spheres, this thermoset is able to form a self-repairing, adhesive filling of additional thermoset resin in the resulting cracks. The extrinsic approach can significantly extend the service life of the composite matrix systems compared to unmodified thermosets or thermosets filled with inactive filler (compare curve “a”). However, the initial mechanical strength is typically further reduced with each subsequent damage. The original strength of the base material is typically not fully restored, and any further damage will lead to a permanent deterioration of the material properties. Nevertheless, this approach is still cost effective as it is based on the incorporation of capsules as self-healing additives into a standard matrix formulation which is easily activated in case of mechanical damage by the damage event itself (autonomous system) or can amend the damage by polymerization at room temperature induced by light, moisture, or atmospheric oxygen (stimulus-responsive system). The material is kept in use for a longer period of time and is only much later recycled. Research and development work in this area is primarily focused on the further development of the reactive additives with regard to (1) increasing their reactivity within the composite matrix, (2) improving the interfacial adhesion between the capsule surface and the resin matrix, and (3) optimizing the reaction kinetics by controlled release through tailor-made polymeric membrane shells (defined shell structure of the hollow microparticles). Further research focuses on the optimization of the self-healing properties by varying size, concentration, and filling level with polymerizable reactant of the microcontainers. Mathematical modeling and simulation of the self-healing efficiency are often used for this purpose.

The course of curve “c” seems to be generally typical for a self-healing thermoset according to such an intrinsic strategy. Due to the need for increased flexibility to ensure the spatial proximity of the polymer segments involved in the self-healing effect, only materials with comparatively lower mechanical strengths are generally possible according to this intrinsic healing strategy. On the other hand, this somewhat lower initial strength over the service life experiences only a relatively small drop in performance compared to the extrinsic strategy-based materials. As already mentioned, this type of modification allows multiple healing events of cuts or cracks in the thermoset matrix, with practically no loss of mechanical properties when the material is subjected to the self-healing cycle. Self-healing is usually initiated by (locally applied) external stimuli, sometimes considerable heat, radiation, or electrical voltage. It is worth mentioning that the new generation of materials, whose self-healing capacity is based on intrinsic healing strategies, usually has additional interesting properties such as shape memory and the possibility of material reuse (recycling).

The curve “d” roughly illustrates the obvious development goals for further improvements in the properties of intelligent, self-healing thermosetting polymers. On the one hand, the level of mechanical performance of the starting material is desired to be systematically increased and the self-healing time reduced (preferably without external stimuli), and on the other hand, the number of self-healing cycles should be as large as possible while maintaining the material performance as fully as possible in order to achieve maximum service life while maintaining the application properties [86]. These development goals are most likely to be achieved by a combination of the two self-healing strategies, and an intelligent combination of extrinsic (“additive”) and intrinsic (“functionalization”) strategies within one and the same thermoset

network is expected to have a positive effect on the development of more environmentally friendly, high-performance thermosets. Accordingly, approaches combining several self-healing strategies, both intrinsic and extrinsic, are increasingly being found in recent literature, thus taking advantage of the benefits of both strategies.

Selected analytical techniques to evaluate self-healing efficiency

General aspects

As shown in Fig. 22.3, an important parameter to describe the effective service life of self-healing materials is the number of healing cycles that can be achieved with the material and the extent to which the original material properties can be restored after a damage event. In principle, therefore, all analytical methods which correctly reflect the performance characteristic of interest (mechanical, thermal, dielectric, etc. properties) of the material before the damaging event and after the healing step are suitable for describing the self-healing capabilities of a material. According to the manifold fields of application of thermosetting polymers there are many analytical parameters in the technical literature which have been used to characterize the self-healing properties. Thus, the polymer systems described in the literature are often only partially comparable with each other with regard to their performance. In this variety, however, there are some particularly interesting analytical approaches which are especially suitable for the time-dependent characterization of material properties and thus for the analytical determination of self-healing properties and healing efficiency (HE). In the present section, we will therefore first discuss

some of the most interesting/important analytical methods for describing the self-healing properties of thermosetting materials and give some illustrative examples for the potential of the analytical tool in terms of what is measured and how the measurement is relevant for self-healing. In subsequent subsections, we will discuss some chemically interesting examples for self-healing materials.

To quantify the self-healing efficiency of thermoset materials and their objective evaluation for complex composite materials, a combination of several analytical methods is usually used. Fig. 22.4 shows the most important methods for the analytical detection of changes in the surface quality of thermoset coatings and volume properties of thermosetting bulk materials.

Depending on the intended use of the composite material to be tested, the methods for testing cured thermoset materials must obligatorily include at least one or more tests for mechanical strength. This may include testing for tensile, compression, flexural, and/or impact strength of the specimen. The mechanical loading may be either static or dynamic with additionally including the action of temperature (thermomechanical methods). The mechanical damage to model specimens in the course of a wear test can be supplemented by combined chemical degradation with salt solutions. This is particularly important, for example, when testing coatings intended for underwater structures.

The ability of a surface to recover from mechanical damage can be assessed particularly advantageously visually by spatially resolved measurement techniques like for example optical, electronic, electrochemical, or chemical imaging methods. Undamaged (original samples), damaged, and healed surfaces are used for comparison. The

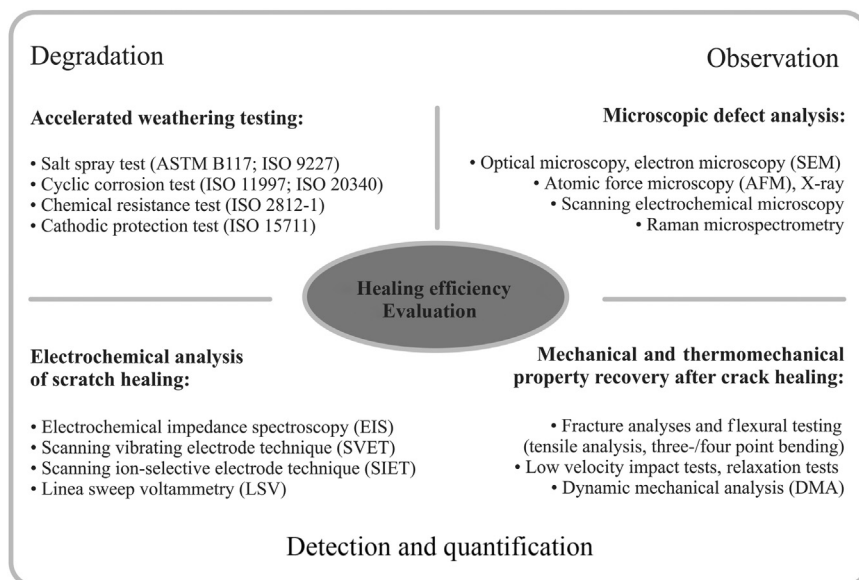


FIGURE 22.4 Degradation tests, methods, and techniques for study of the self-healing surface capability of thermoset coatings as well as the self-healing bulk capability of thermosetting composites.

methods briefly discussed in more detail below are most frequently used to assess self-healing properties.

Electrochemical methods for coating thermosets

Electrochemical examination methods allow a quantitative estimation of the degree of healing of thermoset-based surface coatings on metal substrates. Here the different corrosion tendencies of the metal substrates under the protective coating are quantitatively recorded. The comparison of measuring profiles is usually carried out for samples which have been damaged (scratched) on the metal substrate before and can therefore corrode faster under the influence of salt solutions. An uncoated metal surface that is not coated with a protective polymer and/or a thermoset-coated sample that has no self-healing ability can be examined for comparison. The test samples are usually significantly corroded by salt solutions within a test period of a few days. The relationship between the rate of corrosion and the rate of healing is decisive: if the rate of corrosion does not exceed the rate of healing, the healing ability of the coating under test can be considered sufficient. Various methods can be employed for quantification. As examples for very versatile electrochemical methods, electrochemical impedance spectroscopy (EIS), scanning vibrating electrode testing (SVET), and scanning ion-selective electrode testing (SIET) shall be briefly illustrated using some interesting examples for self-healing surface coatings.

Electrochemical impedance spectroscopy

EIS has been frequently employed to study the corrosion behavior of metal surfaces that were coated with thermosets containing healable microcapsules. The impedance method has been used for a variety of coating systems for metal surfaces, among others, including self-healing epoxy resin-based composite coatings (microcapsules embedded in epoxy resin) [40,49,58,87–93], UV-curable acrylic resins [94] and biobased alkyd coatings [95], shape-memory polyurethane coatings with microcapsule-based healants [65], chemically modified polyurethane networks [96], or a self-healing superamphiphobic coating for efficient corrosion protection of magnesium alloys, which was achieved by combining a compact self-healing epoxy resin coating and a porous superamphiphobic coating [54]. The EIS measurement principle is schematically depicted in Fig. 22.5. Fig. 22.5 also shows a typical measurement result.

Fig. 22.5 provides an overview of the use of EIS in the study of the anticorrosive performance of the scratched metal parts coated with intelligent coating under salt spray conditions. It presents a measurement cell with a three-electrodes setup for EIS measurements in the

damaged area of the coating as well as equivalent circuit models for the partial and complete surface coverage that correspond to the damaged coating state in the early and in the late stage of immersion (Fig. 22.5A) [87]. The EIS device comprises three-electrode systems in which the coating under test acts as the working electrode and either an Ag/AgCl electrode or a saturated calomel electrode acts as the reference electrode. The third electrode is a platinum electrode which functions as a counter electrode. It is aligned in parallel to the coated material to complete the electrochemical cell. As an electrolyte, sodium chloride solutions of various concentrations have proven to be optimal for corrosion tests. When testing coatings to be used under seawater conditions, more highly concentrated salt solutions (about 4%) are employed. If the main focus is on determining kinetic data in the process of early corrosion, significantly lower electrolyte concentrations (less than 1%) are advantageous. The samples are most often tested in the frequency range between 10^5 and 10^{-2} Hz with an AC signal amplitude of 10 mV. The EIS measurement data is primarily presented as a so-called Bode diagram. A Bode diagram shows either the frequency dependence of the absolute impedance values ($|Z| = Z_0$), or their dependence on the phase shift.

The EIS measurement profiles in Bode coordinates for self-healing coating containing hexamethylene diisocyanate microcapsules as well as the kinetics of surface healing with coated microcapsules at 10 wt.% are shown in Fig. 22.5B and C. If there is a defect on the surface of the coating (e.g., an artificial scratch), the impedance at low frequencies drops drastically due to the incipient corrosion process and begins to increase again as soon as the defect begins to heal. Bode diagrams are normally recorded over the period of time in which the impedance returns to its original value, that is, the time in which the coatings completely repair themselves and their protective function is restored. A quantification of the efficiency of the self-repair process is provided by describing the EIS data in the form of a corresponding equivalent circuit diagram. Each component of the coating (corresponding to a cross-sectional segment of the coating) is assigned its own resistance or capacitance value. The change in the number of equivalent circuit components required at the location of the scratch compared to an undamaged reference section provides a direct quantitative measure of the effective self-healing (Fig. 22.5). Using EIS, for example, the influence of microcapsule diameter, microcapsule weight percentage and coating thickness on the anticorrosive properties of the coating can be investigated. The dynamics of anticorrosion behavior after immersion in seawater was monitored also for epoxy-based coating systems in Fig. 22.5D and E. Measuring profiles of steel surfaces coated by a series of modified epoxy resins with polyureaethylene diamine (EDA) microcapsules can achieve the average corrosion resistance efficiency (CRE) of 94% after

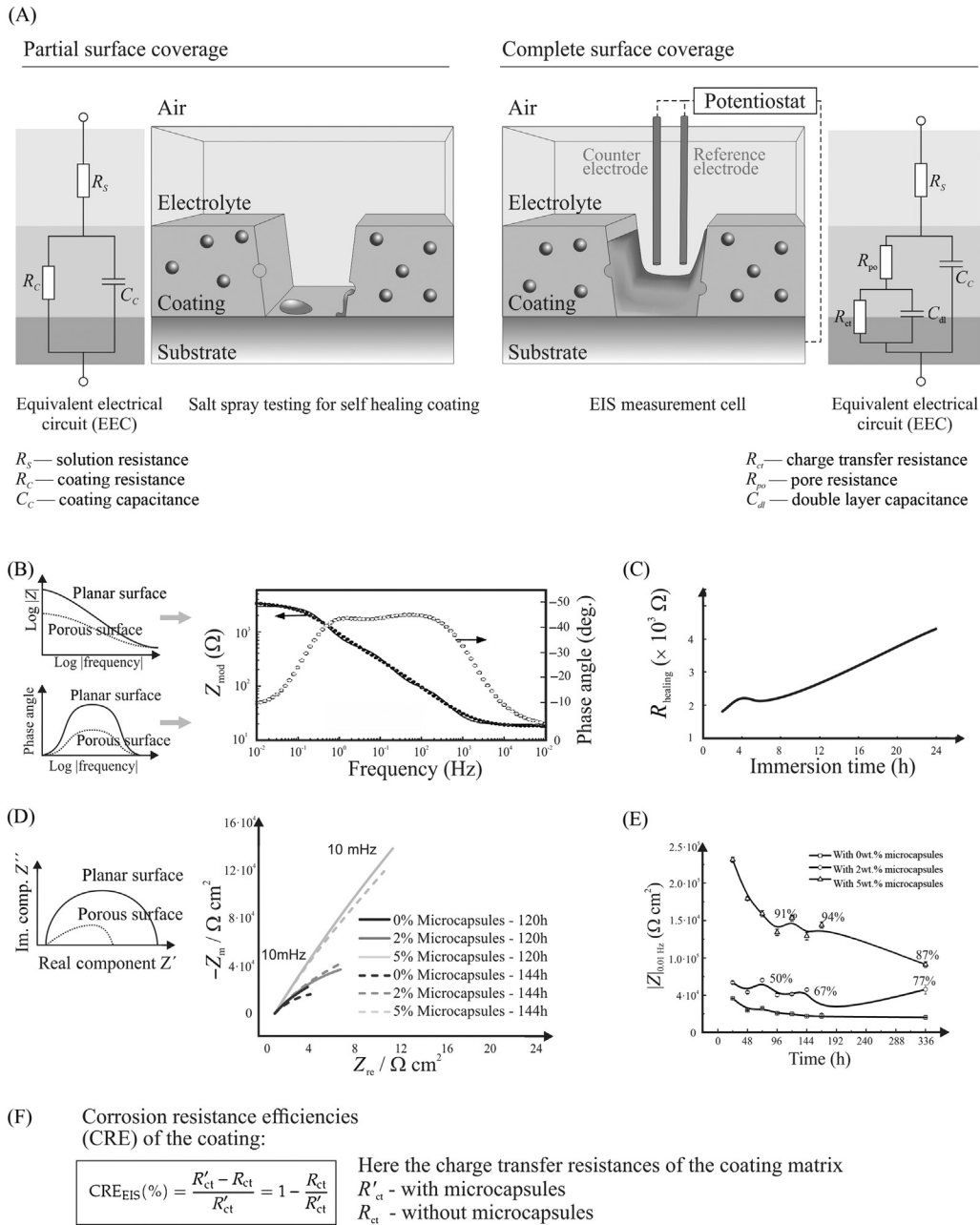


FIGURE 22.5 EIS study of the anticorrosive performance of the scratched samples under accelerated corrosion conditions (salt test): (A) Equivalent circuit models for the partial and complete surface coverage with self-healing coating and the measuring EIS cell with the three-electrodes setup. (B, D) Theoretically expected and practically obtained measurement EIS profiles in terms of Bode and Nyquist diagrams. (C) Kinetics of self-healing process characterized by EIS measurement when the scratched coating was exposed to salt solution. (E) Impedance modulus ($f = 0.01$ Hz) of the scratched epoxy self-healing coating with different contents of microcapsules (0, 2.0 and 5.0 wt.%) after immersion in seawater. (F) Calculation of the corrosion resistance efficiencies (CRE) of the coating: R'_{ct} and R_{ct} are the charge transfer resistances of the coating matrix with and without microcapsules, respectively. *EIS*, Electrochemical impedance spectroscopy. Figures (B) and (C) were modified according to Huang M, Yang J. *Salt spray and EIS studies on HDI microcapsule-based self-healing anticorrosive coatings*. *Prog Org Coat* 2014;77(1):168–75. Available from: <https://doi.org/10.1016/j.porgcoat.2013.09.002> [87]. Figures (D) and (E) were modified according to Ma Y, Zhang Y, Liu J, Sun Y, Ge Y, Yan X, et al. *Preparation and characterization of ethylenediamine-polyurea microcapsule epoxy self-healing coating*. *Materials (Basel)* 2020;13(2):326. Available from: <https://doi.org/10.3390/ma13020326> [89].

immersion for 120 h at a maximum treatment capsule content of 5.0 wt.% [89].

EIS was, for example, used to test the self-healing properties of epoxy coatings containing hollow microspheres that

were filled with linseed oil [59]. Fig. 22.6 shows schematically the pin-shaped friction and wear tester used to test the mechanical stability of the epoxy coating applied to the surface of steel plates. The epoxy coatings with self-healing

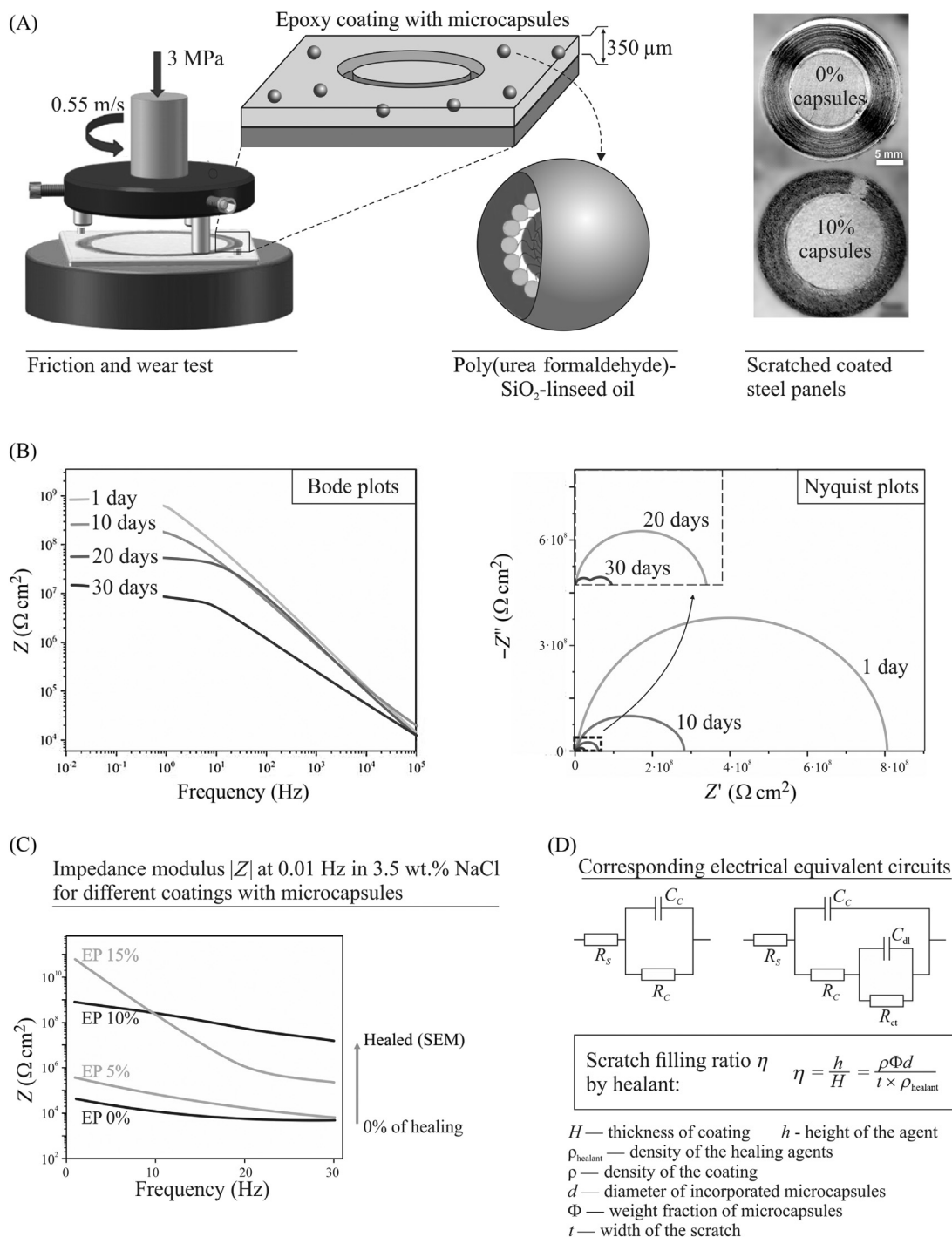


FIGURE 22.6 (A) Friction and wear test of an epoxy coating comprising 10 wt.% poly(urea-formaldehyde)-SiO₂ hybrid hollow microspheres containing linseed oil [59]; (B) EIS plots of scratched coatings with 10 wt.% microcapsules immersed in 3.5 wt.% NaCl solution for 30 days; (C) scratched coated steel plates immersed for 30 days in 3.5 wt.% NaCl solution with a pure epoxy coating having a thickness of 0.35 mm and self-healing epoxy coating comprising 5–15 wt.% microcapsules (D) corresponding equivalent electrical circuits [59] and calculation of scratch filling ratio or scratch filling efficiency (SFE) by extrinsically embedded healant [87,92]. *EIS*, Electrochemical impedance spectroscopy. Modified after Li K, Li H, Cui Y, Li Z, Ji J, Feng Y, et al. Dual-functional coatings with self-lubricating and self-healing properties by combining poly(ureaformaldehyde)/SiO₂ hybrid microcapsules containing linseed oil. *Ind Eng Chem Res* 2019;58(48):220–329. Available from: <https://doi.org/10.1021/acs.iecr.9b04736> [59].

properties contained encapsulated linseed oil. The linseed oil was entrapped in an inorganic-organic hybrid hollow sphere consisting of poly(urea-formaldehyde)/SiO₂ of 20 μm

diameter. Different contents (5–15 wt.%) in functional microspheres were investigated. The wear tests showed that a bifunctional coating with 10 wt.% microcapsules after 4 h of

friction had low wear loss and excellent corrosion inhibition properties for microcracks. The test protocol for self-curing coatings using EIS included the following steps: (1) scratching the coating to a depth down to the surface of the steel plates; (2) exposing the scratched surfaces to air for 72 h so that the released drying oil could completely cross-link and form a protective film on the steel substrate; (3) performing an EIS test at an electrochemical workstation with the three-electrode electrochemical cell depicted in Fig. 22.5.

Fig. 22.6B shows the Bode diagram for a frequency range of 10^5 – 10^{-2} Hz (with an AC signal amplitude of 10 mV) for coating samples with different microcapsule contents after several days of storage in salt solution. Better corrosion protection properties at low frequencies are indicated by higher impedance values. An increase in the concentration of microcapsules in the coatings increased the resistance of scratched coatings at low frequencies (0.01 Hz). This effect was already clearly visible after the first days of immersion: the resistance increased from 4.2×10^4 to $3.2 \times 10^6 \Omega \text{ cm}^2$ at 5 wt.% microcapsules and to $8.0 \times 10^8 \Omega \text{ cm}^2$ at 10 wt.% microcapsules. After 30 days of exposition to the salt solution, the EIS results showed a stronger increase in the impedance modulus for the modified epoxy coating: the impedance modulus for the coating with 10 wt.% microcapsule concentration was about four orders of magnitude higher than the impedance modulus for the unmodified epoxy resin.

At the frequency of 0.01 Hz for all coating samples, the values of the impedance modulus in the Bode diagram and the arc radius in the Nyquist diagram were reduced with increasing immersion time. This can be explained by diffusion of electrolyte into the scratches of coatings. The coatings with microcapsules of 10 wt.% showed a consistently high electrochemical impedance after 1 month of immersion in the electrolyte and thus excellent corrosion protection properties. Depending on the impedance, suitable electrical equivalent circuits were selected after 1, 10, and 20 days of immersion and after 30 days of immersion (Fig. 22.6B–D). Unfortunately, the authors do not quantify the healing efficiency (HE) but confirm the efficiency of self-healing after 1 month of EIS testing using electron microscopy (Fig. 22.6C). For example, the values of the impedance modulus over $10^7 \Omega \text{ cm}^2$ indicate sufficient corrosion protection of films based on cross-linked linseed oil in the crack area of epoxy coatings.

Scanning vibrating electrode testing

SVET is another important electrochemical examination method. SVET can be used to detect the beginning of a corrosion process. The onset of corrosion is characterized by a local change in the electrochemical potential and the corresponding current density. With SVET, an electric field is initiated over the electrochemically active surface

of the studied microzone. The investigated surface fragment is graphically displayed as a contour map of the current densities calculated from the measurement of the electrical potential. The method provides a quantitative estimate of the changes in local current densities of the corrosive current in real time with high resolution. For this purpose, a vibrating reference electrode must be used to measure the electric field. The vibration modulates the signal to be filtered and amplified in the blocking amplifier, thus increasing the signal-to-noise ratio and sensitivity. Fig. 22.7A–B schematically shows the test setup for the SVET measurement technique. The central component of the electrochemical cell is a microelectrode with a scanning probe. The area of the sample to be tested is firmly fixed by a holding device and immersed in the electrolyte. A computer program controls the vibrating microelectrode with the scanning probe. The scanning probe oscillates in x and z direction to the surface and the results are recorded as a current density map of the microzone (Fig. 22.7C). Such xz -SVET maps provide information on the distribution of the current propagating from the surface as well as on the magnitude and location of the direction of the current. If the z -component of the current is positive (anode activity), it is usually shown in red on the map, while the negative z -component (cathode activity) is, for instance, depicted as blue. Areas without electrochemical activity on the surface are green (Fig. 22.7C).

SVET is a relatively simple and yet very informative method for monitoring corrosion processes on metal surfaces (Fig. 22.7C–D). However, there are some limitations of the method to obtain an adequate evaluation of the processes of surface self-healing: SVET does not detect currents flowing below the investigated surface or currents beyond the map, that is, currents occurring in bubbles, pores, and microdefects of the surface (Fig. 22.7E). Therefore, the SVET method is usually always used in combination with other complementary electrochemical techniques, for example to investigate the quality of rubber-based composite coatings. EIS is most often used in combination with SVET to supplement a traditional SVET map with a detailed description of the defective area, as corrosion phenomena can change their spatial position and move below the surface coating. Moreover, the combination of SVET and SIET can be useful when the current density map needs to be supplemented with information about pH values or the concentration of specific other ions.

Scanning ion-selective electrode technique

In general, SIET uses ion-selective miniature electrodes to identify ions involved in the corrosion process. The acidity of the solution in the electrolyte is most frequently monitored, since cathodic reactions can increase the pH value and the hydrolysis of the metal cations formed in

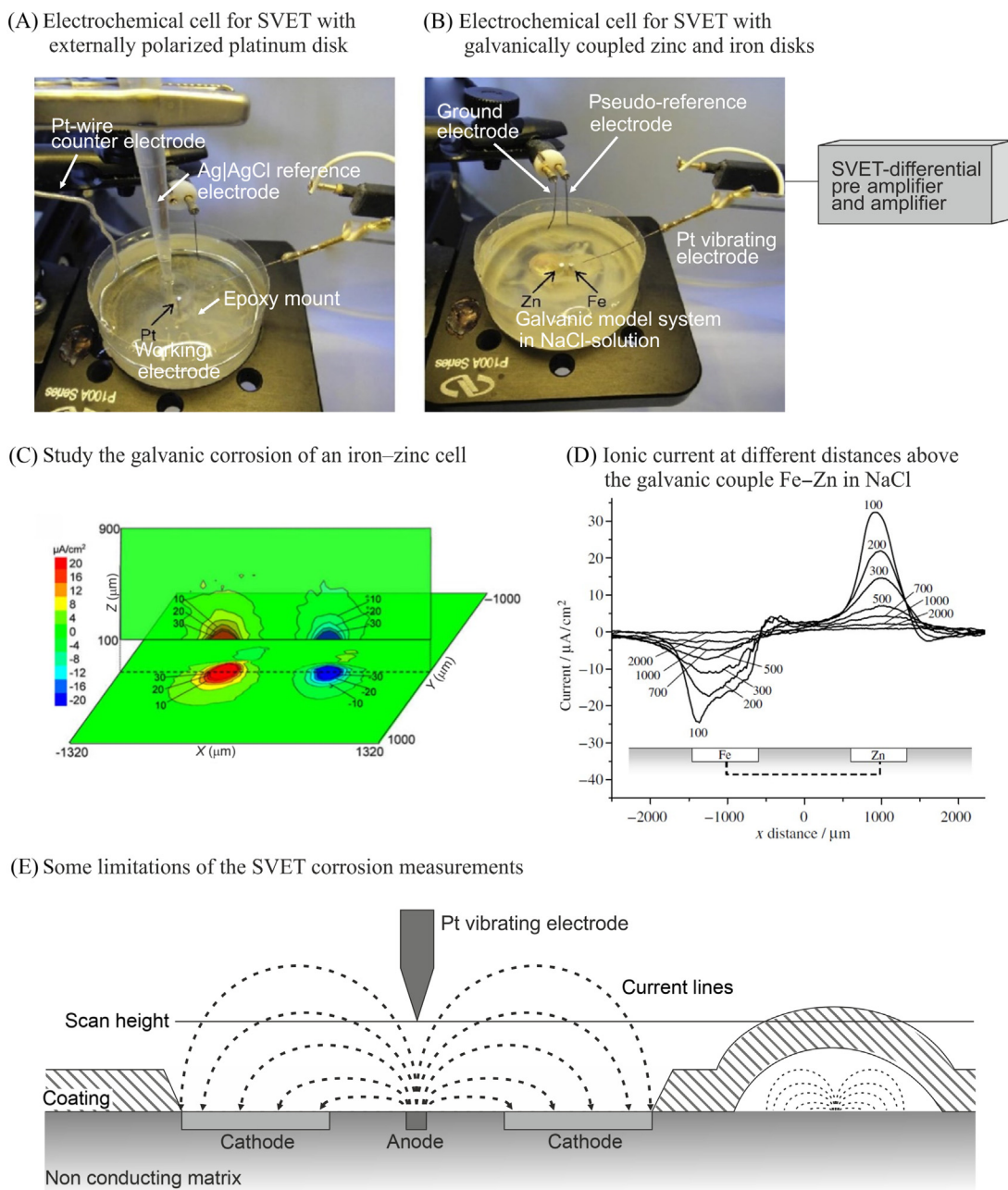
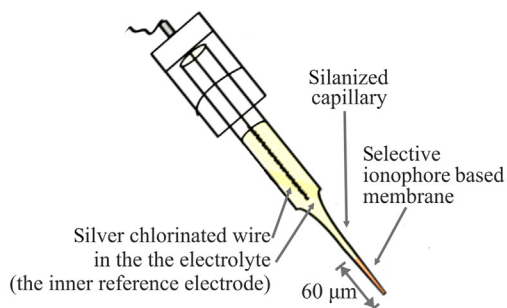


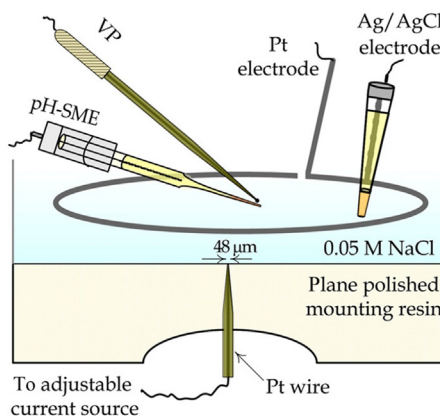
FIGURE 22.7 (A) Electrochemical cells for SVET measurements with Pt-disk (a working electrode is the sample to test); (B) Example of the SVET-cell for a galvanic couple in 0.005 M NaCl: 1 mm diameter Zn and Fe disks, embedded in epoxy resin and electrically connected. [97a]; (C) SVET maps of the ionic currents of a galvanic couple (Fe–Zn) in 0.1 M NaCl solution measured in the xz and xy planes. Typical distribution of anodic, cathodic and inactive SVET regions on the sample surface. The positive z values (red) correspond to zinc oxidation and the negative current (blue) corresponds to the oxygen reduction process at the iron electrode with the production of hydroxide [97b]; (D) Scanner height effect on the detection of the ionic currents above the Fe–Zn galvanic couple immersed in electrolyte solution [97c]; (E) An example of a corrosion cell of the galvanic type in which electrons flow with ions of the electrolyte solution from the anodes to the cathodes (traditional positive charge direction) and limitations of the use of SVET in coatings [97d].

the anode reaction promotes local acidification of the solution [97d]. The concentration of electrolyte ions and the control of some corrosion inhibitors leached from the coating can also be monitored by SIET. The working principle and experimental set-up of the SIET

measurement cell is depicted schematically in Fig. 22.8. Microelectrodes employed in SIET can have a double tip consisting of two capillaries, so that the same housing contains both membrane-ion-selective microelectrodes and a reference electrode. The results of measurements in

A glass-capillary H⁺-selective microelectrode pH-SME

SVET and micro-potentiometry (SIET)



Corrosion cell and reactions

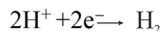
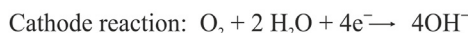
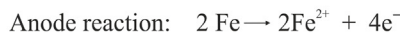
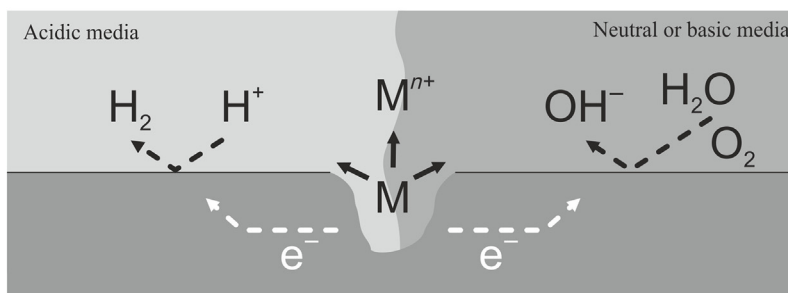


FIGURE 22.8 A liquid membrane ion-selective microelectrode pH-SME and a typical cell for quasi-simultaneous SVET-SIET measurements: the micro-potentiometric measurements are conducted under zero current conditions using a pH-SME and an external reference silver-chloride electrode. A computerized stepper-motor system can be used to move the ISMEs over the sample [97e]. Typical reactions during corrosion of the metal surfaces that influence pH [97d].

SIET are activities or concentrations of ions in the form of a map, lines, or single point measurements over time.

The visualization of corrosion by monitoring the location, density, and shape change of anode and cathode areas over time has been used by many authors to assess the kinetics of self-healing coatings on a corroding metal sample. In order to obtain complete information on the quality of self-healing ability of coatings and to adequately assess their potential for applications, SVET measurements are usually supplemented by chemical information provided by SIET [97]. Thus, the combination of these methods with additional acidity control has been successfully applied to the corrosion activity on coated carbon steel surfaces containing artificial defects [98]. Fig. 22.9A shows microscopic images of isophorone diisocyanate (IPDI) microcapsules incorporated in the epoxy protection coating used for carbon steel. The diameter of the microcapsules is about 20 μm

and enables its use for thin coatings (less than 100 μm). The self-healing ability of epoxy coatings modified with 2 and 3 wt.% of microcapsules investigated by combining electrochemical techniques SVET and SIET is shown in Fig. 22.9B and C. Optical and electrochemical images were acquired during the first 12–13 h of immersion in 0.05 M NaCl of coated carbon steel samples. The kinetics of distribution of anodic and cathodic areas on corroding samples coated with pure epoxy thermoset clearly shows the progress of corrosion over time (SVET maps), which is also confirmed by SIET data on stable alkalinity in the corroded area (Fig. 22.9B). At the same time, in just 2 h the capsules are able to heal damaged areas in the coating to minimize corrosion by forming a protective barrier layer due to the moisture-cured isocyanate polymer (Fig. 22.9C). In the latter case, the acidity of the solution remains stable neutral according to SIET.

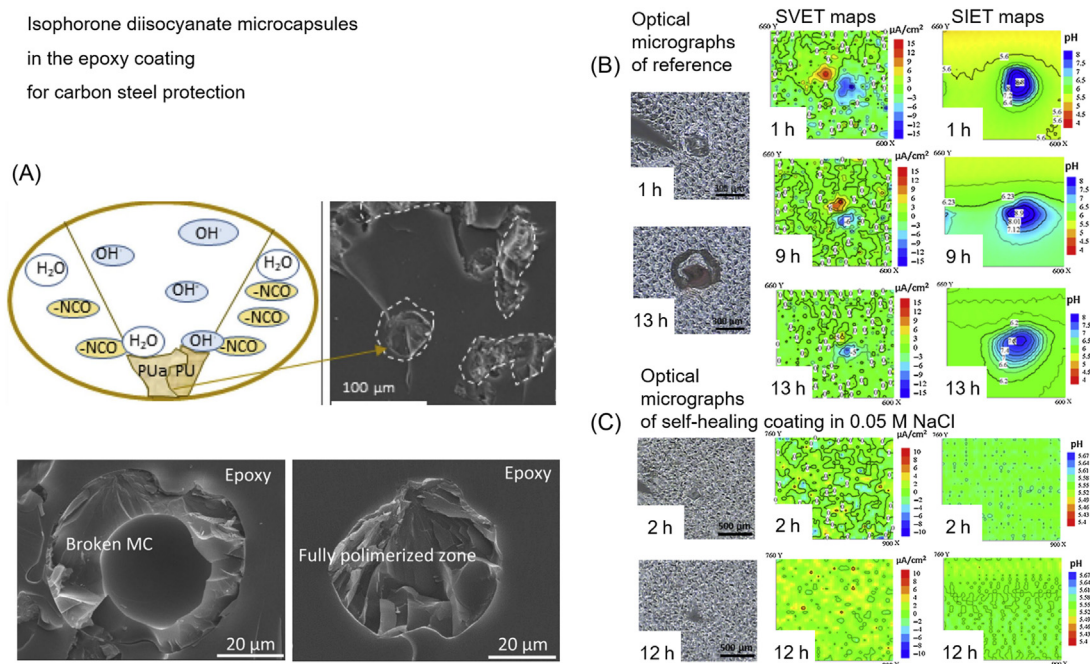


FIGURE 22.9 SVET-SIET analysis of corrosion activity on coated carbon steel surfaces: (A) SEM images of isophorone diisocyanate microcapsules in the epoxy coating, (B) Optical images, SVET and SIET maps acquired during the first 13 h of immersion in 0.05 M NaCl of carbon steel samples coated with epoxy (reference) and (C) IPDI-capsule-modified epoxy coatings [98]. SVET, Scanning vibrating electrode testing; SIET, Scanning ion-selective electrode testing; IPDI, isophorone diisocyanate. Modified after Attaei M, Calado LM, Taryba MG, Morozov Y, Shakoor RA, Kahraman R, et al. Autonomous self-healing in epoxy coatings provided by high efficiency isophorone diisocyanate (IPDI) microcapsules for protection of carbon steel. *Prog Org Coat* 2020;139:105445. Available from: <https://doi.org/10.1016/j.porgcoat.2019.105445> [98].

Mechanical methods for bulk thermosets

Fracture analysis

Fracture toughness testing is often used to measure the tensile strength of tough composites with relatively low viscosity. The simple testing procedure and straightforward interpretation of the measurement signal for layered, laminated, or vascular thermoset structures explain the popularity of this method. The essence of the method is to measure the amount of stress required to propagate an existing defect. A defect is created in the material as a sharp, artificial notch from which a fatigue crack can grow if the material is locally subjected to external mechanical strain at a certain speed up to the maximum possible stress. The fracture toughness limit is characterized by the stress intensity factor (K). A subscript index with Roman numbers indicates the loading mode. The fracture toughness (K_{IC}) is the highest value of stress intensity that a material can withstand under plane deformation conditions without breaking. The mechanical fracture tests of adhesives which are intended for use in aerospace, automotive, and construction applications often estimate the critical tensile strain energy release rate or, in other words, the toughness in terms of tension, (G_{IC}) of the adhesive joints.

Fig. 22.10 shows three types of programmable load that are targeted at crack opening under tensile stress

(mode I) and are targeted at crack sliding as well as crack tearing under friction (modes II and III). The measurement profiles of material failure in these three modes are recorded in load-displacement coordinates. The most important information to assess the quality of the material from a mechanical point of view is the information regarding critical tensile load at crack release moment, P_{max} . These values can be used directly in the calculation of fracture HE if measurements are performed under tensile stress using Tapered Double-Cantilever Beam (TDCB) specimen geometry (Fig. 22.10). The use of other tensile fracture geometries, such as Compact Tension (CT), Single Edge Notch Bend, and Single Edge Notch Tension, requires consideration of the change in length of the cracked front. Thus, the fracture HE is calculated by the ratio of strain energy release rates for mode-I loading (G) as well as by the ratio of stress intensity factors (K). It should be noted that measurements with TDCB as well as with Compact TDCB specimen geometries are the most preferable in assessing the self-healing efficiency of thermosetting composites [104,105]. The use of the TDCB geometry in fracture toughness measurements for the quantification of self-healing has been described in [106]. Different types of measuring profiles for this geometry, as well as practical examples of measuring virgin and healed resin-based materials, are shown in Fig. 22.10B and C. The first graph in Fig. 22.10C “c”

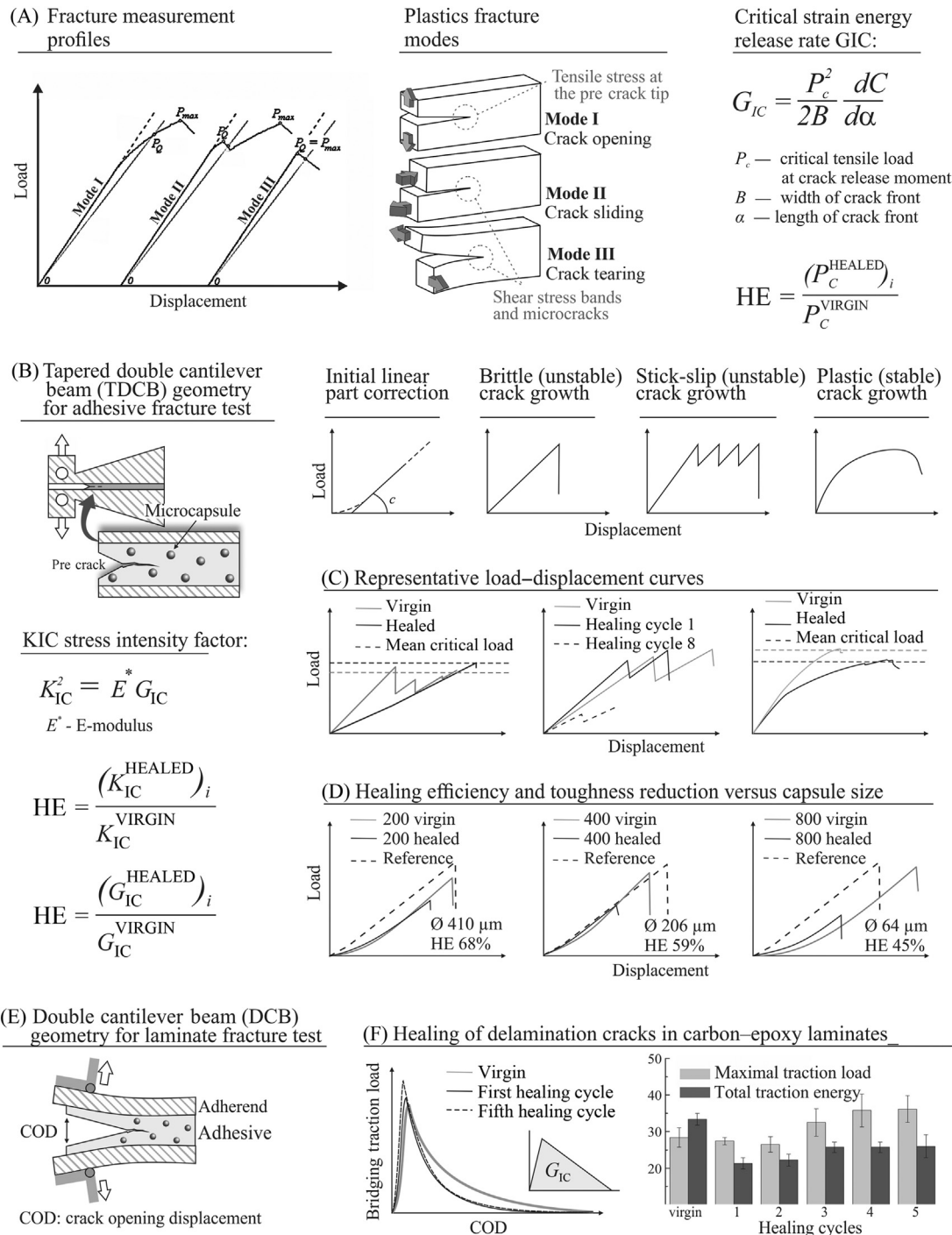


FIGURE 22.10 Self-healing efficiency by fracture testing: (A) types of loading for a crack opening, crack sliding and crack tearing and their measurement profiles in load-displacement coordinates; (B) Tapered Double-Cantilever Beam (TDCB) and typical load-displacement curves measured with TDCB; (C) representative typical load-displacement for self-healing TDCB-fracture tests [99–101]. (D) effect of the capsule size on the healing efficiency of the epoxy thermosetting matrix [102]; (E) Double-Cantilever Beam (DCB) for laminate fracture tests; (F) fracture measurement profiles and effect of number of healing operations on the maximum bridging traction load and total traction energy of the stitched laminate [103].

reflects testing the self-healing PU coatings embedded with the DCPD multilayer microcapsules [99]. During the ring-opening metathesis polymerization of the DCPD core which came in contact with the Grubbs' catalyst

preembedded in the coating, a tightly cross-linked product is formed which effectively heals cracks on the coating and has a positive impact on mechanical properties. The virgin and healed average critical loads were ca. 80 and

94 N, respectively, and their HE was estimated as 118%. The more realistic values in this case could be achieved by considering a significant change in stiffness in the healed area. The second profile reflects the multiple HE of an epoxy matrix using imidazole polymerization. The stiffness of the healed sample was higher than that of the virgin sample because of the restoration of integrity of the precrack by healant injected into the crack plane. The authors note that the change in stiffness between virgin and healed specimens has no effect on the measured fracture toughness [100]. The third system shown in Fig. 22.10C refers to an extrinsically self-healing UV-curable resin embedded with solvent-containing microcapsules and was produced using stereolithographic 3D printing [101]. Commercial photocurable resin modified with anisole and 5% PMMA-containing urea-formaldehyde microcapsules demonstrated 87% recovery of the initial critical toughness. The effect of the capsule size on HE and toughness of epoxy composites was studied in [102]. The size of urea-formaldehyde capsules with epoxy core (DGEBA, Epikote 828) was controlled with agitation rate and varied from 400 to 60 microns, while the stirring rate increased from 200 to 800 rpm (Fig. 22.10D). The fracture self-healing efficiency of the thermoset composite containing the largest capsule size was the highest, reaching 68%. This effect can be explained by the correspondingly higher amount of healant contained in the large capsule, providing for the most efficient healing. Small capsules, as well as the catalyst Aluminum(III) triflate ($\text{Al}(\text{OTf})_3$), are not uniformly distributed within the epoxy matrix and may not get in contact with each other in sufficient quantities. It should be noted that the tendency for HE to increase with the size of the capsules is the opposite in the case of toughness values, that is, for a composite with the largest capsules, toughness decreases by about 80% to 20% of the original value, while the smaller capsules only reduce it by 5%. Healing of delamination cracks in laminates was measured during the tensile fracture of carbon-epoxy material using DCB (Fig. 22.10E and F) [103]. Even after five healing cycles, the maximum traction load is statistically the same as the virgin sample, whereas the total traction energy generated by the bridging stitches/ligaments is slightly reduced, especially during the first two cycles. The traction energy was determined by the area integral of the traction load-crack opening displacement curve and consists of two components, namely the energy absorbed during elastic deformation and the energy absorbed during plastic deformation of the stitches/ligaments. As can be seen from the measurement profile in Fig. 22.10F, a 20%–35% reduction in the total traction energy upon healing was due to a loss in the plastic deformation energy of the stitches. The lower toughness of the repaired stitches and bridging ligaments was probably caused by the higher porosity of the healed

material. However, the mode-I interlaminar fracture toughness can be sufficiently recovered by cross-linked laminates after each healing.

Tensile and bending testing

The evaluation of the failure resistance of softer thermoset materials, that is, of materials with higher toughness, is usually carried out via tensile and compression tests using three- and four-point bending tests. The relevant information on the measuring principle in tensile mode is summarized in Fig. 22.11. Fig. 22.11A shows the mode of mechanical load to which the specimen is subjected and stress-strain profiles obtained by the measurement. The relevant characteristics of material stability under load in the elastic range as well as in the fracture toughness range are indicated as well.

The test specimens are subjected to mechanical load at a constant rate until finally, material failure occurs. During the measurement, the elongation at a certain applied stress is recorded. The resulting stress-strain diagrams show a characteristic profile and allow to determine quantitatively the modulus of elasticity of the material [E_t (MPa)], the maximum value of the applied stress until fracture or break [the tensile strength at break, σ_B (MPa)], the elongation at break, ε_B (%) and the fracture toughness (A). All these mechanical properties of the material are frequently used to characterize the self-healing capacity of intelligent thermoset materials. Fig. 22.11B–D illustrate the application of multiple measuring cycles for a number of subsequent damage/healing events. By comparing the stress-strain diagrams of materials healed under different healing conditions (e.g., applied healing times), the reaction conditions required for good self-healing performance can be readily optimized (Fig. 22.11C, right). Numerical values for the self-healing efficiency can be calculated from the above mechanical parameters using the formulas given in Fig. 22.11 by comparing the values of the undamaged pristine materials with the corresponding values of the materials after damage and self-repair have occurred.

Fig. 22.11 shows the effect of the number of load cycles on the HE in the photo-stimulated self-healing of polyurethane [100] (Fig. 22.11B), in the healing time of polyacrylate coatings [47] (Fig. 22.11C), and in the healing temperature [101] required for disulphide linkages to exhibit healing effects within poly(urea-urethane) networks (Fig. 22.11D).

Dynamic mechanical analysis

The dynamic mechanical analysis (DMA) method is used to track mechanical changes in cross-linked polymers as a function of temperature, as well as to quantify the degree of cross-linking in thermosets and determine the effect of

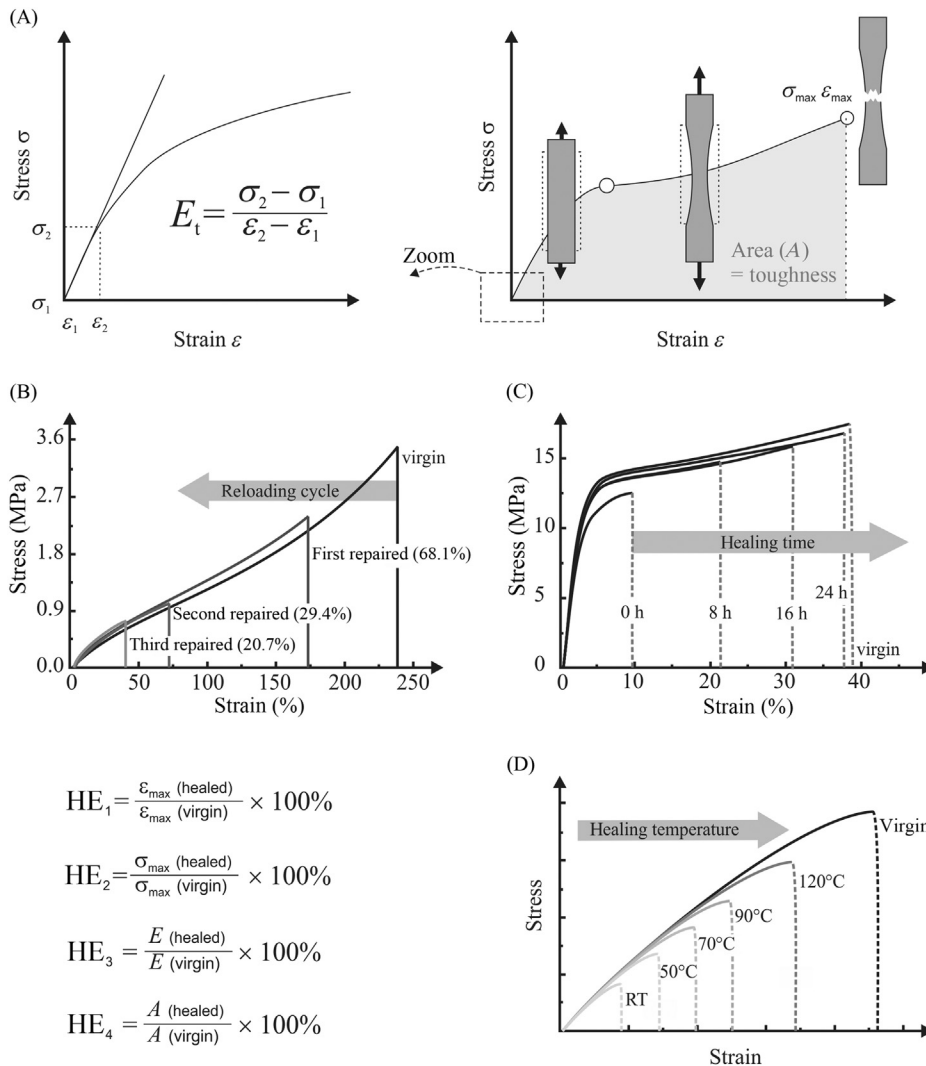


FIGURE 22.11 Self-healing efficiency by tensile testing: (A) calculation of tensile modulus (E_t) in the elastic region of the stress-strain curve; calculation of the stress at break (here $\sigma_{\max} = \sigma_B$), strain at break (here $\varepsilon_{\max} = \varepsilon_B$) as well as toughness of the material (here area, A) from the stress-strain curve. (B) Effect of reloading cycle [107] on photo-stimulated self-healing of polyurethane, (C) on healing time of polyacrylate coatings [73] and (D) on healing temperature [108] of disulphide linkages involved in the healing of poly(urea-urethane) networks on the healing efficiency (HE). Figures (B), (C) and (D) were modified after Ling J, Rong MZ, Zhang MQ. Photo-stimulated self-healing polyurethane containing dihydroxyl coumarin derivatives. *Polymer* 2012;53(13):2691–8. Available from: <https://doi.org/10.1016/j.polymer.2012.04.016>; Zhang Y, Yuan L, Guan Q, Liang G, Gu A. Developing self-healable and antibacterial polyacrylate coatings with high mechanical strength through crosslinking by multi-amine hyper-branched polysiloxane via dynamic vinyl-ous urethane. *J Mater Chem A* 2017;5(32):16889–97. Available from: <https://doi.org/10.1039/C7TA04141A>; Grande AM, Bijleveld JC, Garcia SJ, van der Zwaag S. A combined fracture mechanical – rheological study to separate the contributions of hydrogen bonds and disulphide linkages to the healing of poly(urea-urethane) networks. *Polymer* 2016;96:26–34. Available from: <https://doi.org/10.1016/j.polymer.2016.05.004>, respectively.

modifying additives or additional matrix functionality on changes in glass transition temperature [109]. As is known, exceeding the glass transition temperature, T_g , is accompanied by a drastic change in physical properties of the material and T_g determines the maximum temperature of the operating range of the thermosetting polymer, that is, the temperature range in which the polymer can be used in applications (Fig. 22.12A). It is important to point out the high sensitivity of DMA as compared to differential scanning calorimetry (DSC) and thermal mechanical analysis (TMA) which allows a precise estimation of T_g of densely cross-linked and/or filled composite thermosetting coatings. The high accuracy of determining this temperature transition in the amorphous phase is achieved by a hundredfold change in the mechanical modulus. The value of the elastic modulus (storage modulus, E') at room temperature in the tensile measuring mode can be associated with the Young's modulus and can thus be used to assess the degree of self-recovery of the material,

quite similar to what is done in a classical mechanical test using a universal testing machine. Thus, the loss in the mechanical properties due to damage and the recovery by healing with respect to the virgin thermoset can be easily quantified by DMA [110,111].

In DMA, a cyclic scan of the mechanical properties of a thermoset is performed with the successive segments (1) stress and relaxation at a given temperature and (2) heating and cooling segments at constant stress. DMA provides an understanding of the microstructure of the material, that is, how individual functional groups of the polymer network interact to form thermoreversible covalent bonds. Thus, the method is particularly suitable for characterizing the chemical processes involved in self-healing according to the intrinsic mechanism. It was applied to characterize the self-healing behavior in numerous studies [112–115].

Another important application of DMA is the highly efficient identification of optimal conditions for self-

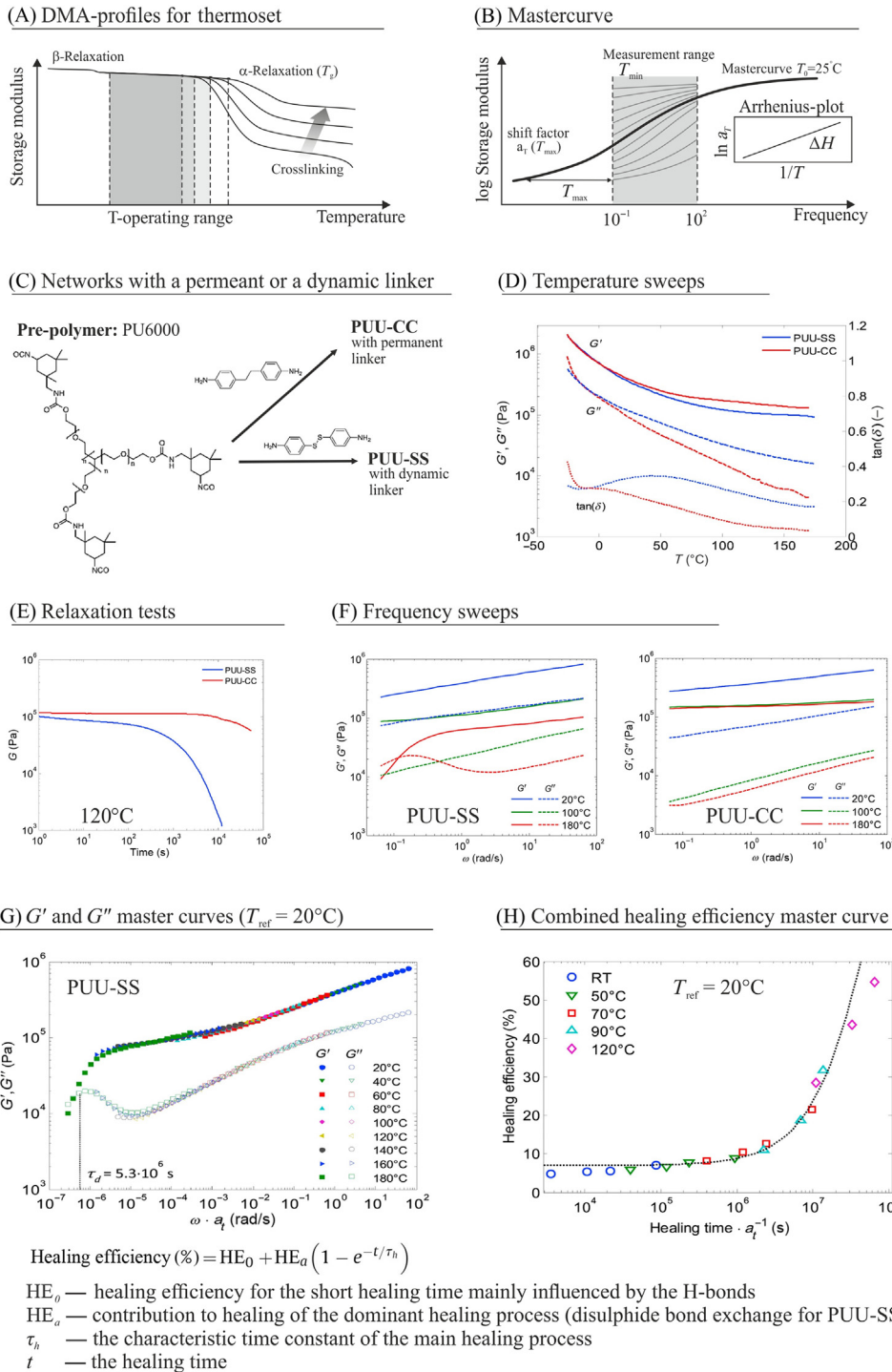


FIGURE 22.12 (A) DMA measuring profiles for the thermosets with various crosslinking density and determination of the operating ranges and (B) a calculation principle of the master curve [109]. (C) Polymer networks with a permanent (PUU-CC) or a dynamic (PUU-SS) linker (“not healable” version containing only the reversible physical bonds and “healable” version containing dynamic covalent linkages). Dynamic and steady-state rheological measurements: (D) Temperature sweeps for PUU-SS and PUU-CC, shear storage moduli (G') and shear loss moduli (G''). (E) Relaxation tests and (F) frequency sweep measurements [108]. (G) Time-temperature dependence of rheological and healing properties: G' and G'' master curves for PUU-SS at the reference temperature of 20°C [108]. (H) Healing efficiency master curve ($T_{ref} = 20^\circ\text{C}$) fitted with Equation (where $HE_0 = 7$, $HE_a = 93$ and $\tau_h = 5 \times 10^7$ s). Figures (C–H) were taken from Grande AM, Bijleveld JC, Garcia SJ, van der Zwaag S. A combined fracture mechanical–rheological study to separate the contributions of hydrogen bonds and disulphide linkages to the healing of poly (urea-urethane) networks. *Polymer* 2016;96:263–4. Available from: <https://doi.org/10.1016/j.polymer.2016.05.004> [108].

recovery of material properties by studying the mechanical response of the material to frequency scanning under isothermal conditions. With such frequency scans one obtains the experimental dependence of the mechanical modulus on two variables, time, and temperature, which change simultaneously. Using the time-temperature superposition principle (TTSP) for matrix resin viscoelasticity

it is possible to generate a master curve for predicting the operating time of thermoset composites in an arbitrary temperature range of interest (Fig. 22.12B). In this context, the accelerated test methodology for predicting the service lifetime of resin-containing laminates over very long periods of time should be mentioned. This approach was described in detail by Miyano and Nakada [116] for

predicting the long-term fatigue strength of CFRP laminates for aircraft and marine use. At the core of this approach is the derivation of universal master curves based on a relatively small number of laboratory measurements that can readily be carried out. From these master curves then, quantitative estimates for properties can be derived by applying the modified TTSP. The predicted statistical long-term tensile static, creep, and fatigue strengths were compared with experimentally obtained time- and temperature-dependent data for resin-impregnated carbon fiber-reinforced laminates.

In principle, predicting service life using this accelerated testing method can also be successfully applied to self-healing resin-based laminates, microcapsule-filled thermosets, and thermosetting micro- and nanocomposites. This approach would make it possible to evaluate the self-healing efficiency of the material under real wear conditions. The most successful combination of applied chemical functionality and/or supplemented additive responsible for the self-healing process could be selected. The construction of such master curves as well as the definition of the service life time of a self-healing epoxy using DMA based on the evaluation of the glass transition temperature was described in [109]. It should be mentioned that the strict application of TTSP for evaluation of polymer system dynamics requires chemical stability of the polymer microstructure with changing temperature. In this case, the relaxation processes under study will be reproduced in the same temperature scenario. In the case of temperature-dependent polymer networks based on noncovalent or dynamic covalent bonds, chemical changes will take place under the influence of temperature. However, for the study of time-dependent relaxation processes in such transient networks, the use of TTSP will undoubtedly be useful.

The investigation of healing processes with special attention to the tracking of changes in the microstructure is necessary above all to elucidate the chemical mechanisms underlying the self-healing effect. Kinetic and mechanistic information is a very important basis for the further development of appropriate dynamic chemical bonds in the case of intrinsic self-healing phenomena. The dynamic chemical equilibria involved in the reversible formation of covalent bonds and their contribution to self-healing are usually investigated with DMA, but also with other thermoanalytical methods such as TMA as well as rheological methods. The influence of temperature on the thermal mobility of polymer chains and the crosslink density in self-healing thermosets has been studied for Diels–Alder (DA) reactions [18,117], and the reversible formation of disulfide bonds [108,118], hydrogen bonding [119], boronic ester bond [120], dynamic iminoboronate boroxine exchange [121], alkoxyamine linkages [122], diarylbibenzofuranone [123], dynamic

Zn(II)-diiminopyridine coordination complexes [124], π - π stacking interactions [125,126], host-guest interactions [127], dynamic covalent disulfide and imine bonds [115]; thiol-isocyanate bonding [128].

The time-temperature correlation between the relaxation of a thermoset network and its macroscopic healing was investigated for poly(urea-urethane) (PUU) networks by Grande et al. [108]. Self-healing thermosets were prepared in such a way that they either contained only hydrogen bonds (PUU-CC) or that they had both hydrogen bonds and dynamic disulfide bonds (PUU-SS, with an additional thermoreversible crosslinker) (Fig. 22.12C). The combination of rheological studies and fracture tests with TTSP allowed to determine the individual contribution of each type of reversible bond to the viscoelastic and self-healing properties. Shift factors were calculated to construct the rheological master curves from individual isothermal measurements of the small amplitude of oscillatory shear (Fig. 22.12F). The same shift factors were then applied to obtain the master curve for fracture healing data as a function of healing time and temperature. In this way, the correlation between the rheological response and macroscopic fracture healing was successfully demonstrated. Fig. 22.12 shows the composition of the master curve from individual isothermal rheological measurements and the correlation between molecular mobility of the thermoset matrix and the achievable degree of self-healing depending on the presence of additional reversible binding sites.

Frequency sweep measurements (Fig. 22.12F) show that at room temperature both polymers similarly display elastic behavior (G'' much smaller than G'). However, at 180°C the predominance of the viscous response (G'') for the disulfide-based system becomes apparent. This is associated with the rupture and reorganization of dynamic covalent bonds. The construction of rheological master curves G' and G'' for PUU-SS using TTSP at 20°C is shown in Fig. 22.12G [108]. The different rheomechanical behavior of the two materials is shown in two modes: a narrow low-frequency terminal relaxation mode ($t > \tau d$) ($\tau d = 1/\omega d$, where ωd is the transition frequency $G'-G''$) and a wide average frequency relaxation mode (intermediate-temporal mode $t < \tau d$). The observed viscoelastic behavior in the PUU thermosets correlates well with two distinct stages of healing: (1) a first low-temperature stage of material healing. This correlates well with a wide intermediate-temporal regime and corresponds to the restoration of properties due to the formation of weak intermolecular hydrogen bonds. (2) A slower relaxation characterized by a significant decrease in the elastic modulus. It correlates with a high-temperature stage of healing associated with intramolecular rearrangements involving dynamic formation of covalent bonds (i.e. the disulfide bonds).

A combined HE master curve of fracture mechanical-rheological behavior of PUU networks was proposed as

the key result of this paper (Fig. 22.12G). The master curve clearly shows two areas: a first area of low efficiency for short-term movements of the network segments (regions of nonthermal relaxation) and a second area of effective healing for long healing times. As can be seen from this curve, the contribution of hydrogen bonds provided by the PUU-CC system to the healing process remains minimal and does not improve over time. Therefore, the evolution of PU-SS HE can be attributed to a single time-dependent healing process and may be described over a broad time (frequency) range using a simple two-step healing model (equation given in Fig. 22.12H). The authors note that the time-temperature rheological data, analyzed by TTSP, allow to investigate healing reactions and the visco-elastic dynamics of self-healing thermosets and improve the understanding of the restoration of interphase strength and the associated relaxation processes.

Optical spectroscopy

Chemical imaging for extrinsic healing

Optical spectroscopic methods are very often used to evaluate the success of extrinsic strategies for the self-healing of polymer systems. With optical spectroscopy the chemical processes during the self-healing process can be observed in real time and kinetic information on structural changes can be derived. This is particularly important because the time dependence of the repair processes is of utmost relevance when optimizing self-healing phenomena. Particularly interesting fields of application are also the control of the structure of microcontainers in thermoset composites, the monitoring of release processes, and the tracing of the distribution of the self-healing agent within the damaged area.

For instance, the presence of fragmented silicone-based microcapsules in the fracture plane of an epoxy matrix has been attempted to be detected spectroscopically in order to show self-healing processes. However, such studies often provide only selective information and are often only to be evaluated qualitatively rather than quantitatively. A numerical evaluation of the self-healing effect down to the depth of the bulk material is often difficult to perform.

The use of FTIR and Raman methods is mainly limited by the accessibility of the self-healing sites for the spectroscopic probes (local resolution). To follow the self-healing process, it is therefore recommended to use chemical imaging methods, that is, to perform spatially resolved spectroscopy (microspectroscopy; Raman imaging, infrared microscopy, spatially resolved fluorescence spectroscopy, etc.).

The use of chemical imaging methods allows the morphology of particles and especially the distribution of

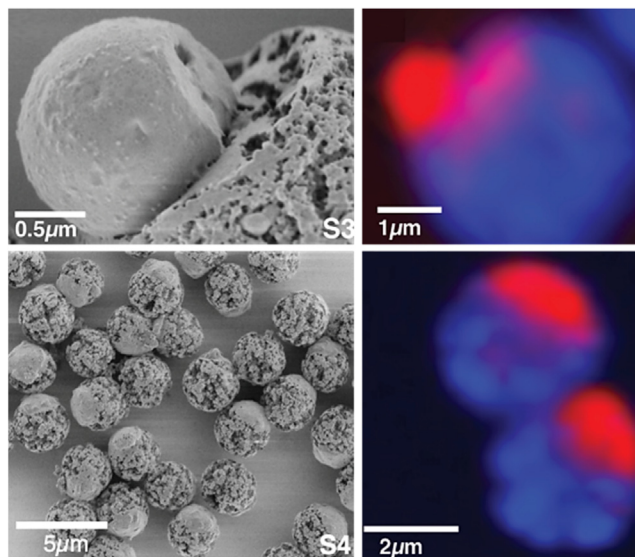


FIGURE 22.13 Electron micrographs and Raman images of two different types of anisotropic polystyrene/poly (glycidyl methacrylate-co-ethylene dimethacrylate) microspheres “S3” and “S4” [129].

chemical species on the particle surface to be characterized very well. The spatially resolved measurement also makes it possible to determine whether and to what extent the contents of microspheres have leaked from the spheres. The performance of this approach is demonstrated very well by the false-color representations of anisotropic polystyrene/poly(glycidyl methacrylate-co-ethylene di-methacrylate) microspheres reproduced in Fig. 22.13 [129].

Fig. 22.13 shows electron microscope (left) and Raman images (right) of Janus particles prepared under different synthesis conditions (particle system “S3,” Fig. 22.13, upper two images, and particle system “S4,” Fig. 22.13, lower two images). The Janus particles consist of two different chemical phases. The two chemical phases are represented in the Raman images (on the right) after chemometric treatment of the original spectra in the false-color representation by the colors “red” (polystyrene) and blue (poly (glycidyl methacrylate-co-ethylene dimethacrylate)) (a color version of Fig. 22.13 is available in the online version of this book chapter). In this example, the Janus architecture of the particles is obtained by extruding the polystyrene phase out of the growing poly (glycidyl methacrylate-co-ethylene dimethacrylate) particles [129]. The different morphology of the particles depending on the reaction conditions can be seen very clearly. This analytical methodology can be transferred very well to the characterization of microparticles, which are developed and optimized for extrinsic self-healing effects. The main advantage of the method is the precise characterization of the chemical composition of the particles. In electron microscopic methods, this is only

possible to a limited extent through element-specific mapping. In addition, the method is usually less time-consuming than, for example, SEM, so that the results of an analysis are usually available much faster.

Difficulties with optical spectroscopic methods may arise when the analytical signals of multiphase systems are to be evaluated and assigned. In this case, physical effects overlay the chemical information one is interested in. Lack of availability of specifically assignable absorbance bands can be a problem. Insufficient or excessive penetration depth of the optical radiation into the sample can also cause difficulties in interpretation and/or signal-to-noise ratio. Information specificity and signal-to-noise ratio can be enhanced by using spectroscopic marker molecules as part of the self-healing formulation. In this respect, a very interesting way to obtain information about the efficiency of self-healing is the so-called “self-reporting” approach.

Self-reporting systems for extrinsic healing

With self-reporting systems, a (therein soluble) spectroscopic marker (typically, a fluorescent dye) is introduced into the extrinsic self-healing agent. The fluorescent dye is released together with the self-healing agent when the microspheres burst in the course of the damage event, and during self-healing they are distributed in the damage zone in a similar form like the self-healing agent. This way, it can be used to track the reactive self-healing agent and to detect the newly formed duroplastic material in the cracks freshly filled with thermoset material (Fig. 22.14). The reactive monomer is premixed with the fluorescent dye. Since only small amounts of the fluorescent marker are required to provide spectroscopic visibility, there is no significant loss in the self-healing efficiency of the filled microcapsules.

The healant can be coencapsulated with a colored dye to visualize its release after damaging the thermoset matrix. The general approaches used in creating self-reporting microcapsules in the self-healing thermosets are as follows: (1) a “simple” release of the encapsulated dyes in the damaged area, surrounding the broken capsules, and stain it; (2) the (colorless) components of the chromic system are embedded separately and after release their physical or chemical interactions induce a self-reporting response; (3) change of optical properties of dye due to its physical transformation, for example aggregating. The aggregation-induced emission (AIE) dyes exhibit drastically increased fluorescence in the solid state compared to the emission efficiency in the soluble state.

In the first case, the dye may be fluorescent [51,130,131] (Fig. 22.14A) or latent acid-based, which reports damages after interaction with the hydroxyl group contained on the surface of the corroded metal (Fig. 22.14B) [94]. Alternatively, a “Turn-On” Mechanism Based on dye-color developer interactions (Fig. 22.14C) [132] may be used. Fig. 22.14D illustrates aggregation-induced optical changes of the AIE

dye (4-TPAE), the “normal” aggregation-caused quenching dye (DCM) as well as their mixture before and after UV-curing of methacryloxypropyl-terminated polydimethylsiloxane with styrene [133,134]. The HE of another curing system based on isocyanate chemistry was investigated using the in situ self-reporting AIE principle with two commercially available tetraphenylethylene-based dyes [135]. The prepared self-healing epoxy coatings with the encapsulated AIE dye-hexamethylene diisocyanate mixture display adaptive repair of the scratched region at a microcapsule concentration of 10 wt.% as well as a high-contrast indication of the healed damage at a content of 0.05 wt.% of AIE dyes.

In situ monitoring of intrinsic healing processes

In addition, the use of optical spectroscopic methods is also of utmost importance when using an intrinsic approach to self-healing. On the one hand, vibrational spectroscopy (infrared, Raman) in particular can theoretically confirm the basic ability of a material to self-heal due to the quickly available information whether the functional groups required for self-healing are present in the spectrum or not (investigation of the self-healing predisposition of the material). On the other hand, spectroscopy can confirm the self-healing effect after the damage event has occurred and after the healing cycle has been completed, by demonstrating the reorganization of chemical or coordinative bonds after healing (depending on the chemistry of the “destruction/and restoration” cycle used). In principle, this is also possible in real time directly under the influence of external stimuli during the self-healing process. A sufficiently homogeneous chemical structure enables the reliable assessment and observation of the self-healing efficiency of such smart coatings. The potential of Raman spectroscopy in the monitoring of intrinsic self-healing processes has been described recently by [137,138].

The mechanism of healing associated with the formation of water-urea clusters was successfully studied in [139] by means of local FTIR studies and supported by Density Functional Theory calculations. For this purpose, nonhygroscopic polyurethanes with repetitive moisture-induced self-healing functions were synthesized from nonhygroscopic polypropylene glycols and urea. Atmospheric moisture was then used to stimulate rapid dynamic exchange between the urea fragments. Fig. 22.15 shows ATR-FTIR spectra collected from undamaged, repeatedly scratched and IR images of healed areas on damaged films. Mean centered bands on nonhydrogen related esters (1730 cm^{-1}) and urethane (1710 cm^{-1}) indicate their synchronous increase in the damaged area and their reduction during recovery. The intensity distribution of the vibrational band of urea with the center 1545 cm^{-1} on the damaged sample shifts towards higher

Coatings with self-reporting and self-healing dual functions. corrosion dynamics

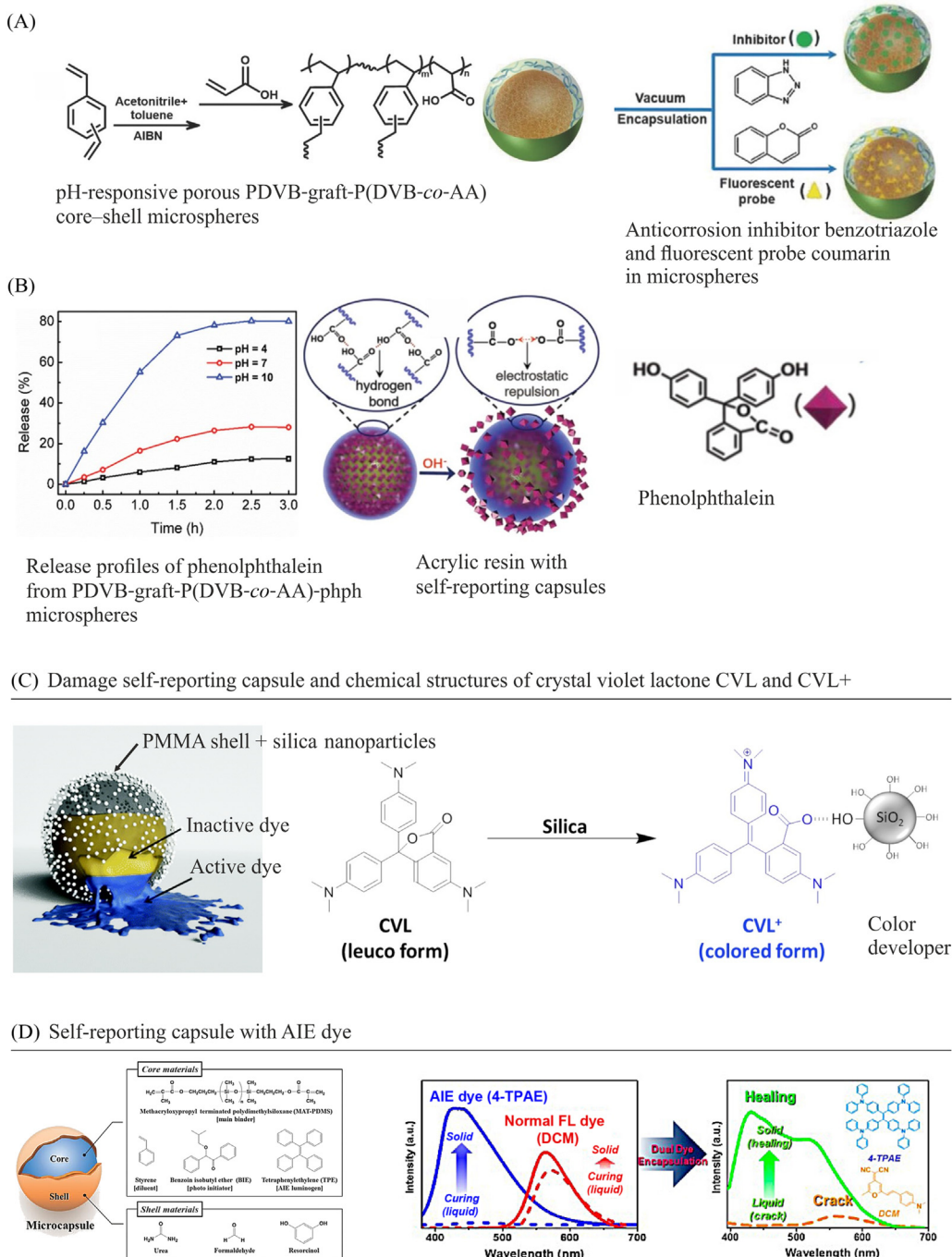


FIGURE 22.14 Self-reporting function in the self-healing thermosetting composites due to (A, B) latent release of the encapsulated dyes into the corroding area of the coating due to pH- pH-sensitive capsule shell [94,136]; (C) “turn-on” mechanism based on dye-color developer interactions [132]; and (D) aggregation-induced optical changes [133,134]. Modified after Wang J-P, Song X, Wang J-K, Cui X, Zhou Q, Qi T, et al. Smart-sensing polymeric coatings with autonomously reporting corrosion dynamics of self-healing systems. *Adv Mater Interfaces* 2019;6(10):1900055. Available from: <https://doi.org/10.1002/admi.201900055>; Wang J-P, Wang J-K, Zhou Q, Li Z, Han Y, Song Y, et al. Adaptive polymeric coatings with self-reporting and self-healing dual functions from porous core-shell nanostructures. *Macromol Mater Eng* 2018;303(4):1700616. Available from: <https://doi.org/10.1002/mame.201700616>; Hu M, Peil S, Xing Y, Döhler D, Caire da Silva L, Binder WH, et al. Monitoring crack appearance and healing in coatings with damage self-reporting nanocapsules. *Mater Horiz* 2018;5(1):51–8. Available from: <https://doi.org/10.1039/C7MH00676D>; Song YK, Lee TH, Kim JC, Lee KC, Lee S-H, Noh SM, et al. Dual monitoring of cracking and healing in self-healing coatings using microcapsules loaded with two fluorescent dyes. *Molecules* 2019;24(9):1679. Available from: <https://doi.org/10.3390/molecules24091679>; Song YK, Kim B, Lee TH, Kim JC, Nam JH, Noh SM, et al. Fluorescence detection of microcapsule-type self-healing, based on aggregation-induced emission. *Macromol Rapid Commun* 2017;38(6). Available from: <https://doi.org/10.1002/marc.201600657>, respectively.

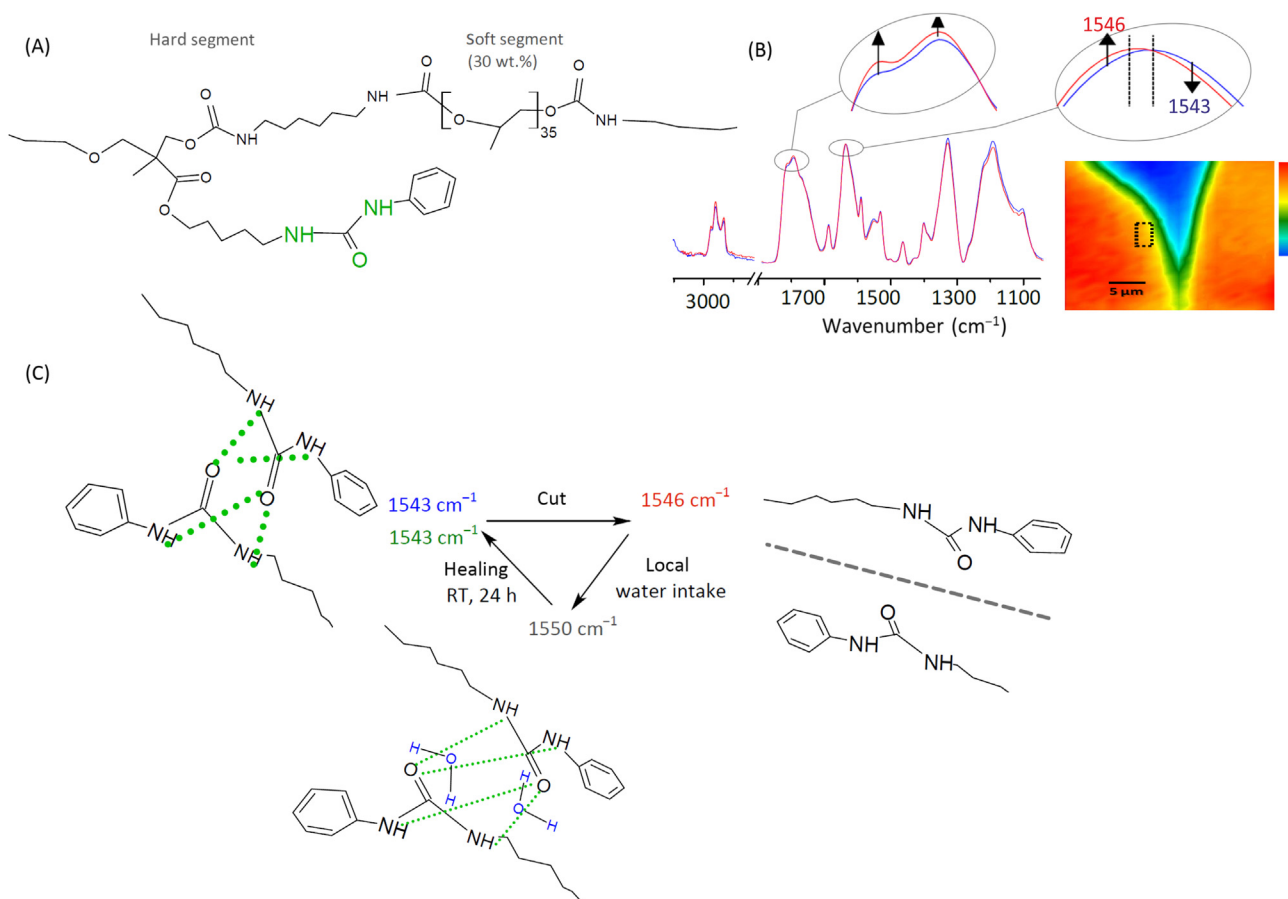


FIGURE 22.15 ATR-FTIR-detection of the polyurethane (PU) healing: (A) structural segment of the self-healing PU with pendant urea groups, (B) spectra collected from undamaged, from scratched and from healed areas by IR imaging of PU films using a μ -ATR-FTIR spectrometer, allowing a spatial resolution: of about $1 \mu\text{m}^2$. Red and blue colors characterize high and low intensity of the vibrational band at 1545 cm^{-1} . (C) IR-detection of the moisture driven healing process via hydrogen bonds. Modified after Willocq B, Khelifa F, Odent J, Lemaur V, Yang Y, Leclère P, et al. Mechanistic insights on spontaneous moisture-driven healing of urea-based polyurethanes. *ACS Appl Mater Interfaces* 2019;11(49):46176–82. Available from: <https://doi.org/10.1021/acsami.9b16858> [139].

wavenumber (up to 1551 cm^{-1} for M-urea and up to 1550 cm^{-1} for polyurethane based on urea) as the water quantity increases) due to the coordinated intensity change in free/hydrogen bound urea. ATR-FTIR control experiments for intact and damaged samples on water surfaces (i.e., at 100% humidity) further illustrated the same vibrational energy changes observed under atmospheric humidity conditions. It also turned out that large amounts of water did not affect the position of the urethane peaks (1710 and 1680 cm^{-1}) in urea-containing polyurethane. Therefore, water molecules more readily interact with urea than with urethane fragments.

Temperature-dependent infrared spectroscopy was used to determine the degree of interaction of hydrogen bonds at different temperatures in a polyurethane amide coating containing carboxylic acid type aromatic disulfides (COOH-SS) [114]. According to the results of the tensile test, such a rigid polyurethane amide matrix based on aromatic disulfides can quickly self-heal up to levels of 8 MPa within 30 s at room temperature. Fig. 22.16

shows changes in N-H stretch (3500 – 3100 cm^{-1}) and amide vibrations (1750 – 1450 cm^{-1}) for PU-COOH-SS during heating. When the temperature increases from 30°C to 120°C , the N-H hydrogen bond stretch vibration frequency shifts systematically from 3373 to 3380 cm^{-1} . As the strengths of hydrogen bonds between carbonyl functionalities and neighboring N-H groups decreases, the amide I mode of the carbonyl group (C=O stretch vibration) shifts to a higher frequency (1730 – 1736 cm^{-1}). Formation of hydrogen bonds between the amide functions and the C=O groups (type iii in Fig. 22.16) is evidenced by the shoulder at a frequency of 1711 cm^{-1} , which shifts to 1701 cm^{-1} with an increase in temperature from 30°C to 80°C . As can be seen in Fig. 22.16, H-bonding interactions in the poly(urethane-amide) system remain rather strong at temperatures up to 80°C and play a major role for self-healing in this temperature range. Upon further increase in temperature from 80°C to 120°C , this hydrogen binding of type iii dissociates faster than it is formed. This leads to a shift of the shoulder

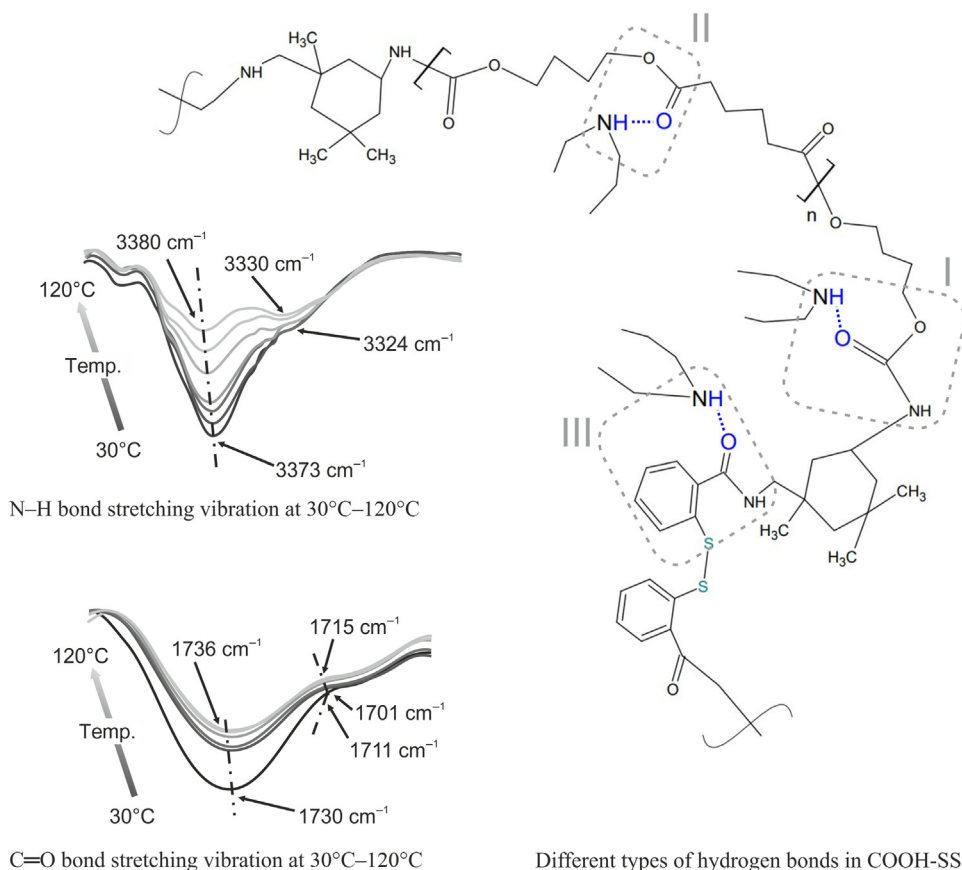


FIGURE 22.16 ATR-FTIR spectra of COOH-SS sample during the heating [114]. The spectra enlarged from 1750 to 1450 cm^{-1} for the carbonyl-group regions as well as from 3500 to 3100 cm^{-1} for the amide-group regions. Three different types of hydrogen bonds in COOH-SS sample. Modified after Zhou J, Yang Y, Qin R, Xu M, Sheng Y, Lu X. Robust poly(urethane-amide) protective film with fast self-healing at room temperature. *ACS Appl Polym Mater* 2020;2(2):285–94. Available from: <https://doi.org/10.1021/acsapm.9b00807> [114].

(from the C=O stretch vibration) from 1701 to 1715 cm^{-1} which is accompanied by a corresponding change in the shoulder characteristic for the N-H of stretch vibration. The results of IR studies in addition to mechanical tensile studies and DMA (with the construction of master curves for COOH-SS) have shown the effectiveness of including acidic chain extenders in the polyamide matrix both in terms of rapid self-healing at different temperatures, as well as in terms of maintaining the mechanical strength. Unique H-bond arrays formed from COOH-SS promote fast and effective healing at low temperatures and allow crystallization under tension while maintaining sufficient strength of the material [114].

Comments on self-healing efficiency

As illustrated so far, the self-healing ability of a material can be described by a variety of complementary methods. It can be defined, with reference to one specific material property, as the extent to which any initial property can be restored by the material itself after an external damage event. Obviously, the self-healing ability seems thus a rather straightforward and easy to determine index which describes and summarizes the ability of a material

to repair itself in relation to a concrete property characteristic.

However, as a rule, due to the complex material property profiles of modern materials, it is in practice not only a matter of “the” ability to self-heal, but actually a whole spectrum of self-healing properties is required, that is, the the material property profile as a whole needs to be restored as comprehensively as possible. Only then it is possible to extend its service life quite reasonably further.

In order to be able to realistically assess this performance and to evaluate and classify it as close to practice as possible, such a self-healing criterion should not only be applied selectively with respect to one property. From an application point of view it is reasonable to choose a more comprehensive approach which considers the effects of self-healing processes, that is, consequences of material-internal reorganization processes in the molecular network of the thermosetting polymer, on several different target properties equally.

Technologically, the challenge is to find out from the wealth of available factual knowledge, experience, available materials and chemical strategies those concepts which are transferable to a specific application and which also prove themselves in practice with respect to a specific, usually quite complex property profile.

An important challenge with regard to metrology continues to be the definition of self-healing materials and their testing methodology to be focused on very specific applications and the correspondingly highly specific property profiles. In order to achieve comparability of different approaches, it certainly makes sense to standardize the evaluation criteria of self-healing thermosetting polymers designed for a very specific application. Among the central application properties of thermosetting polymers with self-healing properties, which should be considered in any case, are the mechanical parameters tensile strength, toughness, and modulus of elasticity at different temperatures, the interfacial adhesive properties, the thermal conductivity and electrical properties, as well as the optical properties such as transparency or color.

The type and extent of material damage can take very different forms and has a strong influence on the result of self-healing processes. An objectivation and standardization of the analysis is complicated by the fact that the nature of the damage also influences the self-healing performance of the material. Damage can range from slight scratches on the surface and microdamage to the 3D networks (microcracks, crack formation), through macroscopic damage to interfaces (delamination phenomena, spalling, holes) to deep cuts and fractures resulting in massive material failure. Accordingly, the damage pattern that the material faces can be very diverse. When comparing the self-healing capabilities of different materials, a more precise specification of the damage event will therefore always be necessary (standardization of damage events).

Extrinsic self-healing of thermoset systems: the “additive” approach

Improving commercial systems by healing additives

Applying the extrinsic approach is in many cases mainly about improving the quality of an existing commercially available polymer system. In this section some representative examples from the recent literature for advanced architectures of autonomous self-healing thermosets are given. The types of self-healing systems and their active components that have been discussed and investigated in particular detail in the recent scientific literature are summarized in Table 22.1. In the majority of the reaction mechanisms covered, the effectiveness of the respective approach and the quality of the self-healing performance has been verified by enhancing commercial or standard epoxy matrix systems. The self-healing agents, which are mainly used to cure defects in such epoxy systems, utilize the following basic chemical systems: isocyanate-based, epoxy-amine, epoxy-thiol, thiol-maleimide, thiol-isocyanate,

siloxane, dicyclopentadiene (DCPD)/ethylidene norbornene (ENB), maleimide-based, vinyl ester, glycidyl methacrylates (GMA), and azide-alkynes.

Recently, many studies have focused on eco-friendly healing systems based on drying oils. These are natural triglycerides containing polyunsaturated fatty acids that readily oxidize to form a thermosetting network. The oxidative polymerization mechanism of drying oils is summarized in [140]. The addition of dryers (metallic salts) reduces the activation energy for oxidation of unsaturated fatty acids, and, in turn, the temperature required to initiate oxidation. The cross-linkable healant is typically obtained from plant oils cross-linking is brought about using radical polymerization with an oxidative mechanism involving the double bonds of the unsaturated fatty acid chains [141]. It should be noted that Table 22.1 contains only systems that are able to cross-link under mild conditions. Some healing systems that may also be regarded as autonomous self-curing systems but require higher temperatures to initiate cross-linking were not included in Table 22.1. This concerns mainly epoxy healing agents that require additional heating up to 120°C–140°C and an epoxy catalyzed by latent hardener (a complex of CuCl_2 and imidazole ($\text{CuCl}_2(\text{Im})_4$), $\text{CuBr}_2(2\text{-MeIm})_4$ or other imidazoline derivatives) that still require heating about 50°C.

Many examples found in the literature on extrinsic healants use standard epoxy polymer systems as the matrix systems. The high interest in establishing self-healing properties with commercial epoxy resin matrix systems is understandable on the one hand considering their wide distribution in industrial and commercial applications and the relatively high costs of these resins. So, in principle the economic interest is comparatively high to increase the durability of materials and products bonded with epoxy resins. On the other hand, epoxy resins have a chemistry that is advantageous for most self-healing approaches: Since epoxies are cured by multifunctional amines, the matrix usually provides excess amino functionalities. These amino groups are able to effectively catalyze the curing of cross-linkable monomer released from the capsules at the crack surface. In this context, the self-healant reaction pairs thiol-maleimide, thiol-epoxy and thiol-isocyanate mechanisms appear particularly promising: The secondary healing network involving these groups already forms at room temperature on the surface of amino-containing epoxy resin [142,143]. Nevertheless, the same chemical strategies can, in principle also be employed to produce self-healing effects also in other thermoset matrix systems. Ultimately, the aim is to develop and have commercially available versatile capsule systems that can be incorporated as general “self-healing additives” into arbitrary thermoset matrix formulations.

TABLE 22.1 Healing systems for the autonomous self-healing approach.

Environmental stimulus/self-healing concept/type of polymerization	Reaction system/commercially available healant (if available)	Comments on efficient curing	References
Moisture-induced curing/isocyanates			
Nucleophilic addition	Healant: HDI. The released HDI can heal the crack in the epoxy coating by reacting with surrounding moisture.	A double-walled polyurea shell provides an excellent resistance to nonpolar organic solvents for paints and coating applications.	[153]
Nucleophilic addition	Healant: IPDI, highly reactive. A one-component catalyst-free healant system; a severely restricted capsulation technology: a multishell is preferable to avoid a penetration of water during the storage process.	The released IPDI reacts with water or moisture to form PU at RT (isocyanate–hydroxyl chemistry); a recovered corrosion resistance of the epoxy and acrylic resin coatings in brine solutions (a factor for the steel corrosion); incorporated IPDI-loaded active lignin capsules slow down the UV-aging of polyurea coatings.	[75,93,154,164]
Nucleophilic addition	Healant: IPDI-based prepolymer and 1,6-diaminohexane as chain extender.	Use of dense MC shell: Double-walled polyurea modified by graphene oxide nanoparticles; applied for marine anticorrosive epoxy coatings.	[155]
Light (UV-radiation or sunlight) induced curing			
Epoxy and cationic photoinitiator Photo-cross-linking via cationic polymerization	Healant: Mixture of epoxy resins E-51 and A1815. Photoinitiator: Mixed triarylsulfonium hexafluorophosphate salts (PI6992), is strongly sensitive in the UV region (200–350 nm), not sensitive to atomic oxygen; E-51:A1815:PI6992 = 1:1:0.6.	Accurate stoichiometric ratio required/the up to 89% curing efficiency of the epoxy resin in 30 min/potential application in aerospace coatings.	[173]
	Healing agents: Epoxy silicon oil (1,3-bis(glycidoxypopyl) tetramethyldisiloxane, B3001) and cationic photoinitiator (mixed triarylsulfonium hexafluorophosphate salt solution in propylene carbonate (30 wt.%), PI 6992).	UV-responsive MC-based system. Effective crack repair of spacecraft coatings due to multitriggered function: under the stimuli of external force and UV radiation.	[27]
	UV-sensitive healant: UV-curable epoxy resin containing 74% DGEBA and 26% <i>o</i> -cresyl glycidyl ether (Epon 813) with 2–4 wt.% UV catalyst THP.	The sunlight-activated self-healing zinc-pigmented epoxy coatings were healed under 365 nm (3.8 mW/cm ²) UV light for 3 h.	[17]
Photo-cross-linking via cycloaddition	Healant: CA-PDMS copolymer combined hydrophobic and flowable PDMS-moiety and the photoreactive cinnamide. Upon photo-irradiation, CA-PDMS generates a viscoelastic substance (a cinnamoyl conversion of 40%–50%) with recoating capability because of reduced flowability and a relatively short irradiation and recoating time: The recoating time increases with increasing photo-irradiation time: CA-PDMS irradiated at 280 nm for 0, 1, 2, 3, and 4 h shows recoating times of 5 s, 20 s, 70 s, 7 min, and 1 h, respectively.	Extrinsic–intrinsic-recoating under UV. The CA-PDMS-based coatings: PDMS-loaded MC: a commercial enamel paint = 1:4. The test 10% NaCl test (EIS) after 48 h: the first and second scribes in the CA-PDMS-based coating were self-healed; catalyst-free, environment-friendly self-healing.	[174]
Thiol-ene UV, DMPA  Radical polymerization to form a thio-ether containing network	In UF-micro- or nanocapsules (1–10 μm or 100–350 nm in size)/polystyrene nanocapsules for dinorbornene: The network formation is accelerated at room temperature by the radical photoinitiator DMPA dispersed in the coating and applying UV irradiation for 1 h.	Very good quantitative healing efficiencies; in acrylate- and epoxy-based materials: rapid and uniform cross-linking, delayed gelation, reduced shrinkage, and insensitivity to oxygen.	[175]
	Tetrathiol (paentaerythritol tetrakis) (3-mercaptopropionate) (tetrathiol) and ether: diacrylate (1,6-hexanediol diacrylate).	Visualization of the healant release: The release of an encapsulated multifunctional thiol in the cut was monitored with a rhodamine–profluorophore dispersed in the poly(methyl acrylate) matrix, which selectively reacts with thiols.	[176]

(Continued)

TABLE 22.1 (Continued)

Environmental stimulus/self-healing concept/type of polymerization	Reaction system/commercially available healant (if available)	Comments on efficient curing	References
Epoxy-acrylate resins Radical polymerization	The components of UV-sensitive healant: (1) epoxy acrylate resin, bisphenol A epoxy acrylate with T_g of 62°C (Cytec Surface Specialties, USA); (2) reactive diluters (liquid monomers): trimethylolethane triacrylate, TMPTA, 1,6-hexanediol diacrylate, HDDA, and tripropylene glycol diacrylate, TPGDA (Cytec Surface Specialties), (3) photocatalyst: 1-hydroxycyclohexyl phenyl ketone (Irgacure-184; Ciba Specialty Chemicals, Switzerland).	A weight ratio of UV-sensitive resin:reactive monomer: photocatalyst was 25:25:2. The curing is initiated by electroluminescence generated during electrical treeing. The MCs are able to direct the propagation of the electrical trees due to a higher dielectric constant relative to the matrix.	[156]
	UV-sensitive healant: The mixture of photosensitive epoxy acrylate resin BAEA resin (Dow Corning), TMPTA (Dow Corning), and photoinitiator: Irgacure 184 (Ciba, Switzerland).	A weight ratio of BAEA:TMPTA:Irgacure 184 = 64:32:4. The released healant is cured in the cracks of the epoxy (EPON 828)–phenol–aldehyde amine matrix under UV exposure for 30 s.	[165]
Oxygen-induced curing. Low-temperature oxypolymerization of drying oils			
Drying oil (linseed oil, tung oil) Oxypolymerization mechanism/radical (chain growth) polymerization	Healant: Linseed oil (unsaturated glycerides of long-chain fatty acids) forms an impermeable film under atmospheric oxygen or humidity condition.	A drying rate of linseed oil is very slow due to the low reactive internal double bonds. The additives of drying agents (metallic salts) accelerate the radical polymerization via unsaturated chain fragments of the fat acids.	[72]
	Healant: Linseed oil (Textron Técnica, S.L., Spain).	Ambient temperature polymerization of the released oil for 24 h.	[177]
	Healant: Linseed oil (Textron Técnica, S.L., Spain). Different amounts of linseed oil (8.5, 10.5, and 12.5 g) containing 1.0 wt.% cobalt (II)naphthenate drier.	Can significantly improve the anticorrosion properties of the damaged coating in short term however it rapidly decreases with time.	[91]
	Healant: Linseed oil in the PU shell (Damao Chemical Reagent Factory). Healing conditions: 5 days at RT, 4 h curing at 80°C.	Epoxy resin Epikoe 862:hardener Epikure F 205:Heloxy 8 = 1:0.58:0.1. The optimal concentrations of oil–PU–MCs are 15–20 wt.%.	[58]
	Healant: Linseed oil (Sigma-Aldrich), with initial decomposition temperature of 310°C; a cross-linking polymerization of the released oil for 72 h in air.	Dual-functional epoxy-amine coatings: Self-lubricating and self-healing functions.	[59]
	Healant: Linseed oil.	The higher interfacial adhesion between matrix and hexamethylene diamine modifier of linseed oil-MC surface results in increased healing performance of epoxy coatings.	[90]
	Healant: Linseed oil (Sigma-Aldrich) with a density of 0.93 g/mL; epoxy resin matrix (Binalood Paint and Resin Company) with a density of 2.1 g/mL.	Low amount of released linseed oil (from 5% of MCs) could not restore corrosion protection after 120 h.	[92]
	Tung oil (a glyceride of an elaeostearic acid, a conjugated triene; 410 mPa s, Guangzhou HanhaoChemical Co. Ltd.); Coating: E-51 epoxy resin with 12 wt.% TEA hardener.	The rapid oxygen-induced cleavage of the carbon–carbon oil chains and subsequent polymerization of highly unsaturated and conjugated molecular fragments.	[57]
Resin monomers based on the oil fatty acid/nonoxyoxidative curing			
	Healant: The alkyd (an oil length of 65%) synthesized from monoglycerides of palm kernel oil and phthalic anhydride to have the groups –COOH and –OH as the reactive sites for the reaction with epoxy resin (Epikote 240) and cycloaliphatic amine (Epikure F205).	A low level of unsaturation makes a palm oil alkyd resistant to oxidation and unable to air dry efficiently. The healing curing process at RT is based on the blends of alkyd with hardener (at ratios 2:8, 1:8, and 1:7) in the epoxy matrix.	[178]

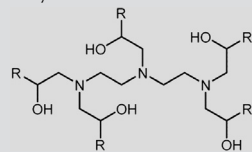
	Healant: Tall oil fatty acid–based epoxy ester resin 7449 (contained 30 wt.% xylene, OPC Polymers, Columbus, Ohio).	Healing conditions: At RT for 72 h.	[179]
	Alkyd resin based on coconut oil (a polycondensation product of polyhydric alcohols and polyacids modified with triglyceride oils) with viscosity 5.6×10^{-4} m ² /s, acid value 6 mg KOH/g, oil length% 62 (Aria Resin Co., Iran).	The carboxyl and hydroxyl groups of the modified alkyd resins react with the epoxy matrix in the presence of amine groups from poly (melamine–urea–formaldehyde) shell. The participation of unsaturated C = C bonds in oxidation curing was not considered.	[88]
Catalyzed low-temperature curing			
Glycidyl methacrylate–based healing system ATRP	Healant: GMA. Catalyst: CuBr/PMDETA in the layer of ATRP-macroinitiator PMMA-Br.	GMA with ATRP-macroinitiator PMMA-Br in the PMMA matrix.	[161]
Acrylate-based healing system Temperature-induced radical polymerization Initiator–accelerator system	Healant: A dental monomer TEGDMA (Esstech, Essington, PA); a dental tertiary amine accelerator: <i>N,N</i> -dihydroxyethyl- <i>p</i> -toluidine, DHEPT (Sigma-Aldrich) soluble and stable in TEGDMA. A healing mixture of TEGDMA and DHEPT was encapsulated.	A free-radical polymerization of TEGDMA-core MCs was initiated by using 0.5 wt.% of BPO in the BisGMA/TEGDMA resins; healing conditions: in a humidior at 37°C for 24 h (67% of the curing conversion).	[180]
Furan maleimide Diels–Alder click reaction	Healant system: (1) furan-functionalized epoxy-amine matrix prepared by curing of DGEBA (Epon 828), furfuryl glycidyl ether FGE (a 3:2 by weight ratio), and biscyclohexanamine; (2) MMIs dissolved in phenyl acetate: 1,6'-bismaleimido-2,2,4-trimethylhexane (MMI-2, Daiwakasei Industries Japan).	Furan functionalities of the epoxy matrix react with a released solution of the MMI in phenyl acetate at RT for 24–48 h. The healing efficiencies between matrixes healed with direct injection of MMI-2 healant and released MMI-2 were compared. Furan functionalities of the epoxy matrix react with a released solution of the multimaleimide in phenyl acetate at RT for 24–48 h.	[181]
Thiol-maleimide with amine catalyst in epoxy matrix 	Healing agents: Tetrathiol (pentaerythritol(3-mercaptopropionate)) and bismaleimide (MBM), tetrathiol and PDM. Amine catalyst from Matrix1: EPON 828 epoxy resin and DETA hardener or Matrix2: The RIM 135 epoxy resin = DGEBA and 1,6-hexanediol diglycidyl ether. Hardener RIMH 137 = alkyl ether amine and isophorone diamine.	Capsule A: Maleimides and Capsule B: amines/thiols. Maleimide–amine reaction proceeds faster than the epoxide–amine or methacrylate–amine reaction.	[143]
Thiol-isocyanate with amine catalyst in epoxy matrix  Nucleophilic addition reaction	System 1: HDI and tetrathiol: (1) with a tertiary amine catalyst: a 100% conversion within minutes; (2) without the catalyst: a very low conversion within 1 h; (3) with a catalyst present in the epoxy matrix: a 70% conversion after 3 h. System 2: HDI3 isocyanurate trimer and tetrathiol: (1) without a catalyst: a 40% conversion after 10 days, (2) with a catalyst present in the epoxy matrix: a 40% conversion after 6 days.	The isocyanate reactivity is high in moisture: the amine-products participate in the cross-linking. Matrix effect: The reactivity of the multifunctional thiol–isocyanate systems (1:1 ratio of the functional groups) was tested in the (1) EPIKOTE 828-DETA epoxy matrix; (2) RIM 135-RIMH 137 (cold-curing epoxy resin).	[142]
Isocyanate-hydroxyl groups of epoxy matrix Nucleophilic addition	Healant: Encapsulated IPDI with thiourethane shell layers (dithiol, trithiol, and tetrathiol); matrix: DGEBA-based epoxy resin (Epidian 5, Organika-Sarzyna Inc. Poland) with TETA hardener/catalyst (ET, Organika-Sarzyna Inc., Poland). Epoxy: ET:MCs = 100:18 (18 or 30).	Self-healing mechanism: A released isocyanate reacts with free secondary hydroxyl groups of epoxy matrix in the presence of tertiary amine ET at RT. The highest self-healing efficiency was observed in the presence of DMP-30 catalyst.	[182]
DCPD- or ENB-cure Grubbs' catalysts (first, second, and	DCPD. ENB. Grubbs' catalyst encapsulated in paraffin wax.	When the Grubbs' catalyst was embedded in paraffin wax microspheres and used in a kinetic study, 69% of the reaction rate was retained after contact with an amine hardener, compared to full loss of reactivity in the unprotected case. Furthermore, this wax protection	[183]

(Continued)

TABLE 22.1 (Continued)

Environmental stimulus/self-healing concept/type of polymerization	Reaction system/commercially available healant (if available)	Comments on efficient curing	References
Hoveyda–Grubbs' second generation) ROMP	Grubbs' catalyst was incorporated in silica-coated polystyrene particles.	only reduced the reaction rate by 9% in comparison to fresh Grubbs' catalyst. It also helped in dispersing the catalyst, leading to a much lower catalyst amount required for self-healing.	
	<i>Multiple release</i> : Hierarchical multiple healing capsule–based system [healing agent (DCPD)/shell poly(thiol-isocyanate) P(TMMP-IPDI)/DCPD].	The protective layer on the iron substrate was completely regenerated after repetitive damage in the same spot.	[167]
	Healant 1: DCPD (gel at RT; $T_m = 32.5^\circ\text{C}$); Healant 2: 5-Ethylidene-2-norbornene(liquid) encapsulated in glass fiber reinforced epoxy matrix (Resoltech 1050/1058 epoxy resin) containing Hardener 1055S and 5% of Grubbs catalyst (HG1).	The efficiency of MC integration into the epoxy matrix was tested using 6 techniques. Healing conditions: 48 h at 40°C .	[184]
	Healant: DCPD (Sigma-Aldrich) encapsulated in multishell MCs; Grubbs' catalyst (Aladdin Industrial Corporation) in PU-matrix (15: 2.5 parts of MCs and Grubbs' catalyst).	The encapsulated DCPD remained highly reactive (DSC-Measurements); healing time of the PU coating: 4 h at 60°C .	[99]
	Liquid healant 5E2N/CNT (5-ethylidene-2-norbornene) 10 wt.% of 5E2N/CNT MCs, 1 wt.% of HG2 catalyst in epoxy and curing agents mixed at a concentration of 100:47.	ROMP of 5E2N depends on reaction temperature: 0.2 min at 45°C ; 142 min at 20°C ; less than 5 min at RT with Grubbs catalyst. 5E2N monomer is active below 0°C (at -15°C); the presence of CNTs in the liquid 5E2N does not affect the reaction kinetics.	[74]
SbF ₅ –epoxy cure, cationic chain polymerization	Epoxy (EPON 828)-loaded MCs:catalysis SbF ₅ · HOC ₂ H ₅ /HOC ₂ H ₅ -loaded MCs = 100:6 wt.% in the matrix EPON 828:MHPA:BF ₃ -DMA: = 100:80:5.	Ultrafast curing at RT (shortened to seconds); significantly improved self-healing speed; the drastic curing exotherm is useful for operation in cold environment.	[185]
BF ₃ –epoxy cure, cationic chain polymerization	In an epoxy matrix (EPON 828): healant cycloaliphatic epoxy (Araldite CY179) catalyzed by the hardener BF ₃ –amine complex loaded in a SiO ₂ capsule. BF ₃ –DMA/BDO, the hardener of both the matrix and the healing agent contained 50% boron trifluoride–2,4-dimethylaniline complex in 1,4-butanediol; curing at RT, 2 h.	Boron trifluoride diethyl etherate ((C ₂ H ₅) ₂ OBF ₃), a commercial catalytic hardener for low-temperature fast-cure epoxy adhesives; the stoichiometric ratio of epoxide/hardener does not require.	[186]
Solvent/diluter epoxy cure (catalyst)	Healant: DGEBA-based epoxy resin and a high-boiling-point organic solvent (EPON 828–ethyl phenylacetate); In the resin paste (SA 70, Gurit) for composite laminate: Healant: solid catalyst (Sc(OTf) ₃) = c. 10:1 wt.%.	Healing conditions: At 80°C for 24 h in the presence of a Lewis acidic catalyst.	[157]

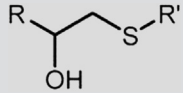
Epoxy–Lewis bases:
Amine epoxy cure
Polyaddition



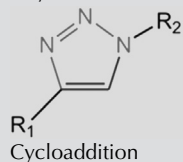
Healant: Epoxy resin (E51 CYD-128, Sinopec Corp and Tianjin FuChen Chemical Reagents Co., Ltd); hardener: TEPA; curing conditions: at RT for 24 h, healing test: at RT for 3 h in open air.	Matrix system: Epoxy:TEPA = 10:1. In the self-healing composite: 10 wt.% of encapsulated epoxy [epoxy core (90%)/silica NP layer/PU-shell] and 5 wt.% of encapsulated TEPA (amine core (82%)/nanoclay layer/PU-shell)	[147]
Healant: DGEBA epoxy resin (DGEBA YD128, KUKDO Chemicals); hardener: polyetheramine (D-230); epoxy:polyetheramine ratio = 3:1; the polyetheramine reacts with epoxy monomer at RT for 24 h.	Effects of dual microcapsulation on the self-healing efficiency of epoxy: it was higher with the dual MCs compared with the single one.	[187]
Healant: A diluted epoxy monomer (EPON 815C is a diluted EPON 828 epoxy resin containing 13.6% n-butyl glycidyl ether); hardener: modified aliphatic polyamine (EPIKURE 3274).	The optimal mass ratio of amine:epoxy capsules was 4:6 (stoichiometric ratio was 4:10).	[188]
Healant: Mixture of epoxy resin and <i>n</i> -butyl glycidyl ether. Hardener: Underwater epoxy hardener, contained primary amine.	8% Epoxy resin-MC and 4% hardener-MC; rapid solidification at low temperature; a new protection strategy for marine and other underwater facilities.	[39]
Epoxy and polyamine (Kian Resin Co., Iran); released epoxy monomer and polyamine react in the ratio 2:1 w/w (stoichiometric) at RT for 1–6 h.	The increased concentration of the encapsulated healant system and healing time result in the enhanced healing.	[49]
Epoxy–polyamine miniemulsion in PVA-based nanofiber: BADGE (EEW = 187 g/eq., Dow Chemical); phenalkamine (NX5454, Cardolite Corp.) with AHEW = 220 g/eq.	A statistical distribution of two separated reactants in close vicinity (<100 nm) in one electrospun PVA–EA fiber provides a favorable reaction stoichiometry and dense cross-linking ability at RT.	[189]
Healant: The low-viscosity epoxy resin (EPIKOTE Resin 240); amine-based hardener (EPIKURE 3370, Hexion) encapsulated in the PAN-nanofibers (400–500 nm): NF1 with 24% w/w of resin amount and NF2 with 37%w/w of amine curing agent.	A fast curing for undamaged NF1 + NF2 was observed at 143°C (reaction initiation)—172°C (peak); the released healing system (broken nanofibers) is cured at 30°C for 360 min (DSC-Analysis).	[190]
Healant: Epoxy resin (EPL 1012R) diluted with diglycidyl ether of 1,6-hexanediol (Inchem ed 180R); a hardener: polyamidoamide based curing agent (Merginamide A280R) from the multi component epoxy matrix (ED180R, EPON 828R).	The curing of released low viscosity epoxy healant at the presence of the unreacted aminoamide group from the matrix's hardener at RT, 24 h; a cost efficient self-healing coating.	[191]
Healant: DGEBA-based epoxy resin (Lapox L12) with density 1.20 g/cm ³ ; hardener: TETA (K6) with density 0.95 g/cm ³ .	A stoichiometric blend ratio of the encapsulated hardener and epoxy monomer was 1:1 by volume and 80% of hardener amount by weight of epoxy resin; the curing (healing) conditions: at 40°C for 4 h followed by RT-healing for 16 h.	[192]
Curing system: (1) <i>Epoxy resin</i> : DGEBA (EPITAL, Russia, an epoxide percentage of 20.0–22.5 wt.%, 191–215 g/eq.); (2) <i>Hardener mixture</i> (low-temperature aliphatic and high-temperature aromatic amines): <i>amidoamide hardener</i> L-20M, a product of TETA, with fatty and rosin acids of tall oil (G.S. Petrov Research Institute of Plastics, Russia); <i>DDS</i> (EPITAL, Russia).	The hardener mixture accelerates the epoxy resin curing (DSC) and increases T_g as well as the rubbery-plateau moduli (DMA). Aliphatic amidoamine reacts with epoxy resin at low temperatures to form the hydroxyl groups which catalyze the further epoxy curing with the aromatic amine.	[193]
DGEBA-epoxy resin, KER 828, (epoxy group content of 5260–5420 mmol/kg, molar mass of 184–190 g) and butyl acetate as diluent; amide-based hardener, Crayamid 140C (amine value of 370–410 mg KOH/g).	No visible sign of corrosion after up to 5 weeks (salt spray test).	[194]

(Continued)

TABLE 22.1 (Continued)

Environmental stimulus/self-healing concept/type of polymerization	Reaction system/commercially available healant (if available)	Comments on efficient curing	References
Epoxy–Lewis acids: (thiol/mercaptan) Thiol epoxy cure (amine catalyst) Nucleophilic polyaddition, the strict stoichiometric ratio of epoxide/hardener is required 	Encapsulated epoxy oligomer–polythiol (hardener)—strong base (hardening accelerator), low-temperature fast curability. Epoxy–mercaptan cure is a nucleophilic addition reaction.	Catalysts' alkalinity and content greatly affected rate of the addition polymerization, curing degree, and bonding strength. As requested by addition polymerization, the stoichiometric ratio of epoxy/mercaptan and uniform mixing at the molecule level are critical for a perfect cure of the healing agent released to the fractured surfaces to be rebonded.	[195]
	Epoxy and mercaptan-based hardener (with a catalyst). Healant: Nondiluted DGEBA epoxy resin, Araldite-F (Ciba-Geigy); curing agent: PETMP and a catalyst 2,4,6-tris(dimethylaminomethyl)phenol (DMP-30).	A fast curing of released epoxy and hardener occurred in a range of 70°C–100°C (DSC analysis); a recovery of mechanical properties was correlated directly with a capsular size and healant concentration as well as with a fracture plane.	[196]
	In polyacrylonitrile shell nanofibers: (1) Healant: epoxy resin (Araldite LY 5052–1, Huntsman, Switzerland) with the viscosity of 1 Pa s; (2) hardener: PETMP with viscosity of 0.45 Pa s (Sigma-Aldrich, USA). A catalyst: <i>N,N</i> -dimethylbenzylamine (BDMA).	The loading contents of epoxy and PETMP are 19 and 25.7 wt.%, respectively. A ratio of the catalyst (BDMA): PETMP was 1:10 wt.%. A fast curing was observed between 60°C and 130°C (gradual release of healants, DSC-Analysis). At 10°C for c. 3h only 70% of epoxy was cured.	[197]
	Healant: Multicore alginate capsules of epoxy resin Araldite 506 (Sigma-Aldrich, 500–700 cps). Hardener 1: Mercaptan hardener pentaerythritol tetra(3-mercaptopropionate) and a tertiary amine catalyst, <i>N,N</i> -dimethylbenzylamine [168]. Hardener 2: DETA, BASF; healing conditions: at 40°C for 48 h [198].	A multiple release from (1) dual-capsule system (epoxy: mercaptan = 1:1) and (2) capsule-catalyst (scandium(III) triflate) self-healing systems. Multiple healing (3–4 times); a higher healing performance for the dual-capsule system at 60°C for 48 h.	[168,198]
	In alkyd coating matrix: DGEBA-based epoxy (EPON828) and pentaerythritol tetrakis (3-mercaptopropionate) healing time: 10 min.	Environment-friendly self-healing coating: UV-curable palm oil-based alkyd coating.	[95]
	Healant: Epoxy resin DTP (a low-viscosity diglycidyl 1,2,3,6-tetrahydrophthalate epoxy resin). Hardener: Tetrathiol and tertiary amine catalyst (BDMA).	Healing efficiency at 20°C 82% after 3 h and 100% after 12 h.	[199]
	Encapsulated healant: A 100% DGEBA epoxy resin—Araldite-F (Ciba-Geigy); encapsulated curing agent—catalyst mixture: PETMP and 2,4,6-tris(dimethylaminomethyl)phenol (DMP-30).	Healing conditions: 24 h at 70°C; an 80% healing efficiency of bulk polymer (Fracture load I), but 57% of the healing efficiency under Fracture load II: it depends on an area of “dry surface” on the fracture surfaces in the healed regions.	[196,200]
	Epoxy-loaded MCs: Epoxy resin EPON 828 and resorcinol diglycidyl ether (J-80); hardener-loaded MCs: tetrathiol PMP; DMP-30; polythiol-loaded MCs: tetrathiol PMP.	Addition of resorcinol caused an increase in fracture toughness (resulting in slower crack propagation during fatigue testing); healing time from 8 to 10 min.	[201]
Isocyanate-amine cure Nucleophilic addition Polyurea formation	Encapsulated healant: (1) hydrophobic IPDI; encapsulated hardener-healant; (2) mixture: hydrophobic amine PAE (polyaspartic acid ester)—TO (TO was dissolved in PAE with a mass ratio 1:1).	Hydrophobic amine instead of traditional water-soluble amine; a 98% self-healing efficiency for dual-component MC coating (capsule content of 20 wt.%: in the air for 12 h at RT).	[202,203]

Copper(I)-catalyzed azide/alkyne-“click”-reaction



Synthesized trivalent alkynes (1, 2) and trivalent azides (3–5) of different hydrophobicity.

Catalyst 1: Cu(PPh₃)₃Br, Catalyst 2: Cu(PPh₃)₃F; Catalyst 3: Cu₂O on graphene-oxide (TRGO-Cu₂O)

Azides: Three-arm star PIB azides; *Alkynes*: mono-, di-, and trisubstituted tripropargylamine alkynes.

Healing conditions: Solvent-free reaction of alkyne with monovalent azido-telechelic PIB in the presence of CuBr(PPh₃)₃ as catalyst and DIPEA as base.

Alkynes: Multivalent poly(acrylate)s (nine atactic random poly(propargyl acrylate-co-*n*-butyl acrylate)s, $M_n = 7000–23,400$ g/mol, alkyne contents ranging from 2.7 to 14.3 mol% per chain); *Azides*: PIBs: five three-arm star azido-telechelic PIBs ($M_n = 5500–30,000$ g/mol) and one three-arm star alkyne-telechelic PIB ($M_n = 6300$ g/mol) in the cross-linking-reaction.

Azide: Liquid, azido-telechelic three-arm star PIB ($M_n = 3900$ g/mol); *Alkynes*: trivalent alkynes were encapsulated into micron-sized capsules and embedded into a polymer-matrix (high-molecular weight PIB, $M_n = 250,000$ g/mol); (Cu(I) Br(PPh₃)₃) as catalyst.

Azide: Azide functionalized carbon nanotubes (MWCNT-*t*-BA-N₃, functionalization via poly(*t*-butyl acrylate)); *Alkynes*: tripropargylpentaerythritol (synthesized and encapsulated); (Cu(I)Br (PPh₃)₃) is a catalyst embedded in the epoxy-amine matrix (1:50:50). Curing conditions: 10 wt parts of MCs:5 wt parts of MWCNT-*t*-BA-N₃.

The click-cross-linking kinetics of trivalent alkyne and azide catalyzed by catalysts 1–3 (1 mol%) was studied (DSC method). The low onset-temperatures were detected for the Cu(PPh₃)₃F-catalyzed reactions of trivalent alkyne 1 and trivalent azides.

[204]

Reactions in the solvent-free state proved to be significantly faster than reactions in solution. Various Cu(I) catalysts and tripropargylamines have been tested for RT “click”-curing reaction with the three-arm star PIB.

[205]

Study of catalysis during the cross-linking reactions of multivalent polymeric alkynes and azides: the significantly increased reaction rate with increasing alkyne concentrations. A kinetic analysis showed autocatalytic effects (up to a factor of 4.3) at RT.

[206]

Crosslinking at 40°C is observed within 380 min and as fast as 10 min at 80°C. Significant recovery of the mechanical properties was within 5 days at RT.

[111]

Increased efficiency of the azide–alkyne curing above 80°C and 50 h; healing efficiency with temperature (120 h): 30%–35% and at 30°C–60°C and 60%–65% at 80°C–140°C correspondently; healing efficiency with time at 100°C: 55%–60% for 50–120 h.

[207]

Acylhydrazine/methacrylate-based cure
Cross-linked acylhydrazone network through acid-catalyzed condensation

Gelators A, a bis-acylhydrazine-terminated poly(ethylene glycol) Gelator B, a tris[(4-formylphenoxy) methyl]ethane; a vascular synthetic system.

Room-temperature polymerization is achieved with addition of the radical initiators and promoters.

[208]

Siloxane cure (catalyst)
Polycondensation

Dimethylvinyl-terminated DMS resin monomer; platinum-catalyst.
The solidification takes about 1–2 days.

The released oil-like resin monomer impregnates cuts in the epoxy matrix and does not undergo polymerization (does not solidify) unless it is in contact with catalyst-contained epoxy matrix.

[209]

Healant: Silanol-terminated polydimethylsiloxane (DMS-S12, Gelest, USA); catalyst: dibutyltin dilaurate; a catalyzed condensation reaction at –20°C for 24 h results in a viscoelastic product (fluorescently visualized using OIL-GLO 44-P, Spectronics, USA). The mass ratio of the healant/catalyst capsules of 18:7 in the commercial enamel paint matrix corresponds to the 10:1 mass ratio of the pure components.

MC-based low-temperature self-healing concept for the commercial enamel paints. Glass slides, steel panels, and mortars were applied to test self-healing coating formulations.

[210]

ATRP, Atom transfer radical polymerization; BADGE, bisphenol A-diglycidyl ether; BAEA, bisphenol A epoxy acrylate; BPO, benzoyl peroxide; CA-PDMS, cinnamide-polydimethylsiloxane; DCPD, dicyclopentadiene; DDS, diaminodiphenyl sulfone; DETA, diethylene amine; DETA, diethylenetriamine; DGEBA, diglycidyl-ether of bisphenol-A; DHEPT, *N,N*-dihydroxyethyl-*p*-toluidine; DIPEA, *N,N*-diisopropylethylamine; DMA, dynamic mechanical analysis; DMPA, 2,2-dimethoxy-2-phenylacetophenone; DMS, dimethylsiloxane; DSC, differential scanning calorimetry; ENB, 5-ethylidene-2-norbornene; GMA, glycidyl methacrylates; HDI, hexamethylene diisocyanate; IPDI, isophorone diisocyanate; MBM, 1,1(methylenedi-4,1-phenyl) bismaleimide; MC, microcapsule; MMI, multimaleimide; PDM, *N,N*-(1,3-phenylene)dimaleimide; PETMP, pentaerythritol tetrakis (3-mercaptopropionate); PIB, polyisobutylene; PMMA, poly(methyl methacrylate); PU, polyurethane; PVA, polyvinyl alcohol; ROMP, ring-opening metathesis polymerization; TEGDMA, triethylene glycol dimethacrylate; TEPA, tetraethylenepentamine; TETA, triethylenetetramine; THP, triarylsulfonium hexafluorophosphate; TMPTA, trimethylolpropane-triacrylate; TO, tung oil.

Influence of the matrix on self-healing performance of the self-healing additive

The catalytic role of industrial epoxy resins and their influence on the curing kinetics of healant on the surface of cracks were estimated using several monofunctional model pairs [143] (Fig. 22.17A). The corresponding multifunctional compounds with the highest potential for rapid healing were then selected. The HE was evaluated using two commercial epoxy materials. Using the tensile fracture method, it was found that although the rate of matrix property recovery was highly dependent on the type of epoxy resin used, the maximum fracture load after healing was the same for both epoxy resin matrix systems tested.

Thus, for a successful self-healing process, not only the degree of restoration of the initial properties is of

great importance, but also the rate at which this original state is achieved again. Therefore, the special features of the healing reagents on the one hand and their (potential) interactions both with the matrix to be healed and with the encapsulating material on the other hand must be considered and investigated in each case. For example, it should be noted that the availability of reactive components such as multifunctional maleimide compounds in extrinsic approaches is strongly related to their encapsulation behavior. When using some reactive components, such as polyamines, it should be considered that a hollow carrier particles are required. The influence of the encapsulation material on the self-healing rate has recently been investigated [144,145]. For example, to estimate the reactivity between cycloaliphatic epoxy healing reagent (Ciba-Geigy, Araldite CY 230) and an amine hardener (TETA hardener, HY 951) the curing kinetics have been

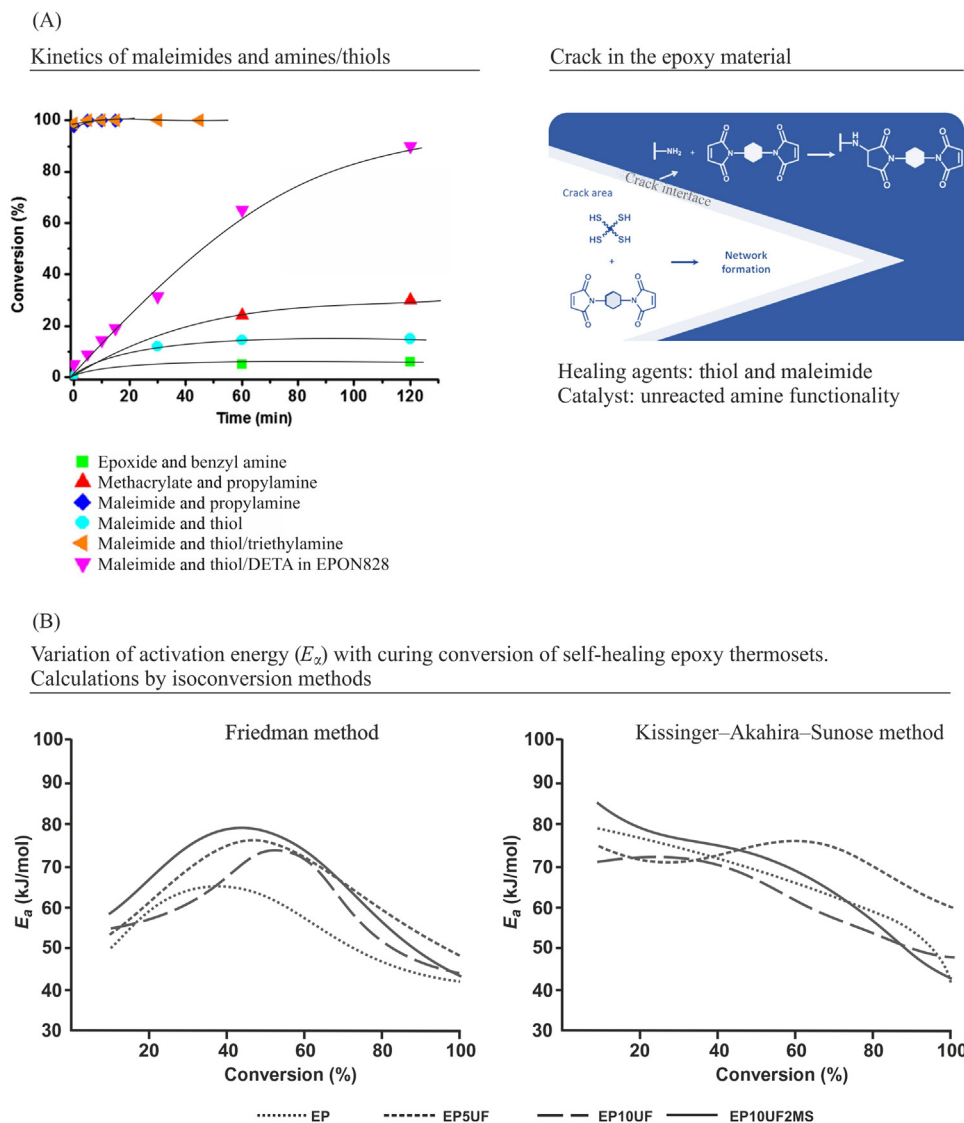


FIGURE 22.17 (A) Kinetics of maleimides and amines-thiols at room temperature on the example of model monofunctional pairs. Crack interface and mechanism of its healing in the epoxy material based on maleimide chemistry [143]; (B) Effect of TETA hardener immobilization on reactivity of cycloaliphatic epoxy healant embedded in urethane formaldehyde shell in the self-healing epoxy thermosets: The estimation of activation energy (E_a) with curing conversion by iso-conversional methods [144]. TETA, Triethylenetetramine. Figure (B) was modified after Tripathi M, Kumar D, Rajagopal C, Roy PK. Curing kinetics of self-healing epoxy thermosets. *J Therm Anal Calorim* 2015;119(1):547–55. Available from: <https://doi.org/10.1007/s10973-014-4128-1>.

investigated by applying kinetic analysis of DSC data [144]. The actual epoxy healant was encapsulated in a polyurethane microcapsule and the amine hardener was immobilized on mesoporous silica (substrate SBA 15). The influence of the finely distributed ceramic additive in the epoxy resin on its curing speed was investigated by nonisothermal DSC. The kinetic parameters of the curing kinetics were determined using the Friedman and Kissinger Akahira Sunose method [144]. These are computational methods typically used to obtain valuable kinetic information about the investigated process by means of relatively simple DSC experiments (see also Chapter 24, Processing and processing control, in this book). As a result of such evaluation methods, one obtains estimates of the (conversion degree-dependent) effective activation energies. Fig. 22.17B shows that the activation energy, (E_a) in the above example, tends to decrease with increasing degree of cure (i.e., with increasing turnover). This reflects the typical autocatalytic character of epoxy curing. However, no influence of the added microparticles on the curing kinetics was observed: The conversion-dependent activation energy was neither influenced by the presence of a ceramic carrier for TETA hardeners in the matrix nor by the presence of a urethane formaldehyde shell for epoxy healant with secondary amines. This shows that in this case the desired strategy of spatial isolation of both reagents could be successfully implemented without any loss of activity. The primary TETA amino groups effectively participate in the curing reaction and do not compete with the secondary amino groups of the capsule shell of the healant chemical [144]. Recently, further preparative methods for encapsulation of fatty amine hardeners were provided in [146,147].

The chemical design of capsule shells is of great importance since the capsule material may exhibit strong effects on the curing of the healant. The curing kinetics of microcapsules containing epoxy healant was studied with different types of formaldehyde resin-based shells in [148]. Capsule shells based on polyvinyl alcohol modified poly (urea-formaldehyde), poly (melamine-urea-formaldehyde), poly (urea-formaldehyde) and phenol modified poly (urea-formaldehyde) were synthesized for incorporation of epoxy resin as core material in self-healing microcapsules. It was found, that the curing process of core-epoxy resin in the microcapsules becomes more difficult compared with nonencapsulated epoxy. Moreover, the curing efficiency of core resin affects the stability of the shell material: the decomposition products of shell may participate in the curing reaction.

The effect of diluent concentration as well as the effect of healant type on the crosslinking degree and reaction conversion was studied for epoxy resin E-51 in [149] as a capsule core for the preparation of self-healing cementitious composites. The optimal fraction of n-butyl

glycidyl ether BGE as well as curing agent MC120D, based on the analysis of activation energy, were determined as 17.5% and 20% respectively. According to the proposed mechanism of the curing reaction E-51 with MC120D it was concluded that not only the epoxy resin E-51 was cured, but also that the BGE contributes to the cross-linking process.

Dye-based inline monitoring of epoxy network self-repair was also applied. The color transitions of pH indicator thymol blue were monitored in-line during the curing process of model thiol-epoxy networks with different multifunctional crosslinkers (Fig. 22.18). At room temperature the thiol-epoxy reactions are catalyzed by organic bases and proceeds via a nucleophilic ring-opening mechanism with autocatalytic effect. During crosslinking the pH continuously increases as the concentration of free basic catalyst increases. This can be tracked by thymol blue as a pH marker when it is premixed with the epoxy resin. A color transition from pink to blue during thiol-epoxy reactions effectively visualizes the progress of crosslinking reactions in self-healing applications, if the crosslinking densities are quantitatively estimated using thermoanalytical methods.

Dual versus single-capsule strategy

The previous examples were typical of the so-called two-capsule approach. In this approach, both the reactive healant additive and the second component required for crosslinking (catalyst or coreactant) are each encapsulated in separate microspheres. This solves the technological problem that the healing reagent has to be safely encapsulated and kept separated from the matrix to be healed until it is damaged, and from the catalyst component, that is, the self-healing agent must not harden prematurely (avoidance of the loss of reactivity). For this purpose, contact with the coreactant or catalyst, in this case also with the catalytically acting epoxy resin, must be reliably prevented.

As an alternative to this two-capsule strategy, increasingly complex container systems are being designed that keep both components of the extrinsic healing reagent effectively separated from each other but still in a common microcontainer. This solves the technological problem that during the extrinsic self-healing process, both types of microcapsules, that is, both healant and coreactant or catalyst capsules, must always be broken open simultaneously in the course of the damaging effect in preferable relative amounts, so that the contents of both capsules can escape at the same time and the two components can mix. Insufficient healing processes in autonomous extrinsic self-healing phenomena can therefore often be caused by unfavorable mixing ratios of the two components, for example, due to a geometrically

Kinetics of low temperature thiol-epoxy crosslinking reactions by using a pH-responsive epoxy resin

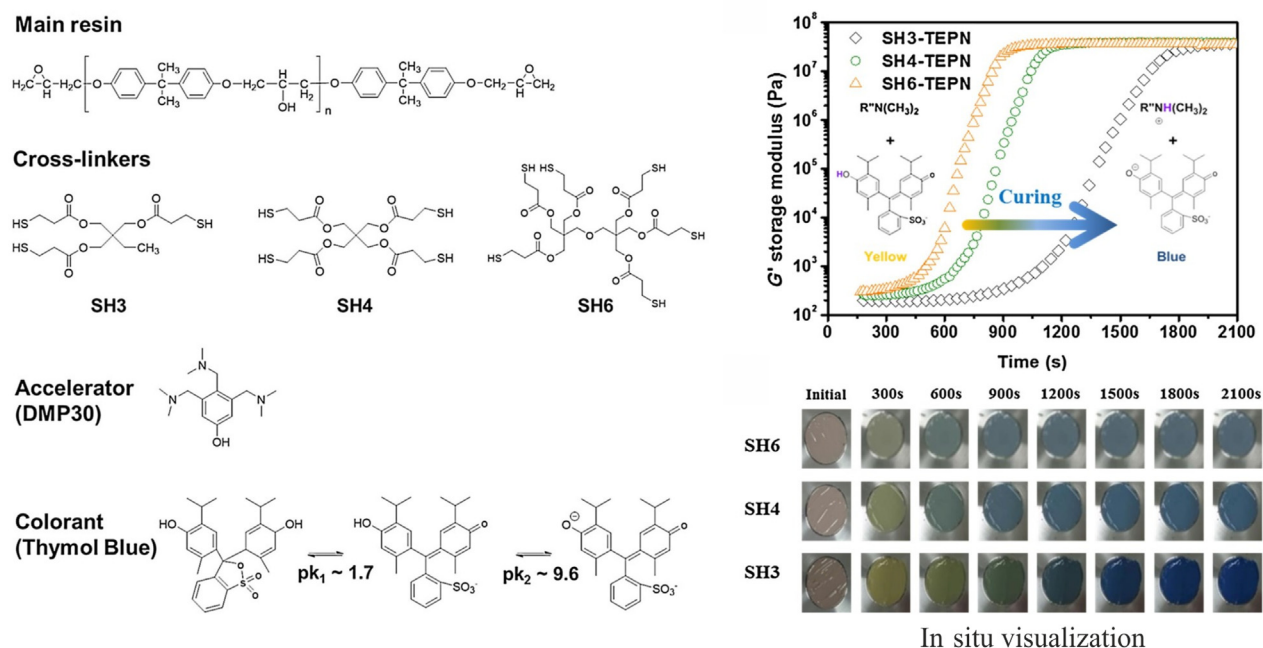


FIGURE 22.18 The curing kinetics of thiol-epoxy in the self-reporting systems. Rheological calibration of curing conversion for in situ visualization of the thiol-epoxy crosslinking reactions [150].

unfavorable damaging event or local segregation phenomena, or by uneven distribution of the microcapsules in the matrix from the beginning. Such difficulties can be avoided by using more complex microcapsule architectures that contain all components necessary for self-healing in separate compartments.

An encapsulation method illustrating this approach, was employed by [151]. Here, TETA amine hardener is packed together with the actual healing prepolymer in a multilayer microcontainer. To this end, in a first step, a double emulsion is produced in a microfluidic glass capillary reactor. This double emulsion consists of an aqueous core phase loaded with aliphatic TETA and an oil shell phase with a reactive acrylate-photoinitiator mixture. This is followed by conversion into microcapsules by the action of UV radiation with UV-induced curing of the reactive shell mixture [151]. Such multilayer particles contain all the necessary self-healing components in separate areas of the particles and upon burst allow the fillings to escape together into the surrounding polymer matrix and heal it. Such strategies are definitely promising for the development of epoxy/amine self-healing concepts also in non-epoxy matrix systems where the matrix may not contribute any catalytic effect to the healing. Analogous strategies for the creation of hierarchically structured microspheres with compartment-structured microsphere architecture are suitable to address the

sometimes serious problems of activity loss of other self-healing chemical systems. For example, this strategy could be suitable for the encapsulation of metal/ligand catalysts for the ring-opening metathesis polymerization (Grubbs' catalyst), or to avoid the deactivation of radical initiators for sunlight-activated crosslinking at low temperatures in the context of thiol-ene chemistry.

Complex containers and design of microcapsule walls

In the following, self-healing systems based on (micro) containers with complex architecture which consist of thermosetting healing reagents and curable resins will be briefly discussed. The rate of release of the reactive component of the microcapsules can be either very fast with complete mechanical destruction of the capsule (instantaneous or break release) or rather slow (controlled delivery or slow release) [152]. In the first case, the self-healing reagents used for high-strength composites are encapsulated in a very mechanically robust envelope. This shell can be (1) a single-layer consisting of urea- or melamine-formaldehyde resins with a high degree of cross-linking, (2) a double-layer containing a poly(urethane)-poly(urea) combination or a (3) hybrid with integrated inorganic nanoparticle monolayer. This ensures the necessary

tightness and resistance to external influences. Such capsules protect, for example, isocyanate [153–155], epoxy acrylate resin [156], epoxy resin–solvent mixtures [157,158], drying oils [59,135] or DCPD [99,159] in a thermoset composite matrix until such a single capsule system is mechanically destroyed, for example, by friction. Compared to instantaneous release upon destruction of the microcapsules, a controlled release strategy allows multiple healing events [160].

The information collected in Table 22.1 suggests that several basic types of composite constructions aiming at an autonomous healing strategy can be identified and schematically assigned to one of the following basic designs (Fig. 22.19). In principle, each basic type of construction design can be implemented for any type of container such as for spherical particles (microcapsules), for vascular systems with nano- or microfibers, and for combinations thereof (mixed systems).

The first type of composite design combines the microencapsulation of only one reactive component, which is usually a liquid oligomer or monomer (system “microcapsule with monomer and nanocapsule of the catalyst”). After release from the capsule, the monomer mixture is polymerized, for instance under the influence of atmospheric oxygen (in the case of drying oils) or humidity (in the case of isocyanates) and self-polymerized in the presence of encapsulated organometallic catalysts distributed in a thermoset matrix (such as ENB, DCPD, or siloxane healants).

The design of the second type follows the double capsule principle. It is applied when both reactive components require effective separation from each other for low-temperature curing. This design is usually used for epoxy monomers with amine or thiol hardeners as well as for azide/alkyne, thiol/isocyanate and thiol/maleimide healing systems. It should be noted that the second type of capsule design also requires the involvement of a catalyst. In this it is similar to the first type of capsule design. In this case, however, the catalyst may already be an integral part of a commercially available curable formulation (e.g., tertiary amine in epoxy resin).

The third type of composite architecture shows the case “all inclusive” or “everything in one capsule.” In this case, the self-healing reagent and the catalyst are isolated from each other by the shell layers of a single multilayer capsule or by smaller capsules integrated in a combined capsule (capsule in capsule) [161,162].

In the second case (the capsule in capsule approach) we are dealing with semipermeable capsule walls of the membrane type. By introducing, for example, ethyl cellulose additives into the wall material of the microcapsule, the release of the liquid reactant can be controlled by specific design of the micro- and nanoporosity [152]. The variation in the concentration and molecular properties of ethyl cellulose effectively affects the size of the microcapsules, their morphology, surface properties, and the speed of reagent passage through the cellulose membrane [152]. In contrast to microcapsules with crack release,

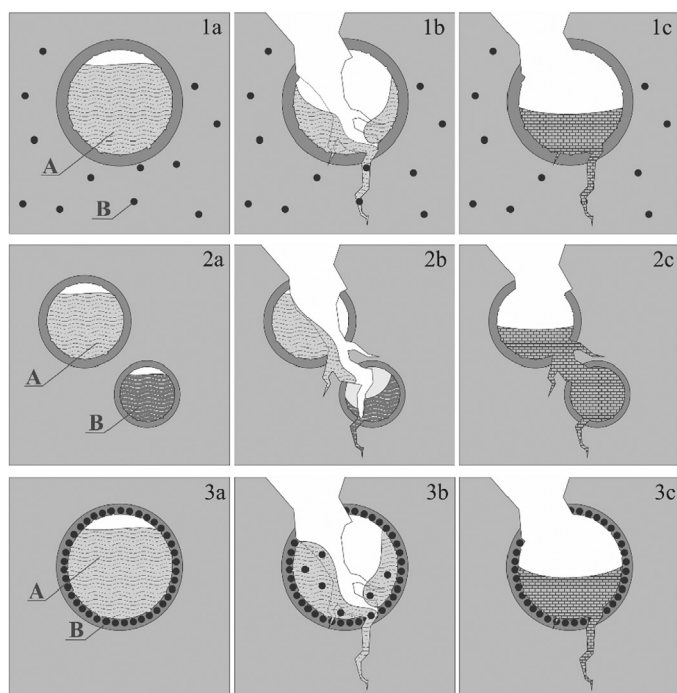


FIGURE 22.19 Self-healing approach based on rupture-release microcapsules: (1) monocapsule or capsule-catalyst systems; (2) dual-capsule system; (3) all-in-one capsule system.

microcapsules with controlled-release properties retain their ability to act as reactive component donors over a longer period of time. This means they are capable of several successive healing processes. This is a major advantage over systems based on the destruction of the microcontainers. The development of controlled-release microcapsules has been a very lively and productive field of research in recent years. Fig. 22.20 schematically summarizes some particle shell architectures developed for this with the potential for controlled and multiple release in thermosetting matrix systems

Multiple self-healing performance in a capsule-based approach can also be achieved by controlled release of healing agent from multicore microcapsules, as well as hierarchical microcapsules. The presence of multistorage cells inside or outside the carrier microcapsules enables repeatable self-healing according to mechanical or electrochemical testing respectively [167,168]. The design of hierarchical microcapsule with multistorage cells (HMMC) includes a central microcapsule made, for instance, of a robust poly(thiol-isocyanate) P(TMMP-IPDI) shell with DCPD as the healing agent, which is tightly packed with an additional portion of active DCPD

(Fig. 22.20K). The outer-layer capsules were obtained using a specially synthesized copolymer dispersion stabilizer based on divinylbenzene and 1,1-diphenylethylene-capped hydrolyzed poly(glycidyl methacrylate). In water such a copolymer covers DCPD microdrops with nonpolar fragments, resulting in a core-shell system which is covalently fixed through radical polymerization. The scratch repair of anticorrosion polyurethane coating containing 15 wt.% HMMC and Grubbs' catalyst was demonstrated by EIS and anticorrosion tests. The protective layer on the iron substrate was completely regenerated after the first damage when the maximum amount of DCPD was easily released from the central cell. After the second and third repetitive damage in the same spot, the outer-layer of the small capsules still supports healing if sufficient amount of the catalyst is present at the crack interface. It should be noted that such capsule systems exhibit a positive effect on the mechanical properties of the PU coating: the peak stress increased by two times (from 3 to 6 MPa) after adding 15% HMMCs in coating [167]. They not only act as self-healing additives but also as reinforcements.

The HE of the multicore capsules was even further extended, namely up to four cycles with an efficiency of

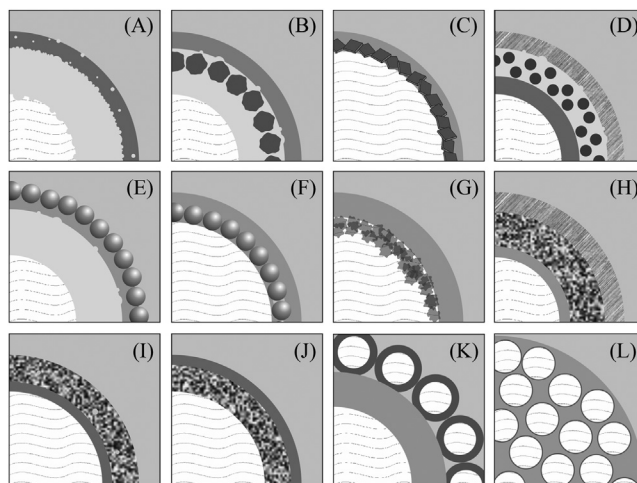


FIGURE 22.20 Capsule design for extrinsic self-healing approach: (A) multilayer wall microcapsules and double-shelled microcapsules: HDI-core/double-layered polyurea microcapsule [153], IPDI-core/polyurea/PVA [163]; double-shelled microcapsules: isophorone diisocyanate (IPDI) core and a polyurethane (PU)/poly(urea-formaldehyde) (PUF) double shell [154]; (B) Multilayer composite microcapsules: healing reagent (isophorone diisocyanate, IPDI)/hybrid shell: urethane-lignin barrier/MF-shell [93]; (C) with nanoclay layer: amine core/nanoclay layer/PU-shell [147]; IPDI-core/NaLS (sodium lignosulfonate capsule)/polyurea hybrid shell [75]; DCPD core/nanoclay-PUF shell [159]; (D) double stimuli-responsive microcapsule: linseed oil/PUF shell/PEI/benzotriazole in PSS/PEI [40]; multilayer microreactor: GMA-core/PMF shell/catalyst CuBr/PMDETA in the layer of ATRP-Macroinitiator PMMA-Br/paraffin wax [161] (E) with multilayered shell structure: DCPD core/PU inner layer/PF outer-layer/PGMA layer (spheres) in PU coatings [99]; IPDI-core/PPG-TDI-SiO₂ NP [164]; (F) Photoabsorbing Hybrid Microcapsules: photosensitive epoxy acrylate resin (core)/poly(urea-formaldehyde) PUF/TiO₂ (organic-inorganic hybrid shell) [156,165], [27]; Linseed Oil core/SiO₂-Poly(urea-formaldehyde) Hybrid shell [59,135]; (G) Sunlight-activated microcapsules: epoxy acrylate core/carbon black particles/PUF shell [17]; (H) Graphene oxide (GO) modified double-walled microcapsules: 1, 6-Diaminohexane (inner core) and isophorone diisocyanate (IPDI)-based prepolymer (outer core)/GO-modified double-walled polyurea shell [155]; (I, J) core (commercially available polyurethane precursor)/epoxy coating/cementitious shell; polyurethane precursor core/cementitious shell/epoxy coating [166]; (L) multiple release: hierarchical multiple healing capsule-based system (healing agent (DCPD)/shell poly(thiol-isocyanate) P(TMMP-IPDI)/DCPD) [167]; (K) multiple release: a multicore capsule epoxy core/alginate and a multicore capsule mercaptan hardener core (pentaerythritol tetra(3-mercaptopropionate))/alginate [168]. HDI, Hexamethylene diisocyanate; PVA, polyvinyl alcohol; GMA, glycidyl methacrylate.

70%–90% according to mechanical testing [168]. The dual-capsule healing system consisted of (1) epoxy resin (diglycidyl ether of bisphenol A) encapsulated as discrete portions in alginate and (2) mercaptane hardener mixed with catalyst, a tertiary amine, which were encapsulated in alginate matrix by electrospray technique. Large multi-core microcapsules of 300–400 μm diameter with 74% core content for epoxy microcapsules and 59% core content for the hardener microcapsules were embedded in the epoxy composite Epikote 828 and tested for healing ability. After the first damage, the HE was achieved about 90% through a nucleophilic ring-opening reaction with the epoxide groups. The following three damage-healing cycles were characterized by some reduction of efficiency to about 70% at a capsule loading of 20 wt.%. A high efficiency of multiple healing processes of an epoxy composite can be achieved for the capsule-catalyst healing system containing alginate-epoxy microcapsules and catalyst Scandium (III) Triflate ($\text{Sc}(\text{OTf})_3$), if the catalyst is reliably protected against moisture. Further variations in capsule design are summarized in Table 22.2.

The development of new target designs for the healing microcapsules is followed by optimization of their size and concentration in composite matrixes. Usually, larger capsules with maximum healant filling are preferred because more healing material is released per unit of crack area [102]. The study notes that HE improves proportionally with increasing capsule size and yields a 68% maximum load recovery. However, the use of the largest capsules significantly reduces the mechanical performance of the thermosetting composite, and determining the optimal capsule size from a mechanical viewpoint requires additional testing. Some authors have solved the problem of mechanical strength by adding ceramic or carbon nanotubes to capsules with maximum size. Thus, the micro-co-encapsulation of multiwalled carbon nanotubes with liquid healant (5-ethylidene-2-norbornene) into poly(melamine-urea-formaldehyde) shells (MUF-CNT/5E2N microcapsules) was found to have significant effect on both the mechanical and the electrical properties of healed epoxy composites (Fig. 22.21), thus making them highly suitable for applications in aerospace [74].

The optimization of microspheres quality (volume for internal filling, monodispersity, morphology, and wall thickness) depending on the synthesis conditions is extremely time-consuming and does not always result in an effective solution. A statistical experimental design approach (DoE) was used to optimize the synthetic parameters and obtain optimal characteristics of microcapsules [169,170]. The potential of encapsulated healants for microcracks recovery in self-healing thermosetting composite is reviewed in some publications [4–6,12–14,25,33,104,171,172].

Microvascular strategies

The second basic possibility to realize the extrinsic approach to incorporate self-healing properties into thermoset matrix systems is the integration of microvascular structures. In this case, microcapsules are not used to store the healing liquid, which are subsequently added to the basic thermoset during formulation. Instead, during the production of the thermoset material, channel systems are built into the matrix of the bulk structure, which are filled with the self-healing liquid. These microchannel systems are modeled on natural vein systems and run through the entire thermoset structure. They are designed to avoid the spatial restrictions to which capsule systems are subjected. Vascular systems are not based on the addition of standard thermoplastic materials but use special manufacturing processes (increasingly based on additive manufacturing technologies) to create 3D hollow channel systems that are filled with healing fluid within the thermoset matrix. A detailed and critical presentation of different strategies for the design and fabrication of vascular structures was recently presented by [77]. In this paper, the emerging technologies based on 3D printing and additive manufacturing are briefly presented and their advantages and disadvantages are discussed.

In the following, some examples are briefly described, which show how 3D hollow channel structures can be designed and produced to enable vascular self-healing in thermosetting polymer matrix systems.

One of the classical concepts of vascular self-healing is the incorporation of filled hollow fibers into the thermoset matrix. This approach is closely related to the addition of polymers with micro hollow spheres, except that one-dimensional (fibrous) filler materials are used instead of zero-dimensional (spherical) fillers. The most suitable fibers for this purpose are hollow glass fibers. Hollow glass fibers can be loaded with self-healing liquid by using capillary phenomena and vacuum. For example, glass fibers with an inner diameter of 5 μm were loaded with healing fluid and incorporated into composite materials [211]. Glass fibers loaded with healing fluid can be incorporated into fiber composites together with carbon fibers or standard glass fibers as reinforcing fibers and processed according to standard procedures. If two-component systems are used as healing reagents, two differently loaded hollow fiber types must be used. If care is taken during fiber insertion to ensure that both fiber types can be introduced into the matrix system in appropriate proportions and suitable (random) orientation, a vascular self-healing fiber composite can be obtained. Textile glass fiber structures (fiber mats with defined 3D architecture) are also conceivable on the basis of filled hollow fibers. The use of multilayers of reinforcing and self-healing glass fiber structures leads to composite materials with

TABLE 22.2 Self-healing performance of thermosetting composites with encapsulated healing systems.

Microcapsules (MCs)			Performance/comments	Reference
Core: healing agent/loading capacity, wt. %	Shell/preparation	Size, μm /concentration (wt. %) for the best performance in matrix	HE, %/Tests/comments	
Single (component) capsule healant system				
DGEBA-epoxy resin diluted with a ethyl phenylacetate (25 wt.%)	PUF/in situ polymerization; a shell thickness was varied by concentrations of reagents, stirrer speed and sonication	4–180 μm /carbon fiber composite laminate	Healed/mode-I interlaminar fracture test	[157]
Epoxy in ethylphenylacetate (EPA at 5 wt. %)/54 (S1) - 74 (S5)%	PUF/in situ polymerization	410 (S1) - 64 (S5) μm /20 wt.% of MCs in epoxy matrix: epoxy resin cured with cyclo-aliphatic amines (100:50); 3 wt.% of Al(OTf) ₃ catalyst	Enhanced HE (68%), but reduced mechanical performance (18%) for the larger capsules (TDCT-fracture test in tensile)	[102]
Epoxy resin (EPL 1012R)/54%	PUF/in situ polymerization	2.13 μm /10 wt.% of microcapsules in the epoxy coating	Excellent corrosion resistance in scratched coatings/salt fog corrosion test, electrochemical detection (48 h)	[191]
Epoxy resin E-51	PUF/in situ polymerization	55.7 μm /2% in the epoxy resin composite coating	Recovery of corrosion resistance; the corrosion resistance was best with its service life prolonged by about 4 time	[158]
Epoxy resin (multicore)/79%	Alginate microcapsules (pore size of 5 – 100 μm)/electrospraying method	320 μm /20 wt.% of MCs in the epoxy matrix with diethylenetriamine DETA	HE of 86%, 3-time in situ healing with DETA/Impact test; HE of 76%, one-time healing/TDCB-fracture test	[198]
Mixture of epoxy resins: cationic photoinitiator (100:9)/87%	SiO ₂ shell/a combined interfacial and in situ polymerization	20–30 μm /the self-healing coating of epoxy resin: amine hardener: MCs with a mass ratio of 5:2:3	High self-healing performance for scratches in the epoxy matrix (SEM)	[173]
Epoxy silicon oil with cationic photoinitiator/25%–29%	Inner polyacrylate-based shell/outer pure TiO ₂ -NP (50 nm) shell (by UV-initiated polymerization of Pickering emulsions)	4 μm /50–60 wt.% of UV-responsive microcapsules in the silicone resin coating (12 μm)	Anti-aging stability/confirmed by SEM after crack formation and accelerated weathering treatment (216 h); potential application in aerospace coatings	[27]
Epoxy ester based on tall oil fatty acid/67%	PUF/in situ polymerization	101 μm /10 wt.% of MCs in the epoxy coating	Sufficient corrosion resistance recovery after 14 days/Salt spray test, SEM, EIS	[179]
Palm oil-based alkyd/90%–95%	PMUF/in situ polymerization	300–500 μm /1%–6% of MCs in the epoxy matrix	Sufficient recovery of mechanical and surface properties	[178]
Tung oil/80%	PUF/in situ polymerization	105 μm /10 wt.% of MCs in epoxy coatings	Recovery of corrosion resistance/salt-immersed corrosion test	[57]
Linseed oil	Multishell: PUF shell (in situ polymerization)/PEI/benzotriazole in PSS/PEI (layer-by-layer assembly)	2 μm /ca. 5 wt.% of MCs in epoxy coatings	Recovery of active corrosion protection due to the stimuli-responsive release of healant/EIS	[40]
Linseed oil/69% (1100 rpm) –77% (700 rpm)	PUF/in situ polymerization	116 μm (700 rpm), 53 μm (900 rpm) and 28 μm (1100 rpm)/5–10 wt.% of MCs the epoxy coating	Recovered corrosion resistance of the scratched coatings/salt spray test after 6 days: the bigger MCs and the higher their concentration result in an improved corrosion resistance	[91,177]

Linseed oil/74%	PU-shell/interfacial polymerization	65 μm /15–20 wt.% of MCs in epoxy coatings	Recovery of corrosion resistance/EIS and salt spray tests	[58]
Coconut oil-based alkyd resin/55%	PMUF/in situ polymerization	1 – 8 μm /10% of MCs in the epoxy coating	Recovery of corrosion resistance in 5 wt.% NaCl solution for 7 days/potentiodynamic polarization and EIS/The effect of the MCs incorporation on the gloss, adhesive strength and mechanical properties of the coating has been studied for commercial viability: increased MCs concentration reduces these properties of the coatings	[88]
IPDI/81%	Multilayer: MF-lignin-shell thickness of 4.5 μm / Pickering emulsion templates by in situ and interfacial polymerization	From 40 μm (1.0 wt.% lignin) to 117 μm (0.01 wt.% lignin)/a mass ratio of epoxy:hardener:MCs is 100:25:15	Recovered corrosion resistance/brine-submersion corrosion-accelerating test (10 wt.% NaCl for 120 h), EIS	[93]
IPDI	Tris (p-isocyanatophenyl) thiophosphate as a shell forming agent/via emulsification followed by interfacial polymerization	5 – 20 μm /epoxy coatings	Recovery of barrier properties of modified coatings (EIS)/Recovery of corrosion resistance (LEIS, SVET, SIET)	[98]
IPDI	Polythiourethane shells: (a) 3,6-dioxa-1,8-octanedithiol (DODT), (b) trimethylolpropane tris(3-mercaptopropionate) (TTMP), (c) pentaerythritol tetrakis(3-mercaptopropionate) (PETMP)/interfacial polymerization	18 and 30 parts by weight per 100 parts of the epoxy matrix (improved adhesion between MCs and epoxy matrix due to reaction of thiourethane shell with epoxy ring)	Recovery of mechanical and surface properties/ three-point bending test and scratch test (after 24 h); Effect of shell wall structure on self-healing efficiency: epoxy composites with embedded IPDI-PETMP/18 MCs have the best self-healing efficiency and virgin mechanical properties	[182]
Dicyclopentadiene, DCPD/72%–75%	PU/PF/PGMA-NP multishell/interfacial polymerization, in situ polymerization and self-assembly (Pickering emulsions template)	80 (S1) -130 (S5) μm /PU- coatings with 15:2.5 parts of MC: Grubbs' catalyst	Recovery of corrosion resistance and mechanical performance/SEM, EIS, TDCB-fracture analysis (118%)	[99]
Dicyclopentadiene, DCPD/72%	PUF/in situ polymerization	250 μm /15 vol.% of MCs in epoxy matrix containing a Grubbs catalyst (HG1)	Three-point bending tests: flexural strength of 81% for the healed PUF-DCPD-epoxy resins	[184]
5-ethylidene-2-norbornene, ENB/74%	MUF/in situ polymerization	100 μm /10 vol.% of MCs in epoxy matrix containing a Grubbs catalyst (HG1)	Three-point bending tests: flexural strength of 77% for the healed MUF-ENB -epoxy resins	[184]
5-ethylidene-2-norbornene (5E2N) with CNTs additives	PMUF shells/in situ polymerization	70 μm /10 wt.% of MCs in epoxy matrix with 1 wt.% Hoveyda-Grubbs (HG2) catalyst	ca. 80% of the fracture toughness after complete failure, 82% of the electrical conductivity; highly suitable for aerospace applications	[74]
Healing mixture: triethylene glycol dimethacrylate (TEGDMA) and N,N-dihydroxyethyl-p-toluidine (DHEPT)/70%	PUF/in situ polymerization	70 \pm 24 μm /10 – 20 wt.% of MCs in the dental BisGMA-TEGDMA resins	A self-healing efficiency of 65% (fracture toughness tests); the fibroblast viability was similar for all dental resins	[180]
Multimaleimide (1,6'-bismaleimido-2,2,4-trimethylhexane) dissolved in phenyl acetate/88%	PUR/in situ emulsion polymerization	100–185 μm /10 wt.% of MCs in a furan-functionalized epoxy-amine thermoset	Load recovery of 71%/fracture test	[181]
Tripropargylpentaerythritol synthesized from pentaerythritol and propargyl bromide/78%	PUR/in situ condensation	50 μm /9% of MCs in the epoxy-amine matrix containing azide	A 60%–65% recovering of the mechanical properties of the epoxy composite (healing at 80°C–140°C for 120 h)/fracture toughness test	[207]

(Continued)

TABLE 22.2 (Continued)

Microcapsules (MCs)			Performance/comments	Reference
Core: healing agent/loading capacity, wt.%	Shell/preparation	Size, μm /concentration (wt.%) for the best performance in matrix	HE, %/Tests/comments	
		functionalized carbon nanotubes (MWCNT-t-BA-N ₃) and CuBr(PPh ₃) ₃		
Dual (component) capsule healant system				
MCs A: epoxy resin (multicore)/74%; MCs B: mercaptan/tertiary amine hardener (multicore)/59%	Alginate microcapsules/electrospraying method	300–400 μm /20 wt.% of MCs in the epoxy matrix	HE of 68%–85%, 4-time healing/Charpy impact test	[168]
MCs A: DGEBA-epoxy resin/96.7%; MCs B: curing agent- catalyst mixture/93.1%: pentaerythritol tetrakis(3-mercaptopropionate) (PETMP)/92.5% and 2,4,6-Tris (dimethylaminomethyl)phenol/ 0.6%	MF/in situ polymerization	Type A: 110 μm ; 136 μm ; Type B: 65 μm ; 66 μm /5.3%wt./wt. of MCs (MC1:MC2 = 1:1) in the three interlayers of carbon fiber/epoxy (CF/EP) laminates	Type A: 80% (Mode-I interlaminar fracture) and 51%–63% of healing efficiencies (Mode-II interlaminar fracture toughness testing); Type B: 57% of maximum healing efficiencies (Mode-I interlaminar fracture)	[196,200]
MCs A: an epoxy monomer diluted with n-butyl glycidyl ether; MCs B: a modified aliphatic polyamine	MCs A: PUF/in situ polymerization method; MCs B: PUF/polycondensation; vacuum infiltration of polyamine (EPIKURE 3274) into hollow MCs	113–117 μm /7 wt.% amine capsules and 10.5 wt.% epoxy capsules in epoxy matrix; a ratio of epoxy:amine capsules was 6:4	The highest HE of 91% (TDCB-fracture test); up to 6 months of healing with a 68% HE (ambient aging studies)	[188]
MCs A: epoxy resin DGEBA/54%; MCs B: triethylenetetramine hardener/22%	PMMA shells/solvent evaporation technique	(37–32) \pm 5 μm /10% of MCs in the epoxy adhesive matrix	89% of self-healing efficiency/fracture testing	[192]
MCs A: mixture of epoxy resin and n-butyl glycidyl ether/90.42%; MCs B: Underwater amine-based hardener/78.67%	MCs A: PUF (5.5 μm)/in situ emulsion polymerization; MCs B: PMMA (2.5 μm)/ solvent evaporation technique	200 μm /8% MCs A and 70 μm /4% MCs B in epoxy coatings for marine	Recovery of corrosion resistance (corrosion tests)/ the underwater self-healing coatings with antibiofouling functions due to zwitterionic surface modifier	[39]
MCs A: epoxy/7.5% of pure epoxy fraction in 39 wt.% of core; MCs B: polyamine/16% of pure polyamine fraction in 44 wt.% of core	Carbon hollow spheres/a silica templating method: carbonization of polysaccharide shells formed on the surface of silica templates/a solvent evaporation method for encapsulation of the epoxy or polyamine	0.24 μm /10% of epoxy and 5% of polyamine MCs in the epoxy nanocomposite coatings	Recovery of corrosion resistance at RT (24°C–36°C)/salt spray (5% NaCl), EIS (3.5% NaCl) and SVET (0.3% NaCl) tests	[49]
MCs A: TetraThiol (methyl benzoate diluent)/75%–85%; MCs B: a low toxic isocyanate (HDI 3, trimer)/70%	MF walled Tetrathiol-MC/an interfacial polycondensation; PUR walled HDI3-MC/ interfacial polymerization	150 μm /20% in the epoxy matrix EPIKOTE 828	A mechanical recovery of 54% is reached at RT after 5 days/TDCB- fracture tests	[142]
MCs A: silanol-terminated polydimethylsiloxane/71%, MCs B: catalyst dibutyltin dilaurate in a chlorobenzene/18% and 67%	PUF/in situ polymerization; PU/interfacial polymerization methods	240 μm and 90 μm /the mass ratio of MCs A: MCs B: commercial enamel paint is 18:7:5	Recovery of corrosion resistance/corrosion, electrochemical, and saline solution permeability tests (25% NaCl, 48 h)	[210]

Notes: The microcapsule shells: PUR, polyurea; PU, polyurethane; MF, melamine–formaldehyde; PMUF, poly(melamine-urea-formaldehyde); PUF, poly(urea-formaldehyde); PMMA, poly(methyl methacrylate).

Electron microscopy of microcapsules and carbon nanotubes and size-distribution histogram of microcapsules

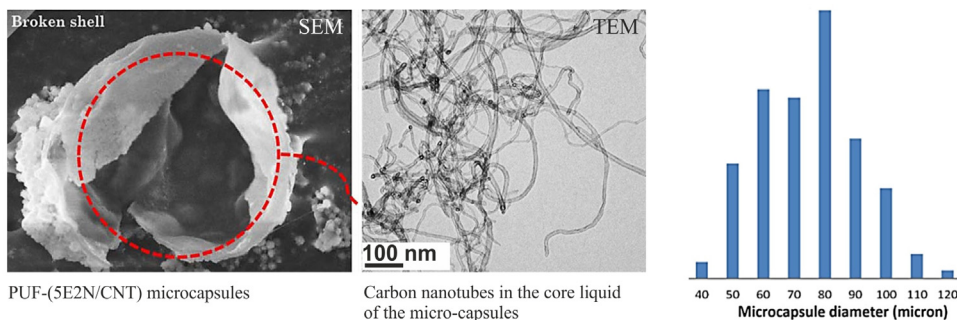
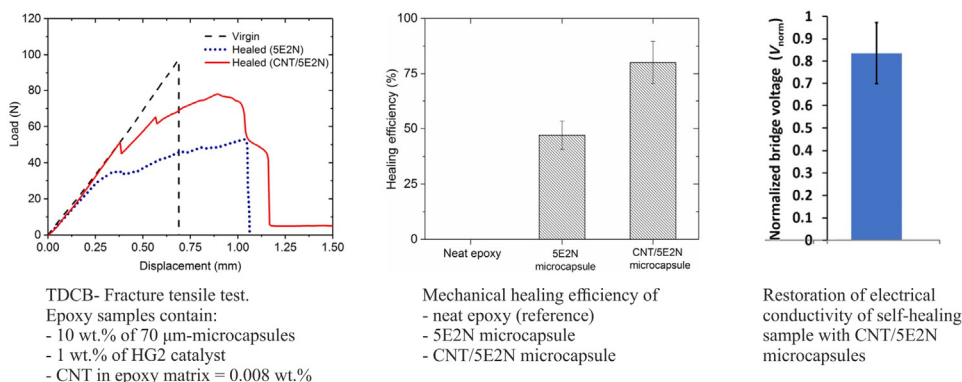


FIGURE 22.21 Electron microscopy of PUF-(5E2N/CNT) microcapsule (SEM image) and CNTs in the core liquid of the microcapsules (TEM image). Size-distribution histogram for microcapsules. Mechanical HE (up to 80% of the fracture toughness) using the TDCB-load-displacement curves in mode-I fracture test and the efficiency of electrical conductivity restoration (82%) of the epoxy matrix modified with PUF-(5E2N/CNT) microcapsules [74]. PUF, Poly(urea-formaldehyde); TDCB, tapered double-cantilever beam. Modified after Zamal HH, Barba D, Ai'ssa B, Haddad E, Rosei F. Recovery of electro-mechanical properties inside self-healing composites through microencapsulation of carbon nanotubes. *Sci Rep* 2020;10:2973. Available from: <https://doi.org/10.1038/s41598-020-59725-6>.

Mechanical healing efficiency and the restoration of electrical conductivity of the self-healing epoxy



self-healing properties across the cross-section of the composite material. As with microcapsule systems, the prerequisite is that the fibers do not break during processing and pour their contents into the thermoset matrix. Particularly in the case of hot-pressing processes, attention must be paid to the suitability of this process compared to, for instance, resin injection or resin transfer molding processes.

Another approach to vascular self-healing in composite materials was realized on a scale of millimeters by using sandwich structures based on polyvinyl chloride [212–214]. Here, the vascular systems were realized by drilled vertical channels and horizontally embedded commercial PVC tubing in a PVC foam core. This foam core was surface bonded on both sides with a glass fiber-reinforced epoxy laminate. The pipe system was connected to an external reservoir through which the tubular system could be supplied with self-healing fluid. Analogous systems were also realized on the basis of polyurethane foam cores [215].

In addition to embedding tubular hollow systems in polymer matrix systems, cavities can also be created directly in the bulk thermoset. For this purpose, a sacrificial material must be used which, during the production of the bulk thermoset structure, occupies the space that is

to be converted into a cavity later and which is subsequently removed. A possible way to do this is to use decomposable or easily removable inks, which are deposited in a defined, 3D pattern to form a 3D network. If this print pattern is infiltrated with a thermoset material, cured, and then the ink is removed, a defined cavity system remains within the cured thermoset matrix. This in turn can be filled with self-healing liquid. Typically, waxes can be used to produce such scaffolds. The production of such connected cavity systems is readily accomplished with direct write assembly [216,217] or direct ink writing (DIW) process [218,219]. Toohey et al. [220,221] for example, developed “interpenetrating networks” for the production of vascular-extrinsically curable epoxy coating systems. They can also be used to produce thermoset structures that can be cured in bulk [218]. One problem of wax-based inks, however, is their insufficient mechanical strength. For example, such cavity structures cannot be pressed nondestructively, so that this technique is not suitable for the production of composite materials. The creation of cavities by pressing the composite together with inserted silicone tubes [222,223] or tubes based on polytetrafluoroethylene [224–226], which are then removed from the composite, can partially solve this problem. More recent approaches to create fiber-

reinforced composites with vascular self-healing properties use polylactic acid (PLA)-based fiber structures as sacrificial material for the creation of the 3D scaffold. For this purpose the PLA fibers are treated with tin oxide. Tin oxide catalyzes the thermal decomposition of PLA and allows the removal of this template later by applying temperatures of ca. 200°C. The PLA fibers can be processed together with glass fibers or carbon fibers to a textile fiber fabric and then impregnated with epoxy resin or another thermoset. After decomposition and volatilization of the PLA template, a fiber-reinforced composite material with a defined hollow structure is obtained. The cavity can then be filled with self-healing liquid accordingly. Since a connection to an external source is possible, used self-healing fluid can, in principle, always be refilled.

However, when designing a composite material comprising both a self-healing extrinsic vascular network system and reinforcing fibers, the self-healing effects have to be carefully balanced versus the achievable matrix reinforcement. The introduction of vascular structures into a thermoset matrix by additive manufacturing leads to an anisotropic material structure. This results in inherent mechanical weaknesses of the resulting material compared to materials produced by classical methods. In order to avoid these intrinsic weaknesses, new materials are required or the available materials must be further adapted and optimized. In addition, the structural integration of the self-healing network into the matrix thermoset needs to be considered also in relation to the amount of reinforcing fibers present in the composite. A thermosetting matrix cannot be loaded with fibers to arbitrarily high filling levels. The self-healing network system acts as a filler in direct competition with the reinforcing fibers. A compromise must be found between the relative proportions of the two integrated network systems. Numerical methods for material optimization are used here to realize the optimal material design accordingly.

The current manufacturing processes for creating and building vascular structures for extrinsic self-healing mainly include variants of additive manufacturing/3D printing technologies and can be summarized as follows.

(1) Processes with an easily removable sacrificial template. A template material is used to build a defined 3D structure. The sacrificial template is destroyed after the material is manufactured, leaving the desired cavity. The following processes are available: extrusion-based printing, DIW, direct laser writing.

(2) Processes with which free-standing cavity structures are directly accessible. In these processes, no sacrificial material is used, but the desired 3D structure is realized directly with a material that is still present in the finished part. These processes mainly include stereolithographic processes and inkjet printing processes. Extrusion-based printing processes also make such materials accessible.

A major problem in the design and creation of vascular 3D hollow structures for self-healing applications is the optimization of mass transport through the channels of the hollow channel network. The flow properties of the self-healing fluid through the vascular network must be guaranteed. A special challenge in current 3D printing processes is the realization of network branching points. Here there is still a need for optimization of the manufacturing process to avoid problems in interconnectivity across different network layers. A difficulty is related to the fact that the reproduction of programmed 3D structures in the manufacturing process is sometimes still inadequate. The accuracy of transferring the structures planned in the computer to the structures actually manufactured is of great importance, especially considering the pipe diameters (flow behavior), wall thicknesses (stability against nondamage), and precision of the branches (clogging of pipes), and is currently still often a challenge for the process used.

Due to the rapid developments in 3D printing and additive manufacturing in recent years, the possibilities for realizing even very complex structures have increased rapidly. Natural vascular systems of living beings (water supply of trees by capillary action, vascular systems of animals through which blood flows) serve as a model for the development and optimization of such systems. Aspects of fluid mechanics (mixing effects, distribution, flow velocities) play an extremely important role in these developments. Due to the continuously improved spatial resolution of 3D printing processes, tube systems can be realized in ever smaller dimensions. Due to this reduction in scale, phenomena in the field of microfluidics in particular are becoming increasingly important in the optimization of architectures, but also in the development of corresponding materials (optimization of interfacial energy or wetting behavior). Limitations in the possible 3D structures result mainly from the resolving power of the printable structures. Another important aspect is the economy of the manufacturing process. It must be ensured that the chosen manufacturing process also allows access to large quantities of the desired textures/materials. Scalability is currently still a major challenge, materials with vascular self-healing properties are generally relatively expensive to produce. Moreover, many 3D printing systems are not capable of producing very large components. This automatically limits the ability to produce only parts with self-healing properties that do not exceed certain dimensions specified by the 3D printing system.

Some important aspects and problems to be solved in the design of vascular structures are discussed in [77]. According to the authors, the major challenges in the design and manufacturing of self-healing vascular networks can be summarized and visualized in Fig. 22.22.

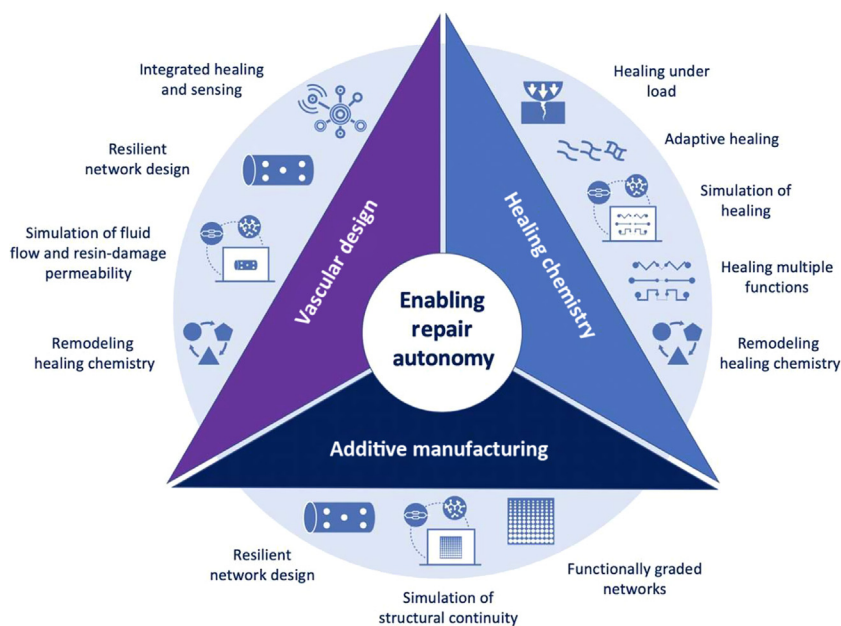


FIGURE 22.22 Challenges in design and manufacture of self-healing vascular network structures [77]. Reproduced from Qamar IPS, Sottos NR, Trask RS. *Grand challenges in the design and manufacture of vascular self-healing*. *Smart Mater Struct* 2020;3(1):13001. Available from: <https://doi.org/10.1088/2399-7532/ab69e2>.

Intrinsic self-healing of thermoset systems: the “chemical design” approach

Covalent reaction mechanisms

As an alternative to extrinsic self-healing approaches, an intrinsic strategy can also be pursued. In this strategy, a reversibly crosslinkable functionality is incorporated into the polymer, which gives the polymer the ability to self-repair. A variety of different chemical functionalities are in principle capable of forming reversible bridges and are thus available for the design of modified thermosetting resins. The selected chemical functionalities should react quickly, reliably, and as completely as possible to form reversible bridges. Chemical reactions that exhibit these desired properties are mainly found under the category of so-called click chemistry [227]. This generally refers to reactions that take place with high yields and practically no side reactions. They are very widely applicable and easy to carry out. The following reaction types are particularly common for intrinsic self-healing processes [6]:

- Cycloaddition reactions, especially of the DA type
- Thiol-sulfide exchange reactions
- Thiol-ene reactions
- Alkyne-azide click chemistry
- Transesterification

The schematic reaction equations for these self-healing mechanisms are summarized in the following figures (Fig. 22.23).

These reaction mechanisms have been applied to a variety of thermoset resin systems. In the following some examples will be briefly presented for illustration.

Noncovalent network formation

In addition to the use of reversible covalent bonds, secondary interactions can also be utilized to design polymers with intrinsic self-healing properties. For example, additional bridges can be formed via coordinative bonds, which help to restore the mechanical strength of a damaged thermoset matrix. For example, in polyurethanes with DA functionalities that were intrinsically self-healing, pyridine units incorporated into the polymer backbone were able to form coordinative bonds with Fe^{3+} ions [82]. These coordinative bonds make an additional contribution to the strength of the material. The mechanical strength can be varied according to the ratio between the number of DA and coordinate bonds present in the polymer. Since the interactions between Fe^{3+} /pyridine are weaker than covalent bonds they are first to be cleaved when exposed to mechanical stress. They therefore have the role of sacrificial bonds. The 3D shape of the material is stabilized by the DA bonds. The regeneration of the coordinative bonds and thus the restoration of mechanical strength can be achieved by treatment with an iron salt solution [82].

Although self-healing is primarily caused by a covalent mechanism, it is often supported by supramolecular interactions based on H-bridges [47,228]. A large number of scientific papers describe the formation of hydrogen bonds as additional reversible and noncovalent cross-linking sites between polymer segments in the context of intrinsic self-healing effects. For example, in aliphatic polyketones that were modified with furan and combined with bis-maleimide in order to exhibit self-healing properties according to the DA reaction mechanism, hydrogen bridges have been described as a significant additional driving force responsible

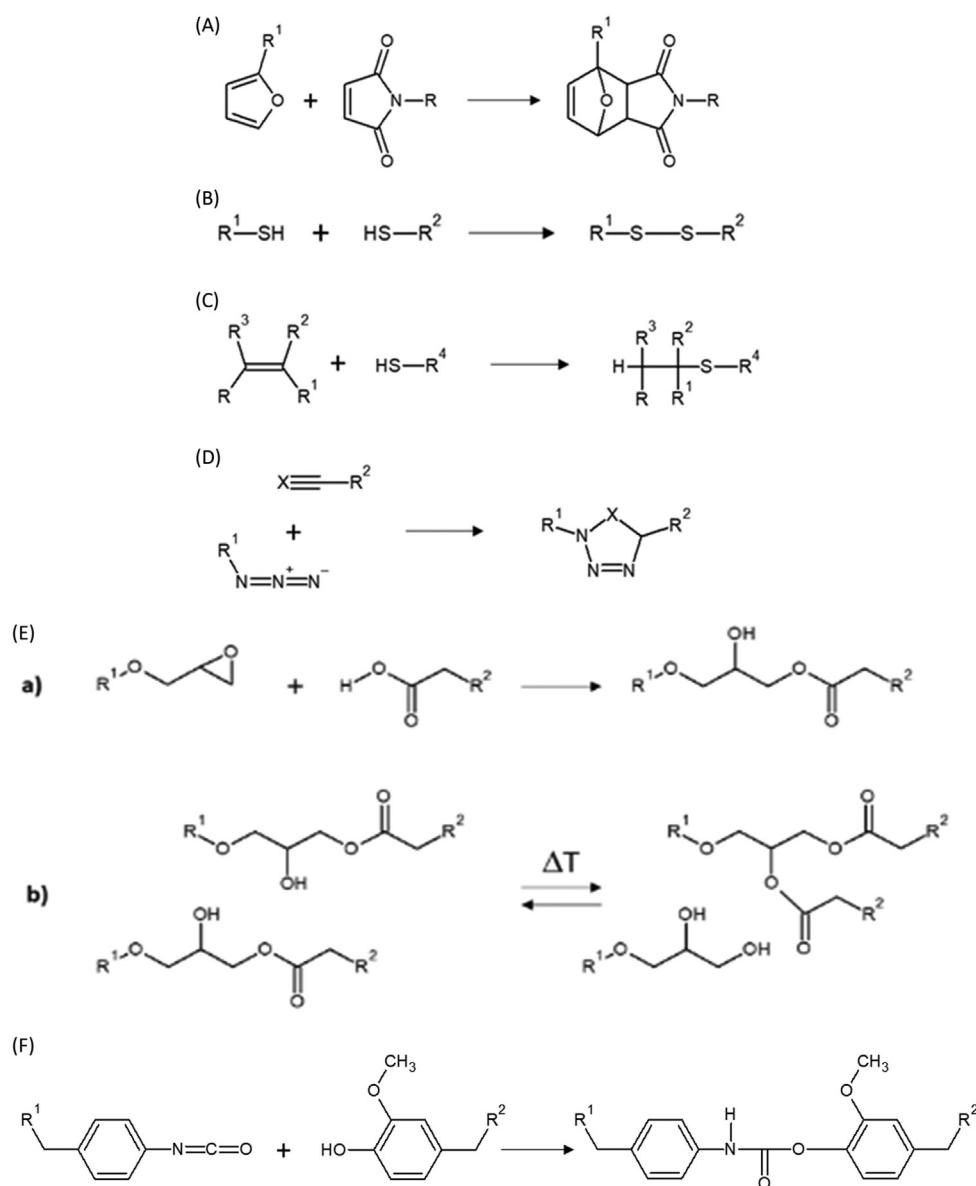


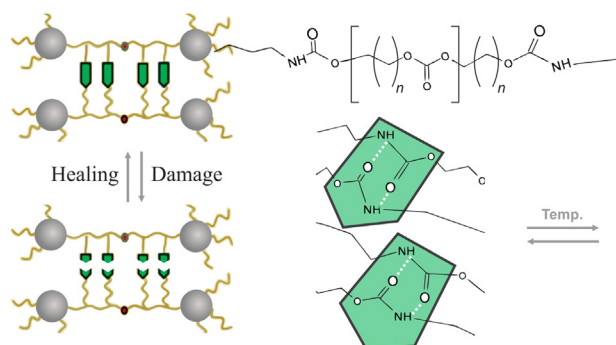
FIGURE 22.23 (A) Diels–Alder (DA) cycloaddition self-healing mechanism. (B) Thiol/disulfide exchange self-healing mechanism. (C) Thiol/ene addition self-healing mechanism. (D) Azide/alkyne click chemistry self-healing mechanism. (E) Transesterification self-healing mechanism. (F) Self-healing by reversible formation of urethane bonds.

for restoring the original material properties [113,117]. Similar contributions of H-bridges to intrinsic self-healing properties have been described for a UV-curable polyurethane developed as a coating with self-healing properties (Fig. 22.24A) [86,229] and other systems. For instance, hydrogen bonds also made an important contribution to the self-healing properties of a linear eugenol/epichlorohydrin-based polymer containing disulfide bridges and a large number of free hydroxyl functions and a polyurethane derived from it [230]. This polymer is interesting because it is partly produced from renewable resources, hence representing an example of an important class of emerging self-healing and bio-renewable thermosetting materials [231]. The healing cycles could be repeated several times. In addition to the photocatalytic self-healing mechanism

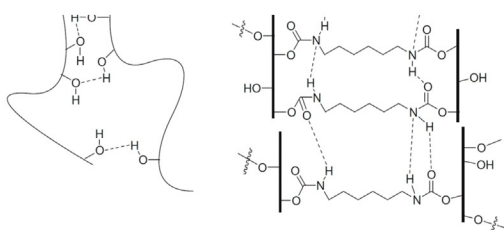
via flexible disulfide bridges, a significant effect via H-bridges was assumed. This effect of reversible hydrogen bonds is schematically summarized in Fig. 22.24B.

A strategy to use only hydrogen bonds to form noncovalent, reversible cross-links in epoxy resins has been described by Guadagno et al. [19,20]. The authors functionalized multiwall carbon nanotubes (MWCNTs) with barbituric acid and incorporated them as functional fillers in epoxy nanocomposites. The result was that the surface of the MWCNTs became more receptive to the formation of stable hydrogen bonds with free hydroxyl functionalities present in the epoxy resin. The strategy is shown schematically in Fig. 22.24C. The effect is based on the strong tendency of barbituric acid to form H-bridges.

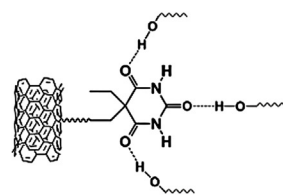
Noncovalent network formation via hydrogen bonds



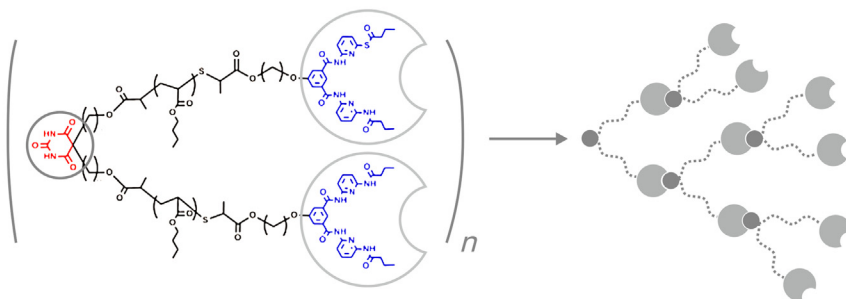
(A) Hydrogen bonds in the soft arm in the polyurethane structure



(B) Free hydroxyl and polyurethane groups



(C) Barbiturate-modified MWCNTs as functionalized fillers



(D) Intermolecular interaction of dendritic structures via hydrogen bonds

Directly barbiturate-functionalized polymers with a pronounced tendency to form hydrogen bonds and a corresponding ability to self-associate under supramolecular structure formation have also been described [232]. The authors describe dendritic macromolecules that can form network-like supramolecular structures by noncovalent interactions between barbiturate functionalities. Such dendrimers can be produced in a one-pot synthesis and should have intrinsically self-healing properties. Fig. 22.24C schematically shows the basic strategy. The individual building blocks are structured according to a key/lock principle. The central structural element is barbituric acid, which is capable of forming stable H-bridges in a form similar to the naturally occurring DNA polymer. This example illustrates particularly clearly the supramolecular

structure formation. The targeted use and optimization of noncovalent, reversible binding sites is an important strategy to further improve and adjust the intrinsic self-healing properties of thermosetting materials.

In the following sections, some examples for intrinsically self-healing thermoset systems are presented that showcase recent developments and interesting ideas. The main focus was given to polyurethanes and epoxies since with these polymer classes the largest number of studies is described in the literature.

Intrinsically self-healing polyurethanes

For polyurethanes, a number of different building blocks with the ability to form dynamic bonds have been

FIGURE 22.24 Noncovalent network formation via hydrogen bonds: (A) Stiff self-healing PU-based coatings with high repair efficiency based on hydrogen bonds of long fatty chains (flexible arms of the rigid aromatic rings as “hard cores”) [229]; (B) Additional contribution to intrinsic self-healing effects by the formation of reversible networks via hydrogen bonds in polymers containing free hydroxyl groups and polyurethanes [230]; (C) Barbiturate-modified MWCNTs as functionalized fillers for enhancing reversible hydrogen bonding as noncovalent reversible bonding mechanism for supporting intrinsic self-healing properties in epoxy resin [20]; and (D) Formation of supramolecular dendritic structures whose cross-linking is based on the intermolecular interaction of hydrogen bonds [232]. Modified after Liu J, Cao J, Zhou Z, Liu R, Yuan Y, Liu X. Stiff self-healing coating based on UV-curable polyurethane with a “Hard Core, Flexible Arm” structure. *ACS Omega* 2018;3(9):11128–35. Available from: <https://doi.org/10.1021/acsomega.8b00925>; Cheng CJ, Li J, Yang FH, Li YP, Hu ZY, Wang JL. Renewable eugenol-based functional polymers with self-healing and high temperature resistance properties. *J Polym Res* 2018; 25(2):57. Available from: <https://doi.org/10.1007/s10965-018-1460-3>; Guadagno L, Vertuccio L, Naddeo C, Calabrese E, Barra G, Raimondo M, et al. Reversible self-healing carbon-based nanocomposites for structural applications. *Polymer (Basel)* 2019;11(5):903. Available from: <https://doi.org/10.3390/polym11050903>. [231] Chen SB, Schulz M, Lechner BD, Appiah C, Binder WH. One-pot synthesis and self-assembly of supramolecular dendritic polymers. *Polym Chem-Uk* 2015; 6(46):7988–94. Available from: <https://doi.org/10.1039/c5py01329a>, respectively.

successfully tested for their potential to induce intrinsic self-healing effects. The structural element of the polyurethane in which the self-healing functionalities are incorporated plays an important role: if the self-healing functionality is embedded within regions of restricted mobility, a less pronounced self-healing ability is often observed compared to polyurethanes that carry the self-healing functionalities in flexible segments. Other important aspects that should be considered when designing self-healing polyurethanes are the required transformation temperatures for the self-healing effect and the intentional utilization of noncovalent interactions for additional contributions to the repair capability. The healing mechanisms most commonly described in the literature for polyurethanes are based on DA/retro-DA reactions and thiol/disulfide chemistry.

Diels–Alder chemistry

Many PU systems have been described in the literature that show intrinsic self-healing effects by means of DA reactions [29,52,81,82,233–235]. Typically, furan is introduced into the polyurethane and reversible crosslinking is performed with maleimides [236]. One reason for the preferred use of furan as a DA component is that with most other cycloaddition reactions of this type, the conversion temperatures are too high for the back reaction and stable (and thus unreactive) aromatic compounds are rather formed instead of the desired dienes and dienophiles.

The self-healing properties of such furan-based polyurethane systems, could be further improved by the addition of polydimethylsiloxane (PDMS) segments [66]. For example, after crack healing at 60°C for 4 h, about 85% of the initial strength could be restored. Comparably low healing temperatures (80°C) were applied to another DA self-healing PU system [47]. Here, the polymer backbone was equipped with functionalities that can additionally form noncovalent interactions based on coordinative bonds and hydrogen bonds, thus enhancing the self-healing effect. The reversible coordinative bonds were achieved by introducing zinc acetate ligands. Similarly, Lin et al. have improved the self-healing effects of the DA reaction by incorporating additional coordinative bonds between pyridine units and Fe³⁺ ions [82].

The combination of self-healing and superhydrophobic properties was achieved by synthesis of a DA curable polyurethane in which the maleimide units were functionalized with POSS. Thus, a contact angle of 141 degrees was achieved and a multifunctional material was realized [52].

The ability to self-heal is particularly pronounced when the functional groups capable of the DA reaction are incorporated in mobile or easily accessible regions of

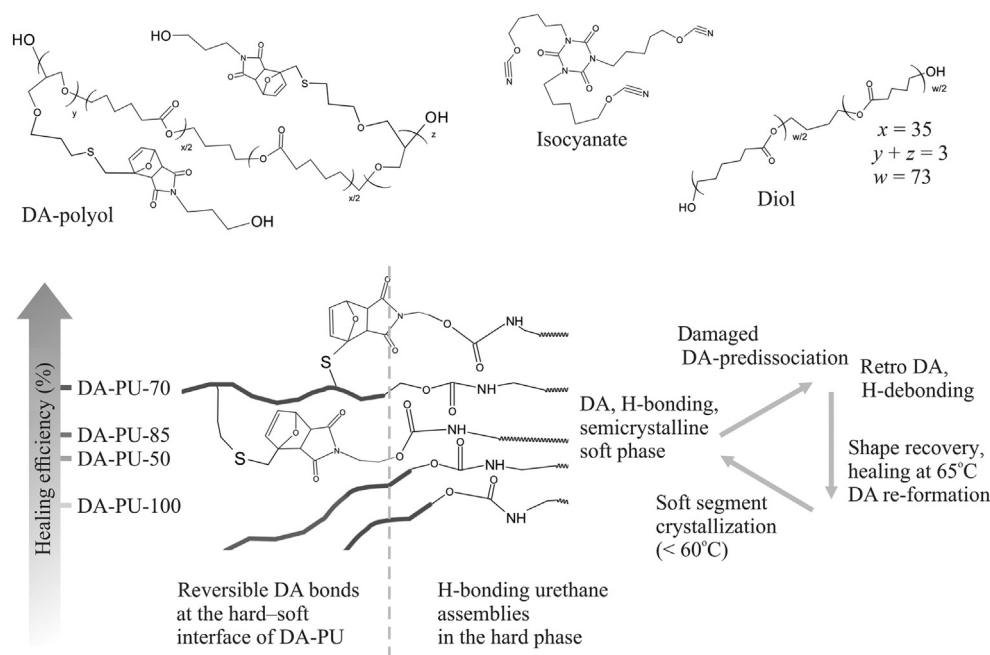
the PU. For this purpose, the microphase structure should be taken into account when designing the self-healing PU. If, for example, the furan units are buried in the hard segment, the temperatures required for the retro-DA reaction may well be in the range between 110°C and 180°C. At these high temperatures, it is more likely that the material is already partially damaged and that homopolymerization of maleimide units occurs. This is the typical undesired side reaction in DA reactions, which irreversibly reduces the ability to self-heal. Truong et al. have preferentially integrated the diene and dienophilic units at the phase boundary between hard and soft domains of the PU [81,234]. As a result, the transformation temperature required to trigger the self-healing reaction could be significantly reduced. Their polymer could readily be cured at 60°C to 70°C. Fig. 22.25A schematically illustrates the self-healing cycle [81].

Disulfide chemistry

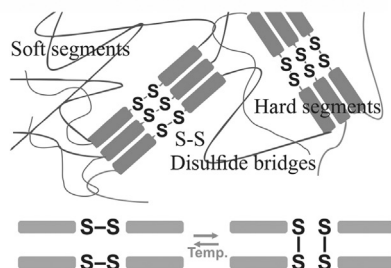
The disulfide mechanism is also frequently found in polyurethanes. Examples of this in recent literature can, for example, be found in [59,73,237–239]. The mechanism of thiol disulfide healing in a water-soluble PU was extensively investigated by Zhang et al. with in situ Raman spectroscopy and DMA [239]. The healing temperature was 75°C. The incorporation of ditelluride bridges instead of disulfide bridges has also been described in the literature [86]. An advantage of ditelluride bridges is the low reaction temperature. Here, self-healing reactions can already take place at room temperature [86].

Lee et al. [237] have incorporated cystamine as a chain extender into the chemical framework of a water-dilutable PU, thus creating intrinsic self-healing effects. The self-healing effect in this case was based on the reversible disulfide-thiol exchange reaction between cystamine and 2-mercapto ethanol. The cleavage of the disulfides produces thiols, which can recombine again to form disulfides. By rearranging the chain segments, new cross-linking disulfide bridges can be formed again and mechanical strength is restored. Fig. 22.25B illustrates this schematically depicting the internal structure of the polyurethane. The depicted microphase separation into rigid, crystalline regions (hard segments) and movable amorphous regions (soft segments) is typical for polyurethanes. Cystamine was incorporated into the hard segments as a thiol unit. The soft segments consist of polyols, which are capable of reversible (noncovalent!) hydrogen bonding and can form additional cross-links. These also contribute to the intrinsic self-healing properties (see subsection on “Intrinsic self-healing approach”). Fig. 22.25B also shows the bond rearrangement of the underlying self-healing mechanism.

(A) Self-healing cycle of polyurethane based on the Diels–Alder/retro-Diels–Alder reaction



(B) Self-healing polyurethane with integrated disulfide/thiol chemistry



(C) Polyphenol comonomers for self-healing polyurethanes

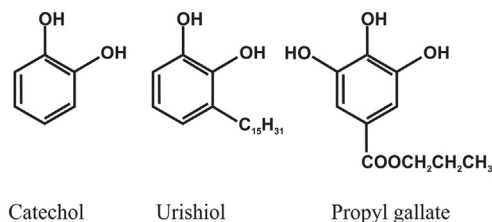


FIGURE 22.25 (A) Self-healing cycle of polyurethane based on the DA/retro-DA reaction mechanism. The reversible bridging sites are incorporated at the phase boundaries between hard and soft domains of the polyurethane [81]; (B) internal structure of a polyurethane with intrinsic self-healing properties based on disulfide/thiol chemistry; (C) polyphenols as comonomers for polyurethanes with intrinsic self-healing properties based on reversible urethane bridge bonds [240]. Figure B modified according to Lee D-I, Kim S-H, Lee D-S. *Synthesis and characterization of healable waterborne polyurethanes with cystamine chain extenders. Molecules* 2019;24(8):1492 [237].

To further improve the self-healing properties, in a related study this disulfide/thiol self-healing mechanism based on cysteine units was combined with another reversible covalent crosslinking mechanism by adding vanillin to the polymer backbone [115]. The vanillin can form additional crosslinking sites by forming Schiff bases between its aldehyde functionality and the amine group present in cysteine. The self-healing effects are achieved through the combined action of disulfide and imine metathesis conversions.

Disulfide bridges are used preferably for rather softer cross-linked PU materials, that is, PU-based elastomer [71]. When using aliphatic disulfide chemistry, the efficiency of the self-healing process seems to be a function

of the crosslink density of the polysulfides on the one hand and the composition of the hard segment on the other hand [71]. The composition of the hard segment plays an important role with respect to chain mobility. The mobility of rigid polyurethanes is severely restricted and, accordingly, their self-healing properties are less pronounced. Disulfide-based cross-linked and self-healing polyurethanes can even be recycled to a certain extent and can be reused. Only relatively mild reaction conditions are required [71].

Aromatic disulfides have also been incorporated into polyurethanes. 2,2'-disulfanediyldianiline was incorporated into a water-soluble PU as a chain extender. The mechanical properties were significantly improved

and the self-healing reaction became possible at body temperature [239].

Azide click chemistry

Self-healing corrosion-resistant coatings for metal substrates based on azide click chemistry were described in the literature [96]. The characterization was performed by EIS (see section “Selected analytical techniques to evaluate self-healing efficiency”, Figs 22.5 and 22.6). After scratching, a high degree of self-repair was found. The underlying healing reaction was based on the formation of triazole units from free azide and propargyl groups in the polymer backbone under mild thermal action [96].

Reversible urethane bonds

Polyurethanes with intrinsic self-healing properties based on the formation of reversible urethane bonds were obtained by incorporation of phenolic residues into the polymer backbone [240,241]. The authors incorporated different polyphenols into the polyurethane, which differed in their substitution pattern in terms of space requirements and electronic properties: catechol, urushiol, and propyl gallate (Fig. 22.25C). The self-healing properties at a reaction temperature of 150°C were most pronounced in the propyl gallate-modified PU, and least pronounced in the catechol-modified PU. The authors argue that the phenolic urethane bond is significantly more stable in the less sterically hindered (catechol-modified) PU and therefore a higher temperature is required to reorganize and rearrange the covalent network. An analogous strategy was pursued by incorporation of vanillyl alcohol [242]. The self-healing temperature in this case was specified as 140°C. The incorporation of eugenol as a phenolic component into the polyurethane backbone has already been described in subsection “Non-covalent network formation”, Fig. 22.24B [230].

The formation of dynamic bonds between propyl gallate units was also used in a polyurethane-based coating system that was subsequently modified on the surface with PDMS to achieve self-cleaning effects [55]. Reversible urethane bonds between isocyanate and phenolic hydroxyl groups were also the chemical basis for self-healing effects in a Tong oil-based polyurethane elastomer [243]. This polyurethane is another example of smart materials based on renewable raw materials.

Photocatalytic self-healing

Coumarin and its derivatives have also been incorporated into polyurethanes [244]. This molecule is particularly interesting because of its photoreactive properties. 7-hydroxy-4-methylcoumarin shows reversible photodimerization (at 365 nm) and photodissociation (at 254 nm). This can be used to cross-link polymer segments

reversibly under the influence of light (dimerization of two coumarin units in adjacent network segments). However, the cycle cannot be repeated as often as desired, since the dimeric coumarin can decay asymmetrically and the reversibility of the process is then lost. It was particularly advantageous to use the dihydroxyl coumarin as chain extender. Coumarin is also interesting from a sustainability perspective, as it can be obtained from renewable raw materials.

Intrinsically self-healing epoxies

As described in the section “Extrinsic self-healing,” epoxy resins are very often used as model systems to evaluate the performance of extrinsic self-healing systems by formulating commercial epoxy systems with different microsphere additives. In addition, many chemically modified epoxy resins have been described in the literature, which chemically anchor functional groups that make the epoxy thermosets intrinsically capable of self-healing. Often the best results are achieved by a combination of intrinsic and extrinsic approaches.

As a general strategy, the most common way to produce intrinsically self-healing epoxies is to use a suitably modified amine- or hydroxyl-based crosslinker. For this purpose, dienes or dienophiles or thiol- or disulfide-based functional groups are bound to a bifunctional crosslinker and these reversibly crosslinkable groups are then incorporated into the epoxy resin in the course of the crosslinking reaction. An important class of epoxy resins with self-healing properties is the class of vitrimers. Because of their importance, these materials are dealt with in a separate chapter in this book and are only briefly mentioned in the present chapter.

Diels–Alder chemistry

Many epoxy resins have been provided with intrinsically self-healing properties by incorporation of maleimides and furans [245], for example, by incorporation of furfuryl alcohol [246,247] or commercial furfurylglycidyl ether [248–251]. The glass transition temperature and thus also the HE can be adjusted within wide limits by varying the amount of DA functionality incorporated [246]. A prerequisite for successful self-healing is that the glass transition temperature of the resulting epoxy resin is lower than the transition temperature at which the retro-DA reaction is initiated ($T_G < T_{rDA}$). The self-healing properties can be controlled by the percentage of built-in DA functionalities. The relationship is summarized for the epoxy system described by Zolghadr et al. in Fig. 22.26.

Coope et al. have also described a modified epoxy system based on conventional epoxy resin with built-in furfuryl and maleimide functionalities. The self-healing

DA-reversibly crosslinkable functionalities in the epoxy resin

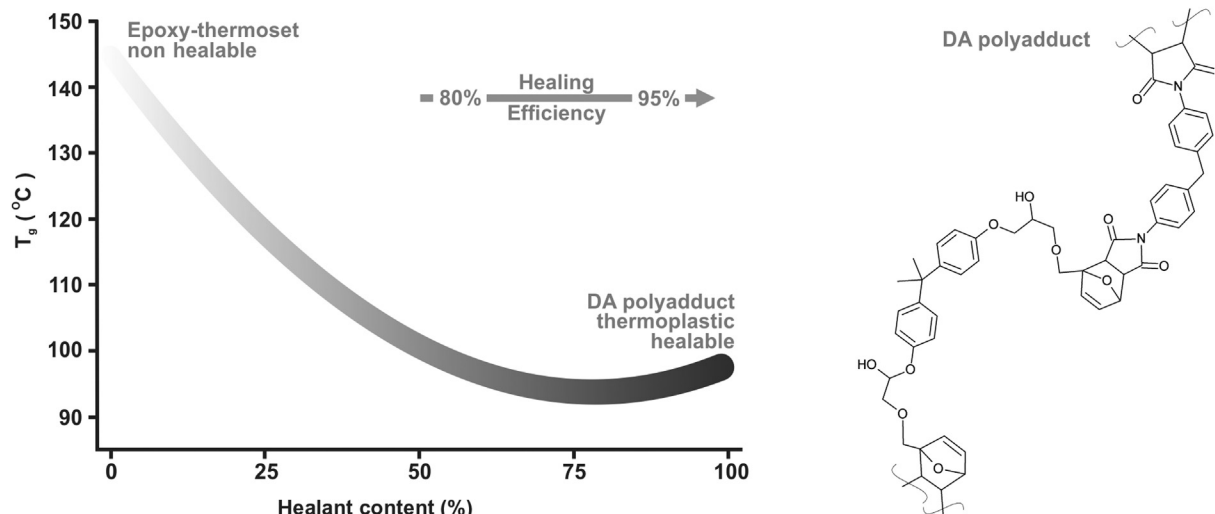


FIGURE 22.26 Relationship between the amount of DA-reversibly cross-linkable functionalities in the epoxy resin and the self-healing efficiency [246]. DA, Diels–Alder.

cycles required a temperature of 150°C (for 5 min). Three self-healing cycles were possible and the material is suitable for aerospace applications due to its property profile [35].

In the production of DA-modified epoxy resins, it is important to ensure that the chemical functionalities that are later required to impart the self-healing properties in the finished network do not lose their reactivity prematurely, for example during synthesis or during the cross-linking reaction. The two most important side reactions that play a role are the Michael addition between maleimides and free amines and the homopolymerization of bismaleimides (BMIs). Both reactions are mainly due to the activated double bond in maleimide. Michael additions can take place at room temperature. In this process, double bonds add to carbon atoms that are activated by electron-withdrawing substituents. Therefore, contact between amino functions (present in the crosslinkers of epoxides) and BMIs should be avoided if possible. Turkenburg and Fischer therefore propose a two-step process for the synthesis of DA-modified epoxy resins [252]. In the first stage, the prepolymer is produced. For this purpose, furfurylamine is reacted with the diglycidyl ether of bisphenol A and an unbranched long-chain prepolymer with the diene component is formed. After the total amount of primary amine has been reacted, the dienophile 1',1'-(methylenedi-4,1-phenylene) BMI is added in a second step. This cross-links the prepolymer by forming DA adducts. This sequence prevents BMI from reacting with the free amine of furfuryl amine in the side reaction under nonreversible formation of covalent C–C bonds. The

second side reaction (homopolymerization of BMI) is prevented primarily by keeping the temperature as low as possible.

Since epoxy resins are mainly used in combination with glass fibers in composites, it is important that such composites also have intrinsically self-healing properties. Glass fiber-reinforced epoxy resins can be equipped with intrinsic self-healing properties using DA chemistry [249]. The behavior at the interfaces between fibers and matrix is of particular importance. Detailed investigations of the kinetic behavior during self-healing with a focus on the behavior at the phase interface were conducted by Peterson et al. Sufficient mobility of the polymer segments is important for effective DA response. Complete restoration of mechanical strength was achieved with a system whose glass transition temperature was 6°C. The authors have performed very interesting single fiber microdroplet experiments for their investigations.

Another noteworthy study on DA network formation under diffusion- and mobility controlled conditions in highly cross-linked polymer networks was performed by Mangialetto et al. The authors used a combination of various thermoanalytical methods (Modulated Temperature DSC, Microcalorimetry, dynamic rheometry, and DMA) to investigate network formation and kinetics of DA reaction in two model systems and mathematically simulated network formation under mobility restricted conditions by applying mechanistic models. They develop a reliable quantitative model that allows to predict the evolution of glass transition temperature in dependence of conversion during DA reaction. The time-profile of the heat capacity

during DA reaction as obtained from TM-DSC was shown to carry valuable information on (partial) vitrification along the reaction path [112,253].

The literature also describes numerous epoxy-based nanocomposites with self-healing properties that make use of DA healing chemistry. Repeatable intrinsic DA-based self-healing effects have been achieved, for example, in an epoxy/graphene nanosheet composite via furan and maleimide functionalities covalently embedded in the epoxy resin matrix [254]. The heat was supplied by irradiation with infrared light. The HE was over 90%. Surface film temperatures were not mentioned by the authors.

Epoxy graphite nanocomposites with self-healing properties have also been described in the recent literature [255]. The aim of this work was to achieve satisfactory self-healing both in bulk thermosetting material (healing within the epoxy matrix) and at the interface between the nanofiller and the embedding matrix. For this purpose, a component of the DA system, BMI, was grafted to the surface of the nanofiller (finely dispersed graphite nanoplates). The other component, furan, was anchored in the epoxy matrix. To make the matrix self-healing as well, BMI was also incorporated into the epoxy matrix. The difficulty here was to distribute the relative proportions of the two DA components between the composite components in such a way that sufficiently high self-healing effects were achieved both at the interfaces and within the matrix [255].

Disulfide chemistry

Disulfide chemistry is also an important self-healing mechanism for epoxy systems. The influence of crosslinking reagents on the cohesive and adhesive self-healing properties was systematically investigated by Lafont et al. The efficiency of self-healing depends very much on the network density and the rigidity of the polymer framework [256]. The authors studied rubber thermosets using triple- and quadruple-branched crosslinking reagents. They were able to achieve complete regeneration of the material at a healing temperature of 65°C if the annealing phase was maintained for periods of between 20 and 300 min. This is also possible with fourfold branched crosslinking reagents, provided that sufficiently flexible chains are used.

Epoxy resin-based composites have also been made intrinsically self-healing not only by DA reactions, but also by using disulfide chemistry. Such glass fiber-reinforced epoxy resin composites have been described, for instance, by Post et al. [84] and Luzuriaga et al. [83].

Recently, an interesting cyclotriphosphazene-based epoxy resin was produced that contained disulfide bridges [257]. The disulfide bridges were introduced into the

system via a modified amine crosslinker during curing of the epoxy resin. This polymer is of special interest. It belongs to a new class of thermosetting materials that have recently gained high interest due to their special physical properties: Vitrimers. Vitrimers behave at room temperature like ordinary cross-linked thermosets. However, if they are heated to high temperatures, their characteristics change and they can be thermoplastically formed. In principle, it is therefore possible to cure vitrimers and subsequently postform them, for example in a hot molding press. This class of thermosets is obviously also of great importance in the context of self-healing thermosets. Therefore, this concrete example will be used to briefly discuss the above mentioned. A detailed discussion of this type of thermoset is not necessary at this point, instead reference should be made to chapter on Vitrimers in this handbook.

The vitrimer described by Zhou et al. obtains its thermoreversible network properties through the incorporation of disulfide bridges. In addition, this epoxy resin with cyclotriphosphazene rings is rich in flame-retardant nitrogen and phosphorous functionalities [257]. The rather complicated structure of this vitrimeric epoxy is summarized in Fig. 22.27A.

Another, more simple epoxy vitrimer was described as a self-healing matrix for glass fiber composites by Luzuriaga et al. [83]. The synthesis of this vitrimer is comparatively straightforward. The crosslinking of the biglycidyl component is performed by a bifunctional aromatic amine, which carries the disulfide functionality (see Fig. 22.27B).

Vitrimers are of particular interest because they show great promise in terms of recycling and reusability. As a rule, thermosetting materials must currently be disposed of or thermally recycled after use. The high potential for reprocessing of vitrimers can be an alternative. The vitrimer shown in Fig. 22.27B was easily recycled and showed no loss of its mechanical properties after recycling [83].

Transesterification

Transesterification chemistry has also been used in epoxy systems [258]. A thiol-epoxy matrix was generated for this purpose. The healing properties of this material could be further improved by adding microcapsules loaded with tung oil. This combination of intrinsic and extrinsic healing approaches led to higher efficiency in self-healing, better mechanical strength and increased corrosion stability [258]. Another epoxy resin with self-healing properties and an additional shape-memory effect based on transesterification self-healing chemistry has also been described recently [63]. This epoxy resin was produced from the

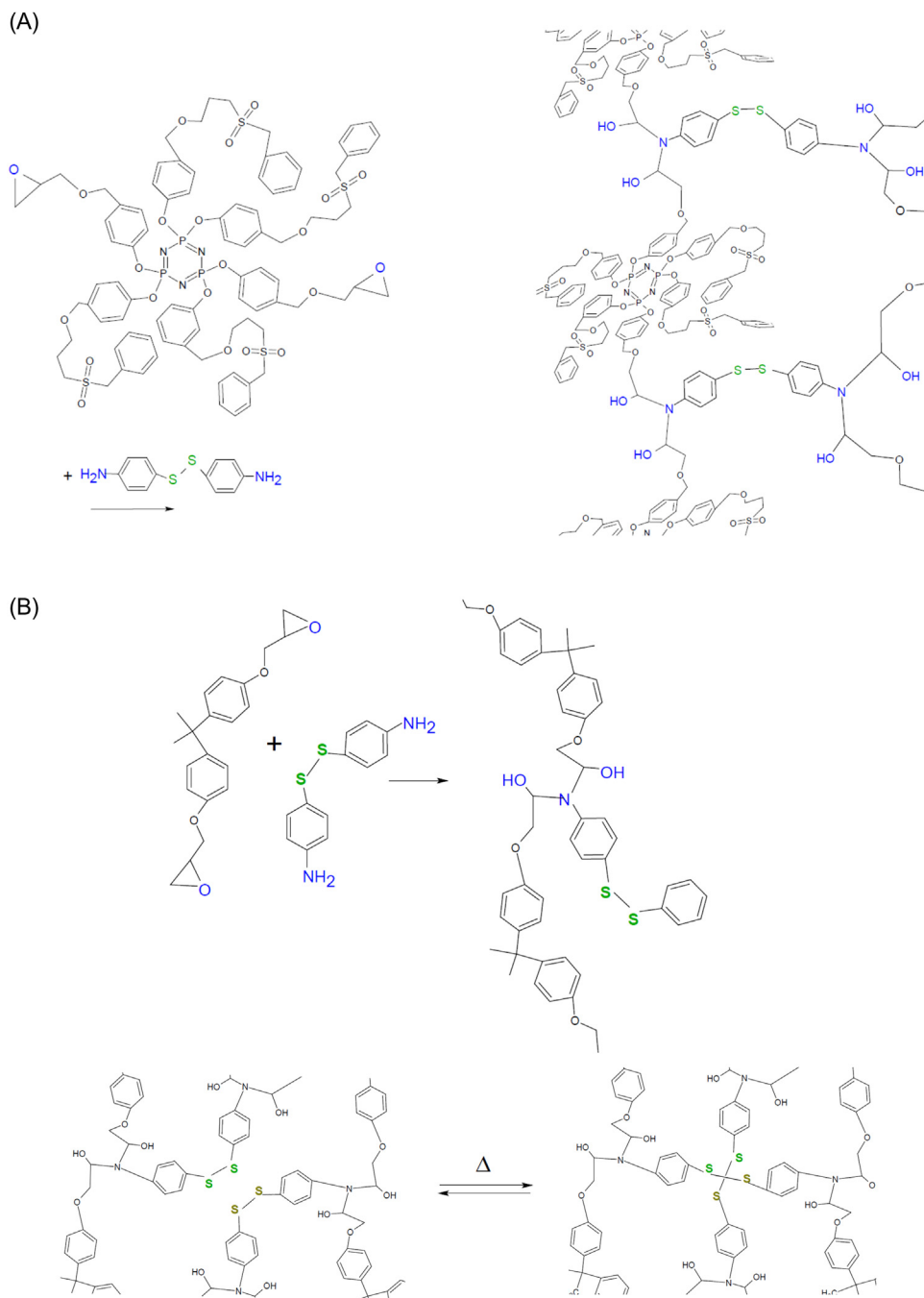


FIGURE 22.27 (A) Structure of a flame-retardant epoxy vitrimer with intrinsic self-healing properties based on disulfide bridges [257]. (B) Vitrimeric epoxy resin based on disulfide bridges. Modified after de Luzuriaga AR, Martin R, Markaide N, Rekondo A, Cabanero G, Rodriguez J, et al. Epoxy resin with exchangeable disulfide crosslinks to obtain reprocessable, repairable and recyclable fiber-reinforced thermoset composites. *Mater Horiz* 2016;3(3):241–247 [83].

diglycidyl ether of bisphenol A by reaction with the tri-functional carboxylic acid tricarballic acid and is temperature stable up to 380°C.

Imine metathesis reaction

Reversible imine metathesis reactions based on Schiff bases have also been used with epoxy resins to induce self-healing

effects [259]. The self-healing chemistry here is completely analogous to the reversible crosslinking mechanism of polyurethanes [240] described in the preceding subsection on “Intrinsically self-healing polyurethanes”. A typical epoxy resin based on the diglycidyl ether of bisphenol A was cross-linked with a hardener containing two hydroxyl groups, which additionally contained imine functionalities. This hardener had been produced by reaction of vanillin and

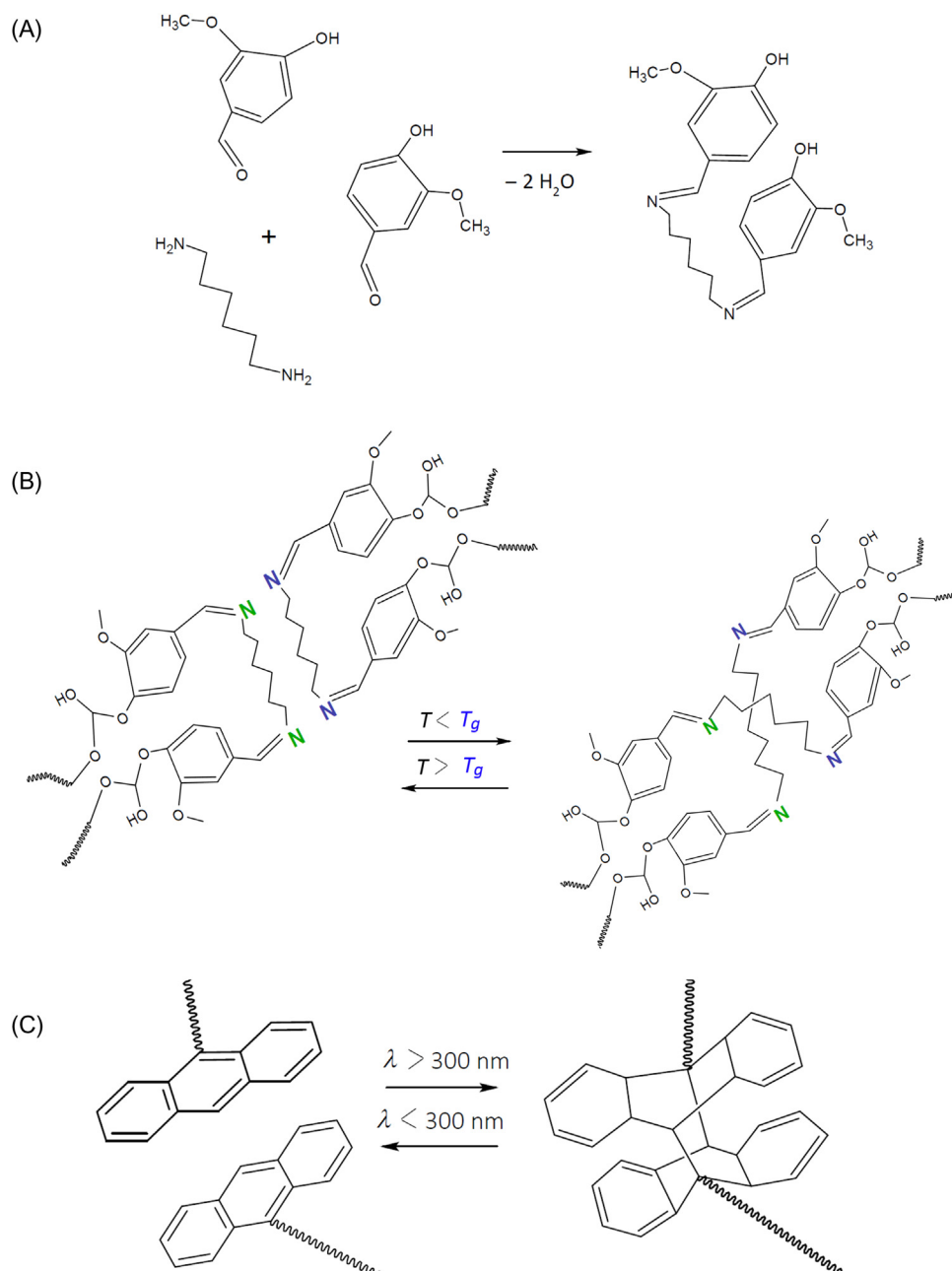


FIGURE 22.28 (A) Production of an epoxy crosslinker based on vanillin with imine functionality [259]. (B) Mechanism of reversible crosslinking by imine functionalities (Schiff bases) using imine metathesis reactions [259]. (C) Reversible photocatalytic dimerization of anthracene units that are covalently bound into different network segments [260].

hexamethylene diamine (see Fig. 22.28A) and is capable of forming dynamic covalent bonds depending on the temperature. The healing temperature for this system was 90°C. The material also showed a pronounced shape memory effect after being subjected to an annealing process in a twisted state [259].

Photocatalytic self-healing

Epoxy systems can also be equipped with intrinsic self-healing properties by means of photocatalytic reactions. For example, anthracene units were covalently integrated

into the epoxy network (Fig. 22.28C) [260]. This was achieved by functionalizing the anthracene units with an amino group and using the amino-functionalized anthracene as amine crosslinker for the epoxy resin. Anthracene is able to dimerize reversibly under the influence of UV light with a wavelength of 365 nm. Bond cleavage takes place with UV radiation of higher energy (at 254 nm).

Other intrinsically self-healing thermosets

A number of other thermosetting polymers have also been modified for intrinsic self-healing. A complete list would

not make sense at this point and is not possible due to vast amount of published material, so here are only presented some additions on recent developments. Most intrinsically healing systems again are based on the application of DA chemistry.

An interesting example for the implementation of the intrinsic strategy to achieve self-healing effects in coatings is the enhancement of melamine resin surfaces with this special property. Melamine resins yield chemically and temperature stable, particularly hard and quite brittle surface films on a variety products in the furniture sector (work surfaces, horizontal, and vertical surface elements of furniture), in interior design (laminated floorings, interior wall cladding), and surfaces in exterior applications (facade elements). Their resistance to chemicals allows them to be used as a coating for laboratory furniture, while their inherent antibacterial properties and resistance to water vapor are favorable for kitchen work surfaces [261]. These advantageous properties are the result of a highly cross-linked, very largely cured polymer network. Standard surfaces based on melamine resin are no longer chemically reactive and have no intrinsic self-healing ability. The polymer segments are practically immobile and practically no longer soften when exposed to temperature [262].

To achieve self-healing effects, the DA reaction was used as the chemical system. Furan groups were incorporated into the melamine–formaldehyde network as chemical functionalities capable of undergoing DA reactions. The thermoreversible reaction took place between these furan units and BMI groups. The self-healing effects were incorporated into the melamine network using various strategies. One strategy was to use reversibly crosslinkable particles based on modified melamine resin as building blocks. In one variant, particles were produced that were composed of two different prepolymers (the pure MF prepolymer on the one hand, which provided the mechanical strength, and furan-modified MF prepolymer on the other hand, which produced the self-healing properties). The two particle types were then crosslinked with maleimides to form a copolymer network [263]. In another variant, particles were produced from a monomer that already combined both functionalities (melamine and furan) in one molecule and the material was again produced by crosslinking with maleimides [264]. In a second strategy, however, the production of particles was abandoned and the surface film was achieved directly by condensation of a new melamine-based monomer that incorporated the self-healing functionalities already into its chemical backbone [18,265] (Fig. 22.29A).

Solid coating films based on papers impregnated and cured with this modified melamine resin show very good self-healing properties over several healing cycles.

Fig. 22.29B illustrates how laminate surfaces look under the light microscope before (Fig. 22.29B-a) and after scratching (Fig. 22.29B-a) and after the healing step (Fig. 22.29B-c). In the experiments, the optical and mechanical properties were almost completely restored. This is an important finding, as the optical appearance plays a particularly important role in all applications of decorative laminates [18].

Other thermosets have also been designed to be self-healing. Silicone resin based on PDMS was made self-healing by incorporation of furan and bismaleimide functionalities using DA chemistry. The annealing temperature was only 60°C and after a single annealing step a mechanical scratch was closed and a restoration of mechanical strength of 84% was achieved [66]. The material also exhibited shape memory behavior. A cross-linked PDMS elastomer with application potential as an artificial muscle, protective coating, or as a material for flexible electronic components was—again by using DA chemistry—chemically modified to exhibit intrinsic self-healing ability. In this case, the additional reversible DA-based bridges significantly improved the mechanical strength [124] and the material could be stretched by 400%.

Superamphiphobic coatings based on acrylates with intrinsic self-healing properties were recently presented by Zhao et al. [53]. These systems made use of the disulfide mechanism and incorporated accelerated self-healing effects into UV-curing acrylates. This coating system is remarkable in that it illustrates that several smart properties are often imparted simultaneously. Self-healing in combination with hydrophobic and oleophobic properties is an important property profile for surface coatings and is often sought after in practice. Another example of a high-performance acrylate as a hybrid polymer with epoxy resin was described by Jin et al. [266]. Thiol-ene click chemistry is used here to achieve intrinsic self-healing. A furan-functionalized polyketone in combination with BMI was recently presented by Zhang et al. [267].

A carborane-containing aromatic polyimide with very high-temperature stability up to 700°C and partially self-healing properties has recently been described [268]. A film of poly(amic acid) based on a copolymer of aromatic dianhydride, aromatic diamine and carborane-modified aromatic diamine was prepared and subsequently imidized at elevated temperature (see Fig. 22.29C). The high-temperature stable, flexible polymer film was examined for its thermooxidative stability and showed self-healing properties in one phase during thermal decomposition. After a short phase of expulsion of volatile components (phase 1 of decomposition), the film temporarily changed into a self-stabilizing state. This stabilizing effect was attributed to multiple boron oxide layers that had formed

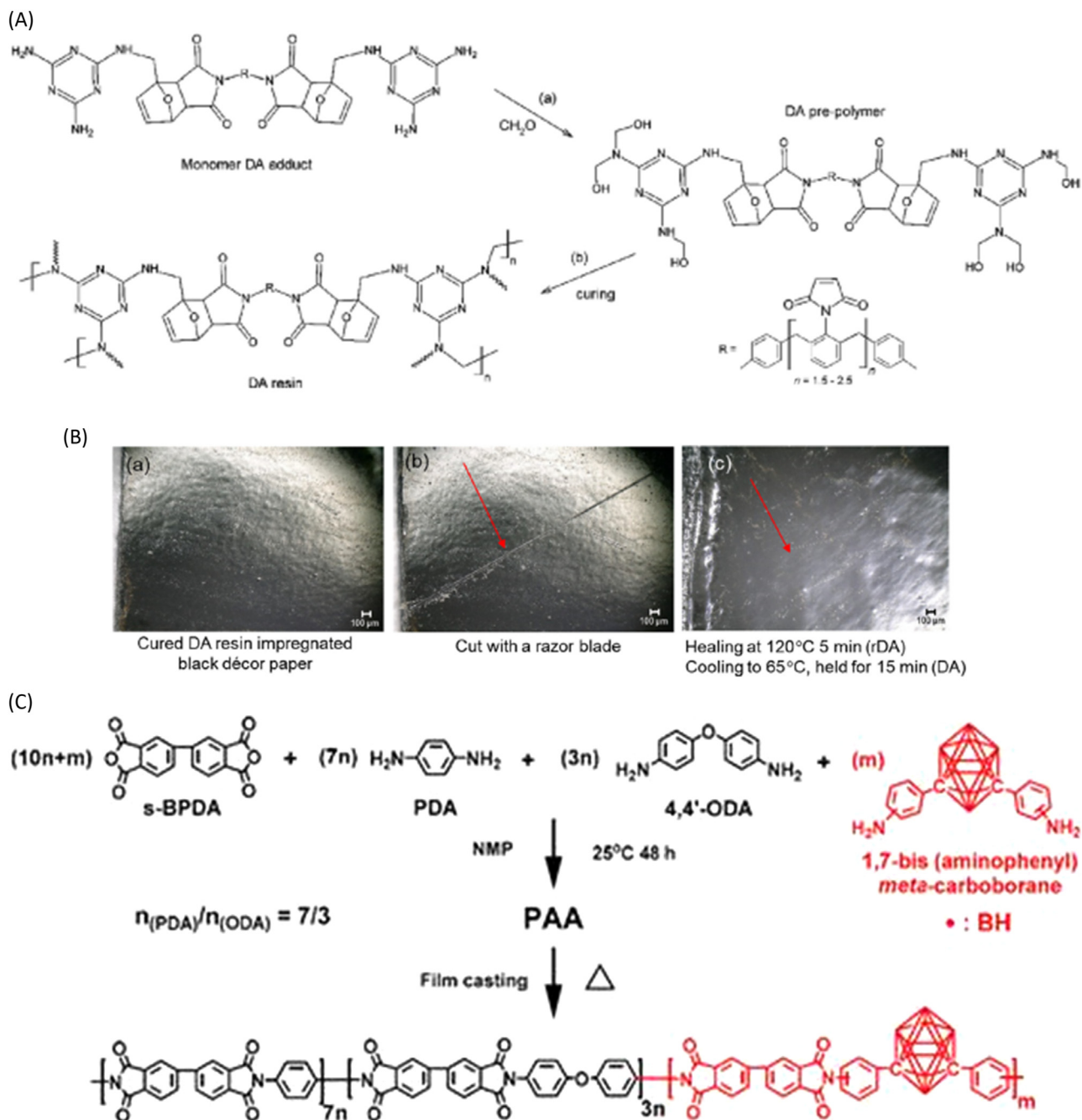


FIGURE 22.29 (A) Structural formula of the monomeric building block for a melamine resin with self-healing properties as well as a schematic reaction equation for the preparation of the prepolymer (a) and its curing to the self-healing thermoset film (b) [18]. (B) Light microscope image (a) of a laminate surface based on black décor paper impregnated with the self-healing melamine resin and cured, (b) same surface after scratching, (c) same surface after thermal healing of the scratch [18]. (C) Production of a high-temperature stable carborane-containing polyimide film [268]. Taken from Liu F, Fang G, Yang H, Yang S, Zhang X, Zhang Z. Carborane-containing aromatic polyimide films with ultrahigh thermo-oxidative stability. *Polymers (Basel)* 2019;11(12):1930. Available from: <https://doi.org/10.3390/polym11121930>.

on the surface of the polyimide film and prevented further degradation [268]. This example illustrates how self-healing film properties in a broader sense can also play an important role in the design of high-temperature applications of polymer systems and advanced coatings.

Summary

Finally, a brief summary of the advantages and disadvantages of the individual strategies for achieving self-healing effects shall be discussed.

In general, liquid reaction mixtures, which are intended for use in the extrinsic approach as fillings of microspheres or vascular structures, must exhibit a number of important properties. Their long-term stability must be sufficiently high so that they do not cure prematurely while they are still encapsulated and stored in the matrix. Their flowability must be sufficiently high so that they can flow quickly into the defect areas and fill them. They should also be able to penetrate into small hairline cracks. If possible, healing fluids should not contain any volatile components that can evaporate quickly during the curing process or diffuse into the matrix system during the inactive storage period, thereby having a negative effect on the matrix properties and no longer being available for healing. Furthermore, the chemical compatibility between the curing reagent and the matrix to be cured must be sufficiently ensured. Otherwise, insufficient wetting and correspondingly weak adhesion properties must be expected. This is very important, as otherwise the mechanical strength of the damaged material will only be restored to a limited extent. There must be no adverse interaction effects between the encapsulated liquid and the matrix to be repaired. For example, there must be no corrosion, dissolution, or softening of the matrix. The strength properties of the healing reagent in the cured state must be at least comparable to the strength of the matrix thermoset and it is preferable that they even exceed the material properties of the matrix polymer. To allow a sufficiently wide temperature range in the application, the self-healing system should have a correspondingly low freezing point and a correspondingly high boiling point. This is of great importance, since rather high temperatures are usually applied during processing and curing of the matrix thermoset. Hence, during the manufacture of the product or molded part, there is a risk that the healing reaction is set off or the additive capsules are deactivated. Since thermosets are technically processed by a variety of methods, standardized healants must be able to withstand the process temperatures of a whole range of manufacturing processes such as hot-pressing, powder coating, extrusion, injection molding, resin transfer molding, and others. Also very important is that the curing behavior is largely independent of the mixing ratio between the hardener/catalyst and the healing fluid. Since exact mixing ratios are usually difficult to achieve in the specific situation, reliable, and extensive curing in a wide stoichiometric ratio between the components involved is required.

Similarly, high demands are imposed on catalysts that accelerate the curing of the healing fluid. The catalysts must dissolve quickly in the healing liquid and form a homogeneous phase. Furthermore, they must not lose their chemical reactivity over an indefinite long period of time. They should not change chemically over a wide temperature range in order to allow a correspondingly

wide range of temperatures in the application of the material. Chemical inertness to the embedding medium is also an important prerequisite. After combining with the liquid causing self-healing, the curing process should be catalyzed as quickly as possible in order to realize the shortest possible repair phases. The curing kinetics in interaction with the self-healing liquid after mixing must be known to be anticipated and adjusted very precisely in the formulation. Ideally, curing is fast and reliable over a wide mixing range between catalyst and healing fluid (healant).

This makes it clear that, depending on the matrix system and the expected damaging effect, the self-healing additives have to be adjusted very precisely to the respective application.

The use of the extrinsic approach has some advantages over the intrinsic approach, but also has some specific disadvantages. In the following, the two basic strategies will be briefly compared and the essential characteristics will be laid out.

A major advantage of the extrinsic strategy using microcapsules is the basically modular structure of the high-performance materials. Various thermosets can be mixed with self-healing additive capsules. In principle, therefore, different commercially available standard thermosets can be upgraded with self-healing additives. During the formulation of the reaction mass, microspheres are added to the thermoset prior to processing. They are, in principle, incorporated in a similar way as flame retardants, fillers or pigments are. In this way, the development of self-healing systems (SH additives) and base polymer development are largely detached. In addition, commercially available polymers can be made self-healing at a later stage if desired and the costly development of special polymers based on particular monomers can be avoided. The extrinsic approach can basically be applied to highly crosslinked thermosets. Depending on the choice of the chemistry responsible for the self-healing effect, a wide range of different types of additives is available. Depending on the thermoset matrix, the most suitable additive can therefore be selected from a wide range of possible additive capsules.

The main disadvantage is that the specific extent of the self-healing effect achievable depends on many partly uncontrollable factors such as the concrete nature and dimension of the damage event and can only be controlled or predicted with difficulty. Usually, when selecting the healing system or formulating the prepolymer mixture, it is necessary to determine what type of harmful effect is to be healed. This means, among other things, that the selection of the capsule type in terms of wall thickness or mechanical strength determines its bursting behavior and thus its response to the damage event. When capsules are used, the healing effect occurs only once and repeated damage cannot be repaired. The self-healing efficiency

can be adjusted by the microsphere content. However, the amount of self-healing additive added cannot be arbitrarily high. Too high contents of microspheres lead to adverse effects on the matrix properties just like with other types of fillers.

The use of microvascular systems has several advantages over microcapsules. In particular, larger amounts of healing fluid can be stored in the thermoset material compared to microcapsules. Thus, for example, larger, spatially more extensive damage can be repaired better than with microcapsules. If a vascular system evenly distributed over the entire material is realized, a comprehensive self-healing effect can be better achieved. Although the healing reagent is also used up after healing like with microcapsules, in an extended tubular system healing fluid can flow in from adjacent areas and thus make repeated healing events possible in an area in close proximity to the first damage. In principle, such tubular systems can also be refilled and partially regenerated from the outside. The number of possible healing cycles is generally greater when using vascular systems than with microspheres. However, it is clear that in damaged and once healed areas, the vascular system is interrupted and thus the affected region is permanently separated from the healing network. Healed areas also prevent the flow of healing fluid through this region. Important in the design of vascular systems is that the flow behavior in very small diameter tubes is dominated by the laws of microfluidics. This can cause problems especially in very finely branched tubular systems and places special demands on the development of healing fluids with respect to their rheological and interfacial energetic properties. This has to be considered especially in the case of thin coatings. For example, coating systems in the automotive sector have layer thicknesses in the range of 100–140 μm . This automatically makes it necessary to install tubular systems with very small channel diameters. Compared to the use of microcapsules, the production of microvascular, self-healing thermoset systems is much more complicated. While microspheres can be easily added and the main problem is to achieve a homogeneous stable dispersion without significant segregation effects, the production of microvascular systems is always a multistage process and therefore, as a rule, more expensive.

In contrast, intrinsic approaches to self-healing are in many respects superior to extrinsic strategies. Since the matrix polymer itself is equipped with the ability for reversible crosslinking, the realization of multiple self-healing cycles is no problem. Difficulties in formulation of the thermoset (inhomogeneous dispersions, segregation effects, uneven distribution of the self-healing reagent, complicated vascular structure with correspondingly demanding production processes) are eliminated from the outset. There are no compatibility problems, since no

components foreign to the matrix thermoset have to be used. Loss of self-healing ability due to high process temperatures during processing or storage-related aging effects are not observed either. However, the polymer network must have a minimum degree of mobility so that the reactive groups can orient toward each other. This often has a negative effect on the mechanical properties of the materials. Achieving healing effects usually requires the application of external stimuli such as an increase in temperature (tempering). However, the reversible crosslinking of reactive groups in the polymer usually results in healing effects in a limited space. Since the intrinsic strategy is based directly on the chemical design of the base polymer, this approach requires the development of novel materials with correspondingly chemically integrated functionalities in the basic polymer structure. This means a cost-intensive monomer development. Commercially available polymers cannot be retrofitted but have to be redesigned from scratch using novel monomers. Often monomers with self-healing properties are chemically more complicated than standard monomers. Thus, thermosets with intrinsically self-healing properties are generally more expensive than comparable standard polymers. They are therefore automatically more suitable for special applications. The costs of new self-healing monomers have to be carefully considered in comparison to both the additional cost of (advanced) self-healing microspheres and the enhanced processing costs using the microvascular extrinsic approach.

References

- [1] Yang Y, Ding X, Urban MW. Chemical and physical aspects of self-healing materials. *Prog Polym Sci* 2015;49–50:34–59. Available from: <https://doi.org/10.1016/j.progpolymsci.2015.06.001>.
- [2] Ghosh SK. *Self-healing materials: fundamentals, design strategies, and applications*. Weinheim: Wiley-VCH; 2009.
- [3] Guadagno L, Vertuccio L, Naddeo C, Barra G, Raimondo M, Sorrentino A, et al. Functional structural nanocomposites with integrated self-healing ability. *Mater Today Proc* 2020. Available from: <https://doi.org/10.1016/j.matpr.2020.03.051>.
- [4] Michael P, Döhler D, Binder WH. Improving autonomous self healing via combined chemical/physical principles. *Polymer* 2015;69: 216–27. Available from: <https://doi.org/10.1016/j.polymer.2015.01.041>.
- [5] JE PC, Sultan MTH, Selvan CP, Irulappasamy S, Mustapha F, Basri AA, et al. Manufacturing challenges in self-healing technology for polymer composites—a review. *J Mater Res Technol* 2020;9(4):7370–9. Available from: <https://doi.org/10.1016/j.jmrt.2020.04.082>.
- [6] Urdl K, Kandelbauer A, Kern W, Muller U, Thebault M, Zikulnig-Rusch E. Self-healing of densely crosslinked thermoset polymers—a critical review. *Prog Org Coat* 2017;104:232–49. Available from: <https://doi.org/10.1016/j.porgcoat.2016.11.010>.

- [7] Wang Z, Scheres L, Xia H, Zuilhof H. Developments and challenges in self-healing antifouling materials. *Adv Funct Mater* 2020;30(26):1908098. Available from: <https://doi.org/10.1002/adfm.201908098>.
- [8] Xie C, Guo H, Zhao W, Zhang L. Environmentally friendly marine antifouling coating based on a synergistic strategy. *Langmuir* 2020;36(9):2396–402. Available from: <https://doi.org/10.1021/acs.langmuir.9b03764>.
- [9] Hamdy Makhlof AS, editor. *Handbook of smart coatings for materials protection*. Elsevier; 2014.
- [10] Scheiner M, Dickens TJ, Okoli O. Progress towards self-healing polymers for composite structural applications. *Polymer* 2016;83:260–82. Available from: <https://doi.org/10.1016/j.polymer.2015.11.008>.
- [11] Liu H, Gao S-W, Cai J-S, He C-L, Mao J-J, Zhu T-X, et al. Recent progress in fabrication and applications of superhydrophobic coating on cellulose-based substrates. *Materials (Basel)* 2016;9(3):124. Available from: <https://doi.org/10.3390/ma9030124>.
- [12] Hia IL, Vahedi V, Pasbakhsh P. Self-healing polymer composites: prospects, challenges, and applications. *Polym Rev* 2016;56(2):225–61. Available from: <https://doi.org/10.1080/15583724.2015.1106555>.
- [13] Althaqafi KA, Satterthwaite J, Silikas N. A review and current state of autonomic self-healing microcapsules-based dental resin composites. *Dent Mater* 2020;36(3):329–42. Available from: <https://doi.org/10.1016/j.dental.2019.12.005>.
- [14] Cui G, Bi Z, Wang S, Liu J, Xing X, Li Z, et al. A comprehensive review on smart anti-corrosive coatings. *Prog Org Coat* 2020;148:105821. Available from: <https://doi.org/10.1016/j.porgcoat.2020.105821>.
- [15] Wang S, Wu Y, Dai J, Teng N, Peng Y, Cao L, et al. Making organic coatings greener: renewable resource, solvent-free synthesis, UV curing and repairability. *Eur Polym J* 2020;123:109439. Available from: <https://doi.org/10.1016/j.eurpolymj.2019.109439>.
- [16] Idumah CI. Novel trends in self-healable polymer nanocomposites *J Thermoplast Compos Mater* 2019;24:089270571984724. Available from: <https://doi.org/10.1177/0892705719847247>.
- [17] Odarczenko M, Thakare D, Li W, Venkateswaran SP, Sottos NR, White SR. Sunlight-activated self-healing polymer coatings. *Adv Eng Mater* 2020;22(3):1901223. Available from: <https://doi.org/10.1002/adem.201901223>.
- [18] Urdl K, Weiss S, Christoff P, Kandelbauer A, Muller U, Kern W. Diels-Alder modified self-healing melamine resin. *Eur Polym J* 2020;127:109601. Available from: <https://doi.org/10.1016/j.eurpolymj.2020.109601>.
- [19] Guadagno L, Vertuccio L, Naddeo C, Calabrese E, Barra G, Raimondo M, et al. Self-healing epoxy nanocomposites via reversible hydrogen bonding. *Compos Part B Eng* 2019;157:1–13. Available from: <https://doi.org/10.1016/j.compositesb.2018.08.082>.
- [20] Guadagno L, Vertuccio L, Naddeo C, Calabrese E, Barra G, Raimondo M, et al. Reversible self-healing carbon-based nanocomposites for structural applications. *Polymer (Basel)* 2019;11(5):903. Available from: <https://doi.org/10.3390/polym11050903>.
- [21] Jin Y, Lei Z, Taynton P, Huang S, Zhang W. Malleable and recyclable thermosets: the next generation of plastics. *Matter* 2019;1(6):1456–93. Available from: <https://doi.org/10.1016/j.matt.2019.09.004>.
- [22] Lemesle C, Bellayer S, Degoutin S, Duquesne S, Casetta M, Pierlot C, et al. Flame retardant and weathering resistant self-layering epoxy-silicone coatings for plastics. *Prog Org Coat* 2019;136:105269. Available from: <https://doi.org/10.1016/j.porgcoat.2019.105269>.
- [23] Li A, Challapalli A, Li G. 4D Printing of recyclable lightweight architectures using high recovery stress shape memory polymer. *Sci Rep* 2019;9:7621. Available from: <https://doi.org/10.1038/s41598-019-44110-9>.
- [24] Mersagh Dezfuli S, Sabzi M. Deposition of self-healing thin films by the sol–gel method: a review of layer-deposition mechanisms and activation of self-healing mechanisms. *Appl Phys A* 2019;125(8):350. Available from: <https://doi.org/10.1007/s00339-019-2854-8>.
- [25] P PV, Al-Maadeed M. Self-repairing composites for corrosion protection: a review on recent strategies and evaluation methods. *Materials (Basel)* 2019;12(17):2754. Available from: <https://doi.org/10.3390/ma12172754>.
- [26] An S, Lee MW, Yarin AL, Yoon SS. A review on corrosion-protective extrinsic self-healing: comparison of microcapsule-based systems and those based on core-shell vascular networks. *Chem Eng J* 2018;344:206–20. Available from: <https://doi.org/10.1016/j.cej.2018.03.040>.
- [27] Zhu Y, Cao K, Chen M, Wu L. Synthesis of UV-responsive self-healing microcapsules and their potential application in aerospace coatings. *ACS Appl Mater Interfaces* 2019;11(36):33314–22. Available from: <https://doi.org/10.1021/acsami.9b10737>.
- [28] Du Y, Li D, Liu L, Gai G. Recent achievements of self-healing graphene/polymer composites. *Polymers (Basel)* 2018;10(2):114. Available from: <https://doi.org/10.3390/polym10020114>.
- [29] Menon AV, Madras G, Bose S. Ultrafast self-healable interfaces in polyurethane nanocomposites designed using Diels-Alder “click” as an efficient microwave absorber. *ACS Omega* 2018;3(1):1137–46. Available from: <https://doi.org/10.1021/acsomega.7b01845>.
- [30] Wang X, Guo Y, Su J, Zhang X, Wang Y, Tan Y. Fabrication and characterization of novel electrothermal self-healing microcapsules with graphene/polymer hybrid shells for bituminous material. *Nanomaterials (Basel)* 2018;8(6):419. Available from: <https://doi.org/10.3390/nano8060419>.
- [31] Pulikkalparambil H, Siengchin S, Parameswaranpillai J. Corrosion protective self-healing epoxy resin coatings based on inhibitor and polymeric healing agents encapsulated in organic and inorganic micro and nanocontainers. *Nano-Struct Nano-Objects* 2018;16:381–95. Available from: <https://doi.org/10.1016/j.nanoso.2018.09.010>.
- [32] Chen D, Wang D, Yang Y, Huang Q, Zhu S, Zheng Z. Self-healing materials for next-generation energy harvesting and storage devices. *Adv Energy Mater* 2017;7(23):1700890. Available from: <https://doi.org/10.1002/aenm.201700890>.
- [33] Mphahlele K, Ray SS, Kolesnikov A. Self-healing polymeric composite material design, failure analysis and future outlook: a review. *Polymer (Basel)* 2017;9(10):535. Available from: <https://doi.org/10.3390/polym9100535>.
- [34] Yan HY, Yang HY, Huang C. Advances of self-healing dental composite resin. *Zhonghua Kou Qiang Yi Xue Za Zhi* 2017;52(9):582–4. Available from: <https://doi.org/10.3760/cma.j.issn.1002-0098.2017.09.016>.

- [35] Coope TS, Turkenburg DH, Fischer HR, Luterbacher R, van Bracht H, Bond IP. Novel Diels-Alder based self-healing epoxies for aerospace composites. *Smart Mater Struct* 2016;25(8):084010. Available from: <https://doi.org/10.1088/0964-1726/25/8/084010>.
- [36] Li W, Zhu X, Zhao N, Jiang Z. Preparation and properties of melamine urea-formaldehyde microcapsules for self-healing of cementitious materials. *Materials (Basel)* 2016;9(3):152. Available from: <https://doi.org/10.3390/ma9030152>.
- [37] Vijayan P, AlMaadeed MA. 'Containers' for self-healing epoxy composites and coating: trends and advances. *Express Polym Lett* 2016;10(6):506–24. Available from: <https://doi.org/10.3144/expresspolymlett.2016.48>.
- [38] Zhang P, Li G. Advances in healing-on-demand polymers and polymer composites. *Prog Polym Sci* 2016;57:32–63. Available from: <https://doi.org/10.1016/j.progpolymsci.2015.11.005>.
- [39] Ye ZP, Zhang PS, Zhang JH, Deng LD, Zhang JW, Lin CG, et al. Novel dual-functional coating with underwater self-healing and anti-protein-fouling properties by combining two kinds of microcapsules and a zwitterionic copolymer. *Prog Org Coat* 2019;127:211–21. Available from: <https://doi.org/10.1016/j.porgcoat.2018.11.021>.
- [40] Leal DA, Riegel-Vidotti IC, Ferreira MGS, Marino CEB. Smart coating based on double stimuli-responsive microcapsules containing linseed oil and benzotriazole for active corrosion protection. *Corros Sci* 2018;130:56–63. Available from: <https://doi.org/10.1016/j.corsci.2017.10.009>.
- [41] Fadil M, Chauhan DS, Quraishi MA. Smart coating based on urea-formaldehyde microcapsules loaded with benzotriazole for corrosion protection of mild steel in 3.5% NaCl. *Russ J Appl Chem* 2018;91(10):1721–8. Available from: <https://doi.org/10.1134/S107042721810021X>.
- [42] Ubaid F, Radwan AB, Naeem N, Shakoor RA, Ahmad Z, Montemor MF, et al. Multifunctional self-healing polymeric nanocomposite coatings for corrosion inhibition of steel. *Surf Coat Technol* 2019;372:121–33. Available from: <https://doi.org/10.1016/j.surfcoat.2019.05.017>.
- [43] Sun J, Wang Y, Li N, Tian L. Tribological and anticorrosion behavior of self-healing coating containing nanocapsules. *Tribol Int* 2019;136:332–41. Available from: <https://doi.org/10.1016/j.triboint.2019.03.062>.
- [44] Lee W-J, Cha S-H. Improvement of mechanical and self-healing properties for polymethacrylate derivatives containing maleimide modified graphene oxide. *Polymer (Basel)* 2020;12(3):603. Available from: <https://doi.org/10.3390/polym12030603>.
- [45] Fortunato G, Anghileri L, Griffini G, Turri S. Simultaneous recovery of matrix and fiber in carbon reinforced composites through a Diels–Alder solvolysis process. *Polymer (Basel)* 2019;11(6):1007. Available from: <https://doi.org/10.3390/polym11061007>.
- [46] Raimondo M, Naddeo C, Vertuccio L, Bonnaud L, Dubois P, Binder WH, et al. Multifunctionality of structural nanohybrids: the crucial role of carbon nanotube covalent and non-covalent functionalization in enabling high thermal, mechanical and self-healing performance. *Nanotechnology* 2020;31(22):225708. Available from: <https://doi.org/10.1088/1361-6528/ab7678>.
- [47] Ouyang C, Zhao C, Li W, Wu X, Le X, Chen T, et al. Super-tough, self-healing polyurethane based on Diels-Alder bonds and dynamic zinc–ligand interactions. *Macromol Mater Eng* 2020;305(6):2000089. Available from: <https://doi.org/10.1002/mame.202000089>.
- [48] Trask RS, Williams GJ, Bond IP. Bioinspired self-healing of advanced composite structures using hollow glass fibres. *J R Soc Interface* 2007;4(13):363–71. Available from: <https://doi.org/10.1098/rsif.2006.0194>.
- [49] Haddadi SA, Ramazani SAA, Mahdavian M, Taheri P, Mol JMC, Gonzalez-Garcia Y. Self-healing epoxy nanocomposite coatings based on dual-encapsulation of nano-carbon hollow spheres with film-forming resin and curing agent. *Compos Part B Eng* 2019;175:107087. Available from: <https://doi.org/10.1016/j.compositesb.2019.107087>.
- [50] Mirabedini SM, Farnood RR, Esfandeh M, Zareanshahraki F, Rajabi P. Nanocomposite coatings comprising APS-treated linseed oil-embedded polyurea-formaldehyde microcapsules and nano-clay, part 2: self-healing and corrosion resistance properties. *Prog Org Coat* 2020;142:105592. Available from: <https://doi.org/10.1016/j.porgcoat.2020.105592>.
- [51] Wang X, Chen Z, Xu W, Wang X. Fluorescence labelling and self-healing microcapsules for detection and repair of surface microcracks in cement matrix. *Compos Part B Eng* 2020;184:107744. Available from: <https://doi.org/10.1016/j.compositesb.2020.107744>.
- [52] Behera PK, Mondal P, Singha NK. Self-healable and ultrahydrophobic polyurethane-POSS hybrids by Diels-Alder “Click” reaction: a new class of coating material. *Macromolecules* 2018;51(13):4770–81. Available from: <https://doi.org/10.1021/acs.macromol.8b00583>.
- [53] Zhao D, Du Z, Liu S, Wu Y, Guan T, Sun Q, et al. UV light curable self-healing superamphiphobic coatings by photopromoted disulfide exchange reaction. *ACS Appl Polym Mater* 2019;1(11):2951–60. Available from: <https://doi.org/10.1021/acsapm.9b00656>.
- [54] Zhao X, Wei J, Li B, Li S, Tian N, Jing L, et al. A self-healing superamphiphobic coating for efficient corrosion protection of magnesium alloy. *J Colloid Interface Sci* 2020;575:140–9. Available from: <https://doi.org/10.1016/j.jcis.2020.04.097>.
- [55] Naveed M, Rabnawaz M, Khan A, Tuhi MO. Dual-layer approach toward self-healing and self-cleaning polyurethane thermosets. *Polymers (Basel)* 2019;11(11):1849. Available from: <https://doi.org/10.3390/polym11111849>.
- [56] Li K, Liu Z, Wang C, Fan W, Liu F, Li H, et al. Preparation of smart coatings with self-healing and anti-wear properties by embedding PU-fly ash absorbing linseed oil microcapsules. *Prog Org Coat* 2020;145:105668. Available from: <https://doi.org/10.1016/j.porgcoat.2020.105668>.
- [57] Li H, Cui Y, Li Z, Zhu Y, Wang H. Fabrication of microcapsules containing dual-functional tung oil and properties suitable for self-healing and self-lubricating coatings. *Prog Org Coat* 2018;115:164–71. Available from: <https://doi.org/10.1016/j.porgcoat.2017.11.019>.
- [58] Yang H, Mo Q, Li W, Gu F. Preparation and properties of self-healing and self-lubricating epoxy coatings with polyurethane microcapsules containing bifunctional linseed oil. *Polymer (Basel)* 2019;11(10):1578. Available from: <https://doi.org/10.3390/polym11101578>.
- [59] Li K, Li H, Cui Y, Li Z, Ji J, Feng Y, et al. Dual-functional coatings with self-lubricating and self-healing properties by combining poly(urea–formaldehyde)/SiO₂ hybrid microcapsules containing linseed oil. *Ind Eng Chem Res* 2019;58(48):22032–9. Available from: <https://doi.org/10.1021/acs.iecr.9b04736>.

- [60] Wu J, Zhang Q, Zhu T, Ge J, Zhou C. Development of novel self-healing and antibacterial resin composite containing microcapsules filled with polymerizable healing monomer. *Zhonghua Kou Qiang Yi Xue Za Zhi* 2015;50(8):469–73.
- [61] Kantheti S, Narayan R, Raju KVS. The impact of 1,2,3-triazoles in the design of functional coatings. *RSC Adv* 2015;5(5):3687–708. Available from: <https://doi.org/10.1039/c4ra12739k>.
- [62] Wu J-L, Li T, Gao X, Zhang Q, Liu D, Ge J-H, et al. Effect of water immersion on a dental self-healing and antibacterial resin composite. *Hua Xi Kou Qiang Yi Xue Za Zhi* 2018;36(5):521–7. Available from: <https://doi.org/10.7518/hxkq.2018.05.011>.
- [63] Lu L, Fan J, Li G. Intrinsic healable and recyclable thermoset epoxy based on shape memory effect and transesterification reaction. *Polymer* 2016;105:10–18. Available from: <https://doi.org/10.1016/j.polymer.2016.10.013>.
- [64] Huang Y, Deng L, Ju P, Huang L, Qian H, Zhang D, et al. Triple-action self-healing protective coatings based on shape memory polymers containing dual-function microspheres. *ACS Appl Mater Interfaces* 2018;10(27):23369–79. Available from: <https://doi.org/10.1021/acsami.8b06985>.
- [65] Fan W, Zhang Y, Li W, Wang W, Zhao X, Song L. Multi-level self-healing ability of shape memory polyurethane coating with microcapsules by induction heating. *Chem Eng J* 2019;368:1033–44. Available from: <https://doi.org/10.1016/j.cej.2019.03.027>.
- [66] Nguyen LT, Pham HQ, Phung DTT, Truong TT, Nguyen HT, Doan TCD, et al. Macromolecular design of a reversibly crosslinked shape-memory material with thermo-healability. *Polymer* 2020;188:122144. Available from: <https://doi.org/10.1016/j.polymer.2019.122144>.
- [67] Azcune I, Odrizola I. Aromatic disulfide crosslinks in polymer systems: self-healing, reprocessability, recyclability and more. *Eur Polym J* 2016;84:147–60. Available from: <https://doi.org/10.1016/j.eurpolymj.2016.09.023>.
- [68] Chen J-H, Hu D-D, Li Y-D, Meng F, Zhu J, Zeng J-B. Castor oil derived poly(urethane urea) networks with reprocessability and enhanced mechanical properties. *Polymer* 2018;143:79–86. Available from: <https://doi.org/10.1016/j.polymer.2018.04.013>.
- [69] Gao W, Bie M, Liu F, Chang P, Quan Y. Self-healable and reprocessable polysulfide sealants prepared from liquid polysulfide oligomer and epoxy resin. *ACS Appl Mater Interfaces* 2017;9(18):15798–808. Available from: <https://doi.org/10.1021/acsami.7b05285>.
- [70] Fan W, Jin Y, Shi L, Du W, Zhou R. Transparent, eco-friendly, super-tough “living” supramolecular polymers with fast room-temperature self-healability and reprocessability under visible light. *Polymer* 2020;190:122199. Available from: <https://doi.org/10.1016/j.polymer.2020.122199>.
- [71] Liu Q, Liu YB, Zheng H, Li CM, Zhang Y, Zhang QY. Design and development of self-repairable and recyclable crosslinked poly(thiourethane-urethane) via enhanced aliphatic disulfide chemistry. *J Polym Sci* 2020;58(8):1092–104. Available from: <https://doi.org/10.1002/pol.20190186>.
- [72] Li H, Cui Y, Wang H, Zhu Y, Wang B. Preparation and application of polysulfone microcapsules containing tung oil in self-healing and self-lubricating epoxy coating. *Colloids Surf A Physicochem Eng Asp* 2017;518:181–7. Available from: <https://doi.org/10.1016/j.colsurfa.2017.01.046>.
- [73] Zhang Y, Yuan L, Guan Q, Liang G, Gu A. Developing self-healable and antibacterial polyacrylate coatings with high mechanical strength through crosslinking by multi-amine hyperbranched polysiloxane via dynamic vinylogous urethane. *J Mater Chem A* 2017;5(32):16889–97. Available from: <https://doi.org/10.1039/C7TA04141A>.
- [74] Zamal HH, Barba D, Aïssa B, Haddad E, Rosei F. Recovery of electro-mechanical properties inside self-healing composites through microencapsulation of carbon nanotubes. *Sci Rep* 2020;10:2973. Available from: <https://doi.org/10.1038/s41598-020-59725-6>.
- [75] Qian Y, Zhou Y, Li L, Liu W, Yang D, Qiu X. Facile preparation of active lignin capsules for developing self-healing and UV-blocking polyurea coatings. *Prog Org Coat* 2020;138:105354. Available from: <https://doi.org/10.1016/j.porgcoat.2019.105354>.
- [76] Neisiany RE, Lee JKY, Khorasani SN, Ramakrishna S. Self-healing and interfacially toughened carbon fibre-epoxy composites based on electrospun core-shell nanofibres. *J Appl Polym Sci* 2017;134(31):44956. Available from: <https://doi.org/10.1002/App.44956>.
- [77] Qamar IPS, Sottos NR, Trask RS. Grand challenges in the design and manufacture of vascular self-healing. *Smart Mater Struct* 2020;3(1):13001. Available from: <https://doi.org/10.1088/2399-7532/ab69e2>.
- [78] Mahmood H, Dorigato A, Pegoretti A. Healable carbon fiber-reinforced epoxy/cyclic olefin copolymer composites. *Materials (Basel)* 2020;13(9):2165. Available from: <https://doi.org/10.3390/ma13092165>.
- [79] Zhang ZP, Rong MZ, Zhang MQ. Polymer engineering based on reversible covalent chemistry: a promising innovative pathway towards new materials and new functionalities. *Prog Polym Sci* 2018;80:39–93. Available from: <https://doi.org/10.1016/j.progpolymsci.2018.03.002>.
- [80] Scheutz GM, Lessard JJ, Sims MB, Sumerlin BS. Adaptable crosslinks in polymeric materials: resolving the intersection of thermoplastics and thermosets. *J Am Chem Soc* 2019;141(41):16181–96. Available from: <https://doi.org/10.1021/jacs.9b07922>.
- [81] Truong TT, Thai SH, Nguyen HT, Phung DTT, Nguyen LT, Pham HQ, et al. Tailoring the hard-soft interface with dynamic Diels-Alder linkages in polyurethanes: toward superior mechanical properties and healability at mild temperature. *Chem Mater* 2019;31(7):2347–57. Available from: <https://doi.org/10.1021/acs.chemmater.8b04624>.
- [82] Lin CH, Sheng DK, Liu XD, Xu SB, Ji FC, Dong L, et al. Coordination bonds and Diels-Alder bonds dual crosslinked polymer networks of self-healing polyurethane. *J Polym Sci Pol Chem* 2019;57(22):2228–34. Available from: <https://doi.org/10.1002/pola.29508>.
- [83] Luzuriaga AR, de Martin R, Markaide N, Rekondo A, Cabanero G, Rodriguez J, et al. Epoxy resin with exchangeable disulfide crosslinks to obtain reprocessable, repairable and recyclable fiber-reinforced thermoset composites. *Mater Horiz* 2016;3(3):241–7. Available from: <https://doi.org/10.1039/c6mh00029k>.
- [84] Post W, Cohades A, Michaud V, van der Zwaag S, Garcia SJ. Healing of a glass fibre reinforced composite with a disulphide containing organic-inorganic epoxy matrix. *Compos Sci Technol* 2017;152:85–93. Available from: <https://doi.org/10.1016/j.compscitech.2017.09.017>.
- [85] Hornat CC, Urban MW. Shape memory effects in self-healing polymers. *Prog Polym Sci* 2020;102:101208. Available from: <https://doi.org/10.1016/j.progpolymsci.2020.101208>.

- [86] Liu J, Ma X, Tong Y, Lang M. Self-healing polyurethane based on ditelluride bonds. *Appl Surf Sci* 2018;455:318–25. Available from: <https://doi.org/10.1016/j.apsusc.2018.05.159>.
- [87] Huang M, Yang J. Salt spray and EIS studies on HDI microcapsule-based self-healing anticorrosive coatings. *Prog Org Coat* 2014;77(1):168–75. Available from: <https://doi.org/10.1016/j.porgcoat.2013.09.002>.
- [88] Khorasani SN, Torkaman R, Neisiany RE, Koochaki MS. Self-healing performance of an epoxy coating containing microencapsulated alkyd resin based on coconut oil. *Prog Org Coat* 2018;120:160–6. Available from: <https://doi.org/10.1016/j.porgcoat.2018.03.024>.
- [89] Ma Y, Zhang Y, Liu J, Sun Y, Ge Y, Yan X, et al. Preparation and characterization of ethylenediamine-polyurea microcapsule epoxy self-healing coating. *Materials (Basel)* 2020;13(2):326. Available from: <https://doi.org/10.3390/ma13020326>.
- [90] Navarchian AH, Najafipour N, Ahangaran F. Surface-modified poly(methyl methacrylate) microcapsules containing linseed oil for application in self-healing epoxy-based coatings. *Prog Org Coat* 2019;132:288–97. Available from: <https://doi.org/10.1016/j.porgcoat.2019.03.029>.
- [91] Behzadnasab M, Mirabedini SM, Esfandeh M, Farnood RR. Evaluation of corrosion performance of a self-healing epoxy-based coating containing linseed oil-filled microcapsules via electrochemical impedance spectroscopy. *Prog Org Coat* 2017;105:212–24. Available from: <https://doi.org/10.1016/j.porgcoat.2017.01.006>.
- [92] Hasanzadeh M, Shahidi M, Kazempour M. Application of EIS and EN techniques to investigate the self-healing ability of coatings based on microcapsules filled with linseed oil and CeO₂ nanoparticles. *Prog Org Coat* 2015;80:106–19. Available from: <https://doi.org/10.1016/j.porgcoat.2014.12.002>.
- [93] Yi H, Yang Y, Gu X, Huang J, Wang C. Multilayer composite microcapsules synthesized by Pickering emulsion templates and their application in self-healing coating. *J Mater Chem A* 2015; 3(26):13749–57. Available from: <https://doi.org/10.1039/C5TA02288F>.
- [94] Wang J-P, Song X, Wang J-K, Cui X, Zhou Q, Qi T, et al. Smart-sensing polymer coatings with autonomously reporting corrosion dynamics of self-healing systems. *Adv Mater Interfaces* 2019;6(10):1900055. Available from: <https://doi.org/10.1002/admi.201900055>.
- [95] Saman NM, Ang DT-C, Shahabudin N, Gan SN, Basirun WJ. UV-curable alkyd coating with self-healing ability. *J Coat Technol Res* 2019;16(2):465–76. Available from: <https://doi.org/10.1007/s11998-018-0124-x>.
- [96] Babaei N, Yeganeh H, Gharibi R. Anticorrosive and self-healing waterborne poly(urethane-triazole) coatings made through a combination of click polymerization and cathodic electrophoretic deposition. *Eur Polym J* 2019;112:636–47. Available from: <https://doi.org/10.1016/j.eurpolymj.2018.10.028>.
- [97] (a) Bastos AC, Quevedo MC, Ferreira MGS. The influence of vibration and probe movement on SVET measurements. *Corros Sci* 2015;92:309–14. Available from: <https://doi.org/10.1016/j.corsci.2014.10.038>.
- (b) Bastos AC, Taryba MG, Karavai OV, Zheludkevich ML, Lamaka SV, Ferreira MGS. Micropotentiometric mapping of local distributions of Zn²⁺ relevant to corrosion studies. *Electrochem Commun* 2010;12(3):394–7. Available from: <https://doi.org/10.1016/j.elecom.2010.01.002>.
- (c) Simões AM, Bastos AC, Ferreira MG, González-García Y, González S, Souto RM. Use of SVET and SECM to study the galvanic corrosion of an iron–zinc cell. *Corros Sci* 2007;49(2):726–39. Available from: <https://doi.org/10.1016/j.corsci.2006.04.021>.
- (d) Bastos A. Application of SVET/SIET techniques to study healing processes in coated metal substrates. In: Klein L, Aparicio M, Jitianu A, editors. *Handbook of Sol-Gel Science and Technology*. Cham: Springer International Publishing; 2018. p. 1727–82.
- (e) Lamaka SV, Taryba M, Montemor MF, Isaacs HS, Ferreira MGS. Quasi-simultaneous measurements of ionic currents by vibrating probe and pH distribution by ion-selective micro-electrode. *Electrochem Commun* 2011;13(1):20–3. Available from: <https://doi.org/10.1016/j.elecom.2010.11.002>.
- [98] Attaei M, Calado LM, Taryba MG, Morozov Y, Shakoov RA, Kahraman R, et al. Autonomous self-healing in epoxy coatings provided by high efficiency isophorone diisocyanate (IPDI) microcapsules for protection of carbon steel. *Prog Org Coat* 2020;139:105445. Available from: <https://doi.org/10.1016/j.porgcoat.2019.105445>.
- [99] Zheng N, Qiao L, Liu J, Lu J, Li W, Li C, et al. Microcapsules of multilayered shell structure synthesized via one-part strategy and their application in self-healing coatings. *Compos Commun* 2019;12:26–32. Available from: <https://doi.org/10.1016/j.coco.2018.12.006>.
- [100] Hart KR, Sottos NR, White SR. Repeatable self-healing of an epoxy matrix using imidazole initiated polymerization. *Polymer* 2015;67:174–84. Available from: <https://doi.org/10.1016/j.polymer.2015.04.068>.
- [101] Sanders P, Young AJ, Qin Y, Fancey KS, Reithofer MR, Guillet-Nicolas R, et al. Stereolithographic 3D printing of extrinsically self-healing composites. *Sci Rep* 2019;9(1):388. Available from: <https://doi.org/10.1038/s41598-018-36828-9>.
- [102] Kosarlı M, Bekas DG, Tsirka K, Baltzis D, Vaimakis-Tsogkas DT, Orfanidis S, et al. Microcapsule-based self-healing materials: healing efficiency and toughness reduction vs. capsule size. *Compos Part B Eng* 2019;171:78–86. Available from: <https://doi.org/10.1016/j.compositesb.2019.04.030>.
- [103] Pingkarawat K, Wang CH, Varley RJ, Mouritz AP. Effect of mendable polymer stitch density on the toughening and healing of delamination cracks in carbon–epoxy laminates. *Compos Part A Appl Sci* 2013;50:22–30. Available from: <https://doi.org/10.1016/j.compositesa.2013.02.014>.
- [104] Hillewaere XKD, Du Prez FE. Fifteen chemistries for autonomous external self-healing polymers and composites. *Prog Polym Sci* 2015;49-50:121–53. Available from: <https://doi.org/10.1016/j.progpolymsci.2015.04.004>.
- [105] Thakre PR, Singh R, Slipher G, editors. *Mechanics of composite and multi-functional materials, Volume 6: Proceedings of the 2017 Annual Conference on Experimental and Applied Mechanics*. 1st ed. Cham: Springer International Publishing; 2018.
- [106] Brown EN. Use of the tapered double-cantilever beam geometry for fracture toughness measurements and its application to the quantification of self-healing. *J Strain Anal Eng Des* 2011;

- 46(3):167–86. Available from: <https://doi.org/10.1177/0309324710396018>.
- [107] Ling J, Rong MZ, Zhang MQ. Photo-stimulated self-healing polyurethane containing dihydroxyl coumarin derivatives. *Polymer* 2012;53(13):2691–8. Available from: <https://doi.org/10.1016/j.polymer.2012.04.016>.
- [108] Grande AM, Bijleveld JC, Garcia SJ, van der Zwaag S. A combined fracture mechanical – rheological study to separate the contributions of hydrogen bonds and disulphide linkages to the healing of poly(urea-urethane) networks. *Polymer* 2016;96:26–34. Available from: <https://doi.org/10.1016/j.polymer.2016.05.004>.
- [109] Menard KP. *Dynamic mechanical analysis*. CRC Press; 2008.
- [110] Diaz MM, Brancart J, van Assche G, van Mele B. Room-temperature versus heating-mediated healing of a Diels-Alder crosslinked polymer network. *Polymer* 2018;153:453–63. Available from: <https://doi.org/10.1016/j.polymer.2018.08.026>.
- [111] Gragert M, Schunack M, Binder WH. Azide/alkyne-“click”-reactions of encapsulated reagents: toward self-healing materials. *Macromol Rapid Commun* 2011;32(5):419–25. Available from: <https://doi.org/10.1002/marc.201000687>.
- [112] Brancart J, Verhelle R, Mangialotto J, van Assche G. Coupling the microscopic healing behaviour of coatings to the thermoreversible Diels-Alder network formation. *Coatings* 2019;9(1):13. Available from: <https://doi.org/10.3390/Coatings9010013>.
- [113] Macedo R, Lima G, Orozco F, Picchioni F, Moreno-Villoslada I, Pucci A, et al. Electrically self-healing thermoset MWCNTs composites based on Diels-Alder and hydrogen bonds. *Polym Int (Basel)* 2019;11(11):1885. Available from: <https://doi.org/10.3390/polym11111885>.
- [114] Zhou J, Yang Y, Qin R, Xu M, Sheng Y, Lu X. Robust poly(urethane-amide) protective film with fast self-healing at room temperature. *ACS Appl Polym Mater* 2020;2(2):285–94. Available from: <https://doi.org/10.1021/acsapm.9b00807>.
- [115] Lee S-H, Shin S-R, Lee D-S. Self-healing of cross-linked PU via dual-dynamic covalent bonds of a Schiff base from cystine and vanillin. *Mater Des* 2019;172:107774. Available from: <https://doi.org/10.1016/j.matdes.2019.107774>.
- [116] Miyano Y, Nakada M. Life prediction of CFRP laminates based on accelerated testing methodology. In: Antoun B, Arzoumanidis A, Qi HJ, Silberstein M, Amirkhizi A, Furmanski J, et al., editors. *Challenges in mechanics of time dependent materials*, Vol. 2. Cham: Springer International Publishing; 2017. p. 35–47.
- [117] Araya-Hermosilla R, Lima GMR, Raffa P, Fortunato G, Pucci A, Flores ME, et al. Intrinsic self-healing thermoset through covalent and hydrogen bonding interactions. *Eur Polym J* 2016;81:186–97. Available from: <https://doi.org/10.1016/j.eurpolymj.2016.06.004>.
- [118] Li T, Xie Z, Xu J, Weng Y, Guo B-H. Design of a self-healing cross-linked polyurea with dynamic cross-links based on disulfide bonds and hydrogen bonding. *Eur Polym J* 2018;107:249–57. Available from: <https://doi.org/10.1016/j.eurpolymj.2018.08.005>.
- [119] Yan T, Schröter K, Herbst F, Binder WH, Thurn-Albrecht T. Unveiling the molecular mechanism of self-healing in a telechelic, supramolecular polymer network. *Sci Rep* 2016;6:32356. Available from: <https://doi.org/10.1038/srep32356>.
- [120] Wang Z, Gu Y, Ma M, Chen M. Strong, reconfigurable, and recyclable thermosets cross-linked by polymer–polymer dynamic interaction based on commodity thermoplastics. *Macromolecules* 2020;53(3):956–64. Available from: <https://doi.org/10.1021/acs.macromol.9b02325>.
- [121] Delpierre S, Willocq B, Manini G, Lemaire V, Goole J, Gerbaux P, et al. Simple approach for a self-healable and stiff polymer network from iminoboronate-based boroxine chemistry. *Chem Mater* 2019;31(10):3736–44. Available from: <https://doi.org/10.1021/acs.chemmater.9b00750>.
- [122] Yuan C, Rong MZ, Zhang MQ. Self-healing polyurethane elastomer with thermally reversible alkoxyamines as crosslinkages. *Polymer* 2014;55(7):1782–91. Available from: <https://doi.org/10.1016/j.polymer.2014.02.033>.
- [123] Imato K, Takahara A, Otsuka H. Self-healing of a cross-linked polymer with dynamic covalent linkages at mild temperature and evaluation at macroscopic and molecular levels. *Macromolecules* 2015;48(16):5632–9. Available from: <https://doi.org/10.1021/acs.macromol.5b00809>.
- [124] Wang D-P, Lai J-C, Lai H-Y, Mo S-R, Zeng K-Y, Li C-H, et al. Distinct mechanical and self-healing properties in two polydimethylsiloxane coordination polymers with fine-tuned bond strength. *Inorg Chem* 2018;57(6):3232–42. Available from: <https://doi.org/10.1021/acs.inorgchem.7b03260>.
- [125] Burattini S, Greenland BW, Merino DH, Weng W, Seppala J, Colquhoun HM, et al. A healable supramolecular polymer blend based on aromatic pi-pi stacking and hydrogen-bonding interactions. *J Am Chem Soc* 2010;132(34):12051–8. Available from: <https://doi.org/10.1021/ja104446r>.
- [126] Feula A, Pethybridge A, Giannakopoulos I, Tang X, Chippindale A, Siviour CR, et al. A Thermoreversible supramolecular polyurethane with excellent healing ability at 45°C. *Macromolecules* 2015;48(17):6132–41. Available from: <https://doi.org/10.1021/acs.macromol.5b01162>.
- [127] Xiang Z, Zhang L, Li Y, Yuan T, Zhang W, Sun J. Reduced graphene oxide-reinforced polymeric films with excellent mechanical robustness and rapid and highly efficient healing properties. *ACS Nano* 2017;11(7):7134–41. Available from: <https://doi.org/10.1021/acsnano.7b02970>.
- [128] Fan C-J, Wen Z-B, Xu Z-Y, Xiao Y, Wu D, Yang K-K, et al. Adaptable strategy to fabricate self-healable and reprocessable poly(thiourethane-urethane) elastomers via reversible thiol–cyanate click chemistry. *Macromolecules* 2020;53(11):4284–93. Available from: <https://doi.org/10.1021/acs.macromol.0c00239>.
- [129] Wagner AM, Wagner S, Bredfeldt J-E, Mukherjee A, Kronenberger S, Braun K, et al. Chemical imaging of single anisotropic polystyrene/poly (methacrylate) microspheres with complex hierarchical architecture (2021); manuscript submitted to “Polymers”.
- [130] Schreiner C, Scharf S, Stenzel V, Rössler A. Self-healing through microencapsulated agents for protective coatings. *J Coat Technol Res* 2017;14(4):809–16. Available from: <https://doi.org/10.1007/s11998-017-9921-x>.
- [131] Kim SY, Sottos NR, White SR. Self-healing of fatigue damage in cross-ply glass/epoxy laminates. *Compos Sci Technol* 2019;175:122–7. Available from: <https://doi.org/10.1016/j.compscitech.2019.03.016>.

- [132] Hu M, Peil S, Xing Y, Döhler D, Caire da Silva L, Binder WH, et al. Monitoring crack appearance and healing in coatings with damage self-reporting nanocapsules. *Mater Horiz* 2018;5(1): 51–8. Available from: <https://doi.org/10.1039/C7MH00676D>.
- [133] Song YK, Lee TH, Kim JC, Lee KC, Lee S-H, Noh SM, et al. Dual monitoring of cracking and healing in self-healing coatings using microcapsules loaded with two fluorescent dyes. *Molecules* 2019;24(9):1679. Available from: <https://doi.org/10.3390/molecules24091679>.
- [134] Song YK, Kim B, Lee TH, Kim JC, Nam JH, Noh SM, et al. Fluorescence detection of microcapsule-type self-healing, based on aggregation-induced emission. *Macromol Rapid Commun* 2017; 38(6). Available from: <https://doi.org/10.1002/marc.201600657>.
- [135] Chen S, Han T, Zhao Y, Luo W, Zhang Z, Su H, et al. A facile strategy to prepare smart coatings with autonomous self-healing and self-reporting functions. *ACS Appl Mater Interfaces* 2020; 12(4):4870–7. Available from: <https://doi.org/10.1021/acsami.9b18919>.
- [136] Wang J-P, Wang J-K, Zhou Q, Li Z, Han Y, Song Y, et al. Adaptive polymeric coatings with self-reporting and self-healing dual functions from porous core-shell nanostructures. *Macromol Mater Eng* 2018;303(4):1700616. Available from: <https://doi.org/10.1002/mame.201700616>.
- [137] Vasiliu S, Kampe B, Theil F, Dietzek B, Döhler D, Michael P, et al. Insights into the mechanism of polymer coating self-healing using raman spectroscopy. *Appl Spectrosc* 2014;68(5): 541–8. Available from: <https://doi.org/10.1366/13-07332>.
- [138] Zedler L, Hager MD, Schubert US, Harrington MJ, Schmitt M, Popp J, et al. Monitoring the chemistry of self-healing by vibrational spectroscopy—current state and perspectives. *Mater Today* 2014;17(2):57–69. Available from: <https://doi.org/10.1016/j.mattod.2014.01.020>.
- [139] Willocq B, Khelifa F, Odent J, Lemaire V, Yang Y, Leclère P, et al. Mechanistic insights on spontaneous moisture-driven healing of urea-based polyurethanes. *ACS Appl Mater Interfaces* 2019;11(49):46176–82. Available from: <https://doi.org/10.1021/acsami.9b16858>.
- [140] Mallécol J, Lemaire J, Gardette J-L. Drier influence on the curing of linseed oil. *Prog Org Coat* 2000;39(2-4):107–13. Available from: [https://doi.org/10.1016/S0300-9440\(00\)00126-0](https://doi.org/10.1016/S0300-9440(00)00126-0).
- [141] Seniha Güner F, Yağcı Y, Tuncer, Erciyes A. Polymers from triglyceride oils. *Prog Polym Sci* 2006;31(7):633–70. Available from: <https://doi.org/10.1016/j.progpolymsci.2006.07.001>.
- [142] Hillewaere XKD, Teixeira RFA, Nguyen LTT, Ramos JA, Rahier H, Du Prez FE. Autonomous self-healing of epoxy thermosets with thiol-isocyanate chemistry. *Adv Funct Mater* 2014;24(35):5575–83. Available from: <https://doi.org/10.1002/adfm.201400580>.
- [143] Billiet S, van Camp W, Hillewaere XKD, Rahier H, Du Prez FE. Development of optimized autonomous self-healing systems for epoxy materials based on maleimide chemistry. *Polymer* 2012; 53(12):2320–6. Available from: <https://doi.org/10.1016/j.polymer.2012.03.061>.
- [144] Tripathi M, Kumar D, Rajagopal C, Roy PK. Curing kinetics of self-healing epoxy thermosets. *J Therm Anal Calorim* 2015; 119(1):547–55. Available from: <https://doi.org/10.1007/s10973-014-4128-1>.
- [145] Kwon HJ, Lee EJ, Kim MR, Cheon KH, Park HJ, Lee KY. Encapsulation of peroxide initiator in a polyurea shell: its characteristics and effect on MMA polymerization kinetics. *Macromol Res* 2019;27(2):198–204. Available from: <https://doi.org/10.1007/s13233-019-7094-4>.
- [146] Yuan L, Sun T, Hu H, Yuan S, Yang Y, Wang R, et al. Preparation and characterization of microencapsulated ethylenediamine with epoxy resin for self-healing composites. *Sci Rep* 2019;9(1):18834. Available from: <https://doi.org/10.1038/s41598-019-55268-7>.
- [147] Yi H, Deng Y, Wang C. Pickering emulsion-based fabrication of epoxy and amine microcapsules for dual core self-healing coating. *Compos Sci Technol* 2016;133:51–9. Available from: <https://doi.org/10.1016/j.compscitech.2016.07.022>.
- [148] Tong XM, Zhang M, Yang MZ. Study on the curing kinetics of epoxy resin in self-healing microcapsules with different shell material. *Adv Mater Res* 2011;306-307:658–62. Available from: <https://doi.org/10.4028/www.scientific.net/AMR.306-307.658>.
- [149] Wang X, Zhang M, Xing F, Han N. Effect of a healing agent on the curing reaction kinetics and its mechanism in a self-healing system. *Appl Sci* 2018;8(11):2241. Available from: <https://doi.org/10.3390/app8112241>.
- [150] Lee TH, Park YI, Noh SM, Kim JC. In-situ visualization of the kinetics of low temperature thiol-epoxy crosslinking reactions by using a pH-responsive epoxy resin. *Prog Org Coat* 2017;104:20–7. Available from: <https://doi.org/10.1016/j.porgcoat.2016.11.007>.
- [151] Neuser S, Chen PW, Studart AR, Michaud V. Fracture toughness healing in epoxy containing both epoxy and amine loaded capsules. *Adv Eng Mater* 2014;16(5):581–7. Available from: <https://doi.org/10.1002/adem.201300422>.
- [152] Wang X, Yin H, Chen Z, Xia L. Epoxy resin/ethyl cellulose microcapsules prepared by solvent evaporation for repairing microcracks: particle properties and slow-release performance. *Mater Today Commun* 2020;22:100854. Available from: <https://doi.org/10.1016/j.mtcomm.2019.100854>.
- [153] Sun D, An J, Wu G, Yang J. Double-layered reactive microcapsules with excellent thermal and non-polar solvent resistance for self-healing coatings. *J Mater Chem A* 2015;3(8):4435–44. Available from: <https://doi.org/10.1039/C4TA05339G>.
- [154] Song Y, Chen K-F, Wang J-J, Liu Y, Qi T, Li GL. Synthesis of polyurethane/poly(urea-formaldehyde) double-shelled microcapsules for self-healing anticorrosion coatings. *Chin J Polym Sci* 2020;38(1):45–52. Available from: <https://doi.org/10.1007/s10118-019-2317-x>.
- [155] Ma Y, Zhang Y, Liu J, Ge Y, Yan X, Sun Y, et al. GO-modified double-walled polyurea microcapsules/epoxy composites for marine anticorrosive self-healing coating. *Mater Des* 2020;189:108547. Available from: <https://doi.org/10.1016/j.matdes.2020.108547>.
- [156] Gao L, Yang Y, Xie J, Zhang S, Hu J, Zeng R, et al. Autonomous self-healing of electrical degradation in dielectric polymers using in situ electroluminescence. *Matter* 2020; 2(2):451–63. Available from: <https://doi.org/10.1016/j.matt.2019.11.012>.
- [157] Bolimowski PA, Bond IP, Wass DF. Robust synthesis of epoxy resin-filled microcapsules for application to self-healing

- materials. *Philos Trans A Math Phys Eng Sci* 2016;374(2061). Available from: <https://doi.org/10.1098/rsta.2015.0083>.
- [158] Chenpeng Y, Chengfei Z, Baoqing H. Preparation process of epoxy resin microcapsules for self-healing coatings. *Prog Org Coat* 2019;132:440–4. Available from: <https://doi.org/10.1016/j.porgcoat.2019.04.015>.
- [159] Chuanjie F, Xiaodong Z. Preparation and barrier properties of the microcapsules added nanoclays in the wall. *Polym Adv Technol* 2009;20(12):934–9. Available from: <https://doi.org/10.1002/pat.1342>.
- [160] Esser-Kahn AP, Odom SA, Sottos NR, White SR, Moore JS. Triggered release from polymer capsules. *Macromolecules* 2011;44(14):5539–53. Available from: <https://doi.org/10.1021/ma201014n>.
- [161] Zhu DY, Wetzal B, Noll A, Rong MZ, Zhang MQ. Thermomolded self-healing thermoplastics containing multilayer microreactors. *J Mater Chem A* 2013;1(24):7191. Available from: <https://doi.org/10.1039/C3TA11008G>.
- [162] Tian R, Fu X, Zheng Y, Liang X, Wang Q, Ling Y, et al. The preparation and characterization of double-layer microcapsules used for the self-healing of resin matrix composites. *J Mater Chem* 2012;22(48):25437. Available from: <https://doi.org/10.1039/C2JM34195F>.
- [163] He Z, Jiang S, An N, Li X, Li Q, Wang J, et al. Self-healing isocyanate microcapsules for efficient restoration of fracture damage of polyurethane and epoxy resins. *J Mater Sci* 2019;54(11):8262–75. Available from: <https://doi.org/10.1007/s10853-018-03236-3>.
- [164] Zhou X, Li W, Zhu L, Ye H, Liu H. Polymer–silica hybrid self-healing nano/microcapsules with enhanced thermal and mechanical stability. *RSC Adv* 2019;9(4):1782–91. Available from: <https://doi.org/10.1039/C8RA08396G>.
- [165] Gao L, He J, Hu J, Wang C. Photoresponsive self-healing polymer composite with photoabsorbing hybrid microcapsules. *ACS Appl Mater Interfaces* 2015;7(45):25546–52. Available from: <https://doi.org/10.1021/acsami.5b09121>.
- [166] Anglani G, Tulliani J-M, Antonaci P. Behaviour of Pre-Cracked Self-Healing Cementitious Materials under Static and Cyclic Loading. *Materials (Basel)* 2020;13(5):1149. Available from: <https://doi.org/10.3390/ma13051149>.
- [167] Xue Y, Li C, Liu J, Tan J, Su Z, Yang Y, et al. Fabrication and characterization of hierarchical microcapsules with multi-storage cells for repeatable self-healing. *Colloids Surf A Physicochem Eng Asp* 2020;603:125201. Available from: <https://doi.org/10.1016/j.colsurfa.2020.125201>.
- [168] Lee Hia I, Chan E-S, Chai S-P, Pasbakhsh P. A novel repeated self-healing epoxy composite with alginate multicore microcapsules. *J Mater Chem A* 2018;6(18):8470–8. Available from: <https://doi.org/10.1039/c8ta01783b>.
- [169] de Carvalho ACM, Ferreira EPdC, Bomio M, Melo JDD, Cysne Barbosa AP, Costa MCB. Influence of synthesis parameters on properties and characteristics of poly (urea-formaldehyde) microcapsules for self-healing applications. *J Microencapsul* 2019;36(4):410–19. Available from: <https://doi.org/10.1080/02652048.2019.1638462>.
- [170] Ulutan S. Encapsulation of linseed oil and linseed oil based alkyd resin by urea formaldehyde shell for self-healing systems. *Prog Org Coat* 2018;121:190–200. Available from: <https://doi.org/10.1016/j.porgcoat.2018.04.027>.
- [171] Bah MG, Bilal HM, Wang J. Fabrication and application of complex microcapsules: a review. *Soft Matter* 2020;16(3):570–90. Available from: <https://doi.org/10.1039/C9SM01634A>.
- [172] Zhu DY, Rong MZ, Zhang MQ. Self-healing polymeric materials based on microencapsulated healing agents: from design to preparation. *Prog Polym Sci* 2015;49-50:175–220. Available from: <https://doi.org/10.1016/j.progpolymsci.2015.07.002>.
- [173] Guo W, Jia Y, Tian K, Xu Z, Jiao J, Li R, et al. UV-triggered self-healing of a single robust SiO₂ microcapsule based on cationic polymerization for potential application in aerospace coatings. *ACS Appl Mater Interfaces* 2016;8(32):21046–54. Available from: <https://doi.org/10.1021/acsami.6b06091>.
- [174] Song Y-K, Chung C-M. Repeatable self-healing of a microcapsule-type protective coating. *Polym Chem-Uk* 2013;4(18):4940. Available from: <https://doi.org/10.1039/C3PY00102D>.
- [175] van den Dungen ETA. Self-healing coatings based on thiol-ene chemistry [PhD thesis]. Stellenbosch: University of Stellenbosch; 2009.
- [176] van den Dungen ETA, Loos B, Klumperman B. Use of a fluorophore for visualization of the rupture of capsules in self-healing coatings. *Macromol Rapid Commun* 2010;31(7):625–8. Available from: <https://doi.org/10.1002/marc.200900728>.
- [177] Esfandeh M, Mirabedini SM, Zohuriaan-Mehr MJ, Farnood RR. Preparation and characterization of linseed oil-filled urea–formaldehyde microcapsules and their effect on mechanical properties of an epoxy-based coating. *Colloids Surf A Physicochem Eng Asp* 2014;457:16–26. Available from: <https://doi.org/10.1016/j.colsurfa.2014.05.033>.
- [178] Shahabudin N, Yahya R, Gan SN. Microcapsules filled with a palm oil-based alkyd as healing agent for epoxy matrix. *Polymer (Basel)* 2016;8(4):125. Available from: <https://doi.org/10.3390/polym8040125>.
- [179] Zhang C, Wang H, Zhou Q. Preparation and characterization of microcapsules based self-healing coatings containing epoxy ester as healing agent. *Prog Org Coat* 2018;125:403–10. Available from: <https://doi.org/10.1016/j.porgcoat.2018.09.028>.
- [180] Wu J, Weir MD, Zhang Q, Zhou C, Melo MAS, Xu HHK. Novel self-healing dental resin with microcapsules of polymerizable triethylene glycol dimethacrylate and N,N-dihydroxyethyl-p-toluidine. *Dent Mater* 2016;32(2):294–304. Available from: <https://doi.org/10.1016/j.dental.2015.11.014>.
- [181] Pratama PA, Sharifi M, Peterson AM, Palmese GR. Room temperature self-healing thermoset based on the Diels-Alder reaction. *ACS Appl Mater Interfaces* 2013;5(23):12425–31. Available from: <https://doi.org/10.1021/am403459e>.
- [182] Szmeczyk T, Sienkiewicz N, Strzelec K. Polythiourethane microcapsules as novel self-healing systems for epoxy coatings. *Polym Bull* 2018;75(1):149–65. Available from: <https://doi.org/10.1007/s00289-017-2021-3>.
- [183] Jackson AC, Bartelt JA, Marczewski K, Sottos NR, Braun PV. Silica-protected micron and sub-micron capsules and particles for self-healing at the microscale. *Macromol Rapid Commun* 2011;32(1):82–7. Available from: <https://doi.org/10.1002/marc.201000468>.

- [184] Vintila IS, Iovu H, Alcea A, Cucuruz A, Mandoc AC, Vasile BS. The synthetization and analysis of dicyclopentadiene and ethylidene-norbornene microcapsule systems. *Polymer (Basel)* 2020;12(5):1052. Available from: <https://doi.org/10.3390/polym12051052>.
- [185] Ye XJ, Zhang J-L, Zhu Y, Rong MZ, Zhang MQ, Song YX, et al. Ultrafast self-healing of polymer toward strength restoration. *ACS Appl Mater Interfaces* 2014;6(5):3661–70. Available from: <https://doi.org/10.1021/am405989b>.
- [186] Song YX, Ye XJ, Rong MZ, Zhang MQ. Self-healing epoxy with a fast and stable extrinsic healing system based on BF₃-amine complex. *RSC Adv* 2016;6(103):100796–803. Available from: <https://doi.org/10.1039/C6RA17976B>.
- [187] Li Q, Siddaramaiah, Kim NH, Hui D, Lee JH. Effects of dual component microcapsules of resin and curing agent on the self-healing efficiency of epoxy. *Compos Part B Eng* 2013;55:79–85. Available from: <https://doi.org/10.1016/j.compositesb.2013.06.006>.
- [188] Jin HH, Mangun CL, Stradley DS, Moore JS, Sottos NR, White SR. Self-healing thermoset using encapsulated epoxy-amine healing chemistry. *Polymer* 2012;53(2):581–7. Available from: <https://doi.org/10.1016/j.polymer.2011.12.005>.
- [189] Bijlard AC, Kaltbeitzel A, Avlasevich Y, Crespy D, Hamm M, Landfester K, et al. Dual-compartment nanofibres: separation of two highly reactive components in close vicinity. *RSC Adv* 2015;5(118):97477–84. Available from: <https://doi.org/10.1039/c5ra17750b>.
- [190] Neisiany RE, Khorasani SN, Lee JKY, Ramakrishna S. Encapsulation of epoxy and amine curing agent in PAN nanofibers by coaxial electrospinning for self-healing purposes. *RSC Adv* 2016;6(74):70056–63. Available from: <https://doi.org/10.1039/c6ra06434e>.
- [191] Khorasani SN, Rahnema H, Neisiany RE, Koochaki MS. Single microcapsules containing epoxy healing agent used for development in the fabrication of cost efficient self-healing epoxy coating. *Prog Org Coat* 2018;114:40–6. Available from: <https://doi.org/10.1016/j.porgcoat.2017.09.019>.
- [192] Khan NI, Halder S, Goyat MS. Influence of dual-component microcapsules on self-healing efficiency and performance of metal-epoxy composite-lap joints. *J Adhes* 2017;93(12):949–63. Available from: <https://doi.org/10.1080/00218464.2016.1193806>.
- [193] Ignatenko VY, Ilyin SO, Kostyuk AV, Bondarenko GN, Antonov SV. Acceleration of epoxy resin curing by using a combination of aliphatic and aromatic amines. *Polym Bull* 2020;77(3):1519–40. Available from: <https://doi.org/10.1007/s00289-019-02815-x>.
- [194] Parsaee S, Mirabedini SM, Farnood R, Alizadegan F. Development of self-healing coatings based on urea-formaldehyde/polyurethane microcapsules containing epoxy resin. *J Appl Polym Sci* 2020;137(41):49663. Available from: <https://doi.org/10.1002/app.49663>.
- [195] Yuan YC, Rong MZ, Zhang MQ, Yang GC. Study of factors related to performance improvement of self-healing epoxy based on dual encapsulated healant. *Polymer* 2009;50(24):5771–81. Available from: <https://doi.org/10.1016/j.polymer.2009.10.019>.
- [196] Ghazali H, Ye L, Zhang MQ. Interlaminar fracture of CF/EP composite containing a dual-component microencapsulated self-healant. *Compos Part A Appl Sci* 2016;82:226–34. Available from: <https://doi.org/10.1016/j.compositesa.2015.12.012>.
- [197] Sadeghi SAM, Borhani S, Zadhoush A, Dinari M. Single nozzle electrospinning of encapsulated epoxy and mercaptan in PAN for self-healing application. *Polymer* 2020;186:122007. Available from: <https://doi.org/10.1016/j.polymer.2019.122007>.
- [198] Hia IL, Pasbakhsh P, Chan E-S, Chai S-P. Electrospayed multi-core alginate microcapsules as novel self-healing containers. *Sci Rep* 2016;6:34674. Available from: <https://doi.org/10.1038/srep34674>.
- [199] Yuan YC, Rong MZ, Zhang MQ, Chen J, Yang GC, Li XM. Self-healing polymeric materials using epoxy/mercaptan as the healant. *Macromolecules* 2008;41(14):5197–202. Available from: <https://doi.org/10.1021/ma800028d>.
- [200] Ghazali H, Ye L, Zhang MQ. Mode II interlaminar fracture toughness of CF/EP composite containing microencapsulated healing resins. *Compos Sci Technol* 2017;142:275–85. Available from: <https://doi.org/10.1016/j.compscitech.2017.02.018>.
- [201] Yuan YC, Rong MZ, Zhang MQ, Yang GC, Zhao JQ. Self-healing of fatigue crack in epoxy materials with epoxy/mercaptan system. *Express Polym Lett* 2011;5(1):47–59. Available from: <https://doi.org/10.3144/expresspolymlett.2011.6>.
- [202] Guo M, Li W, Han N, Wang J, Su J, Li J, et al. Novel dual-component microencapsulated hydrophobic amine and microencapsulated isocyanate used for self-healing anti-corrosion coating. *Polymer (Basel)* 2018;10(3):319. Available from: <https://doi.org/10.3390/polym10030319>.
- [203] Guo M, He Y, Wang J, Zhang X, Li W. Microencapsulation of oil soluble polyaspartic acid ester and isophorone diisocyanate and their application in self-healing anticorrosive epoxy resin. *J Appl Polym Sci* 2020;137(12):48478. Available from: <https://doi.org/10.1002/app.48478>.
- [204] Kargarfard N, Diedrich N, Rupp H, Döhler D, Binder WH. Improving kinetics of “Click-Crosslinking” for self-healing nanocomposites by graphene-supported Cu-nanoparticles. *Polymers (Basel)* 2017;10(1):17. Available from: <https://doi.org/10.3390/polym10010017>.
- [205] Schunack M, Gragert M, Döhler D, Michael P, Binder WH. Low-temperature Cu(I)-catalyzed “Click” reactions for self-healing polymers. *Macromol Chem Phys* 2012;213(2):205–14. Available from: <https://doi.org/10.1002/macp.201100377>.
- [206] Dohler D, Michael P, Binder WH. Autocatalysis in the room temperature copper(I)-catalyzed alkyne-azide “Click” cycloaddition of multivalent poly(acrylate)s and poly(isobutylene)s. *Macromolecules* 2012;45(8):3335–45. Available from: <https://doi.org/10.1021/ma300405v>.
- [207] Saikia BJ, Dolui SK. Preparation and characterization of an azide-alkyne cycloaddition based self-healing system via a semiencapsulation method. *RSC Adv* 2015;5(112):92480–9. Available from: <https://doi.org/10.1039/c5ra17666b>.
- [208] White SR, Moore JS, Sottos NR, Krull BP, Santa Cruz WA, Gergely RCR. Restoration of large damage volumes in polymers. *Science* 2014;344(6184):620–3. Available from: <https://doi.org/10.1126/science.1251135>.
- [209] Lee MW, An S, Lee C, Liou M, Yarin AL, Yoon SS. Hybrid self-healing matrix using core-shell nanofibers and capsuleless microdroplets. *ACS Appl Mater Interfaces* 2014;6(13):10461–8. Available from: <https://doi.org/10.1021/am5020293>.

- [210] Kim D-M, Cho Y-J, Choi J-Y, Kim B-J, Jin S-W, Chung C-M. Low-temperature self-healing of a microcapsule-type protective coating. *Materials (Basel)* 2017;10(9):1079. Available from: <https://doi.org/10.3390/ma10091079>.
- [211] Bleay SM, Loader CB, Hawyes VJ, Humberstone L, Curtis PT. A smart repair system for polymer matrix composites. *Compos Part A Appl Sci* 2001;32(12):1767–76. Available from: [https://doi.org/10.1016/S1359-835X\(01\)00020-3](https://doi.org/10.1016/S1359-835X(01)00020-3).
- [212] Williams HR, Trask RS, Bond IP. Self-healing composite sandwich structures. *Smart Mater Struct* 2007;16(4):1198–207. Available from: <https://doi.org/10.1088/0964-1726/16/4/031>.
- [213] Williams HR, Trask RS, Bond IP. Self-healing sandwich panels: restoration of compressive strength after impact. *Compos Sci Technol* 2008;68(15-16):3171–7. Available from: <https://doi.org/10.1016/j.compscitech.2008.07.016>.
- [214] Williams HR, Trask RS, Knights AC, Williams ER, Bond IP. Biomimetic reliability strategies for self-healing vascular networks in engineering materials. *J R Soc Interface* 2008;5(24):735–47. Available from: <https://doi.org/10.1098/rsif.2007.1251>.
- [215] Patrick JF, Sottos NR, White SR. Microvascular based self-healing polymeric foam. *Polymer* 2012;53(19):4231–40. Available from: <https://doi.org/10.1016/j.polymer.2012.07.021>.
- [216] Theriault D, White SR, Lewis JA. Chaotic mixing in three-dimensional microvascular networks fabricated by direct-write assembly. *Nat Mater* 2003;2(4):265–71. Available from: <https://doi.org/10.1038/nmat863>.
- [217] Theriault D, Shepherd RF, White SR, Lewis JA. Fugitive inks for direct-write assembly of three-dimensional microvascular networks. *Adv Mater* 2005;17(4):395–9. Available from: <https://doi.org/10.1002/adma.200400481>.
- [218] Hamilton AR, Sottos NR, White SR. Self-healing of internal damage in synthetic vascular materials. *Adv Mater Weinh* 2010;22(45):5159–63. Available from: <https://doi.org/10.1002/adma.201002561>.
- [219] Hansen CJ, Wu W, Toohey KS, Sottos NR, White SR, Lewis JA. Self-healing materials with interpenetrating microvascular networks. *Adv Mater* 2009;21(41):4143–7. Available from: <https://doi.org/10.1002/adma.200900588>.
- [220] Toohey KS, Hansen CJ, Lewis JA, White SR, Sottos NR. Delivery of two-part self-healing chemistry via microvascular networks. *Adv Funct Mater* 2009;19(9):1399–405. Available from: <https://doi.org/10.1002/adfm.200801824>.
- [221] Toohey KS, Sottos NR, Lewis JA, Moore JS, White SR. Self-healing materials with microvascular networks. *Nat Mater* 2007;6(8):581–5. Available from: <https://doi.org/10.1038/nmat1934>.
- [222] Kousourakis A, Mouritz AP, Bannister MK. Interlaminar properties of polymer laminates containing internal sensor cavities. *Compos Struct* 2006;75(1-4):610–18. Available from: <https://doi.org/10.1016/j.compstruct.2006.04.086>.
- [223] Kousourakis A, Bannister MK, Mouritz AP. Tensile and compressive properties of polymer laminates containing internal sensor cavities. *Compos Part A Appl Sci* 2008;39(9):1394–403. Available from: <https://doi.org/10.1016/j.compositesa.2008.05.003>.
- [224] Norris CJ, Bond IP, Trask RS. Interactions between propagating cracks and bioinspired self-healing vasculature embedded in glass fibre reinforced composites. *Compos Sci Technol* 2011;71(6):847–53. Available from: <https://doi.org/10.1016/j.compscitech.2011.01.027>.
- [225] Norris CJ, Bond IP, Trask RS. The role of embedded bioinspired vasculature on damage formation in self-healing carbon fibre reinforced composites. *Compos Part A Appl Sci* 2011;42(6):639–48. Available from: <https://doi.org/10.1016/j.compositesa.2011.02.003>.
- [226] Huang C-Y, Trask RS, Bond IP. Characterization and analysis of carbon fibre-reinforced polymer composite laminates with embedded circular vasculature. *J R Soc Interface* 2010;7(49):1229–41. Available from: <https://doi.org/10.1098/rsif.2009.0534>.
- [227] Kolb HC, Finn MG, Sharpless KB. Click chemistry: diverse chemical function from a few good reactions. *Angew Chem Int Ed* 2001;40(11):2004–21. [https://doi.org/10.1002/1521-3773\(20010601\)40:11<2004:AID-ANIE2004>3.0.CO;2-5](https://doi.org/10.1002/1521-3773(20010601)40:11<2004:AID-ANIE2004>3.0.CO;2-5).
- [228] Schafer S, Kickelbick G. Double reversible networks: improvement of self-healing in hybrid materials via combination of Diels-Alder cross-linking and hydrogen bonds. *Macromolecules* 2018;51(15):6099–110. Available from: <https://doi.org/10.1021/acs.macromol.8b00601>.
- [229] Liu J, Cao J, Zhou Z, Liu R, Yuan Y, Liu X. Stiff self-healing coating based on UV-curable polyurethane with a “Hard Core, Flexible Arm” structure. *ACS Omega* 2018;3(9):11128–35. Available from: <https://doi.org/10.1021/acsomega.8b00925>.
- [230] Cheng CJ, Li J, Yang FH, Li YP, Hu ZY, Wang JL. Renewable eugenol-based functional polymers with self-healing and high temperature resistance properties. *J Polym Res* 2018;25(2):57. Available from: <https://doi.org/10.1007/s10965-018-1460-3>.
- [231] Zhu M, Liu J, Gan L, Long M. Research progress in bio-based self-healing materials. *Eur Polym J* 2020;129:109651. Available from: <https://doi.org/10.1016/j.eurpolymj.2020.109651>.
- [232] Chen SB, Schulz M, Lechner BD, Appiah C, Binder WH. One-pot synthesis and self-assembly of supramolecular dendritic polymers. *Polym Chem-Uk* 2015;6(46):7988–94. Available from: <https://doi.org/10.1039/c5py01329a>.
- [233] Wang Z, Yang H, Fairbanks BD, Liang H, Ke J, Zhu C. Fast self-healing engineered by UV-curable polyurethane contained Diels-Alder structure. *Prog Org Coat* 2019;131:131–6. Available from: <https://doi.org/10.1016/j.porgcoat.2019.02.021>.
- [234] Truong TT, Nguyen HT, Phan MN, Nguyen LTT. Study of Diels-Alder reactions between furan and maleimide model compounds and the preparation of a healable thermo-reversible polyurethane. *J Polym Sci Pol Chem* 2018;56(16):1806–14. Available from: <https://doi.org/10.1002/pola.29061>.
- [235] Li X, Yu R, He Y, Zhang Y, Yang X, Zhao X, et al. Four-dimensional printing of shape memory polyurethanes with high strength and recyclability based on Diels-Alder chemistry. *Polymer* 2020;200:122532. Available from: <https://doi.org/10.1016/j.polymer.2020.122532>.
- [236] Fang YL, Du XS, Cheng X, Zhou M, Du ZL, Wang HB. Preparation of living and highly stable blended polyurethane emulsions for self-healing films with enhanced toughness and recyclability. *Polymer* 2020;188:122142. Available from: <https://doi.org/10.1016/j.polymer.2019.122142>.
- [237] Lee D-I, Kim S-H, Lee D-S. Synthesis and characterization of healable waterborne polyurethanes with cystamine chain

- extenders. *Molecules* 2019;24(8):1492. Available from: <https://doi.org/10.3390/molecules24081492>.
- [238] Nevejans S, Ballard N, Fernández M, Reck B, Asua JM. Flexible aromatic disulfide monomers for high-performance self-healable linear and cross-linked poly(urethane-urea) coatings. *Polymer* 2019;166:229–38. Available from: <https://doi.org/10.1016/j.polymer.2019.02.001>.
- [239] Zhang M, Zhao F, Luo Y. Self-healing mechanism of micro-cracks on waterborne polyurethane with tunable disulfide bond contents. *ACS Omega* 2019;4(1):1703–14. Available from: <https://doi.org/10.1021/acsomega.8b02923>.
- [240] Cao S, Li SH, Li M, Xu LN, Ding HY, Xia JL, et al. The thermal self-healing properties of phenolic polyurethane derived from polyphenols with different substituent groups. *J Appl Polym Sci* 2019;136(6):47039. Available from: <https://doi.org/10.1002/App.47039>.
- [241] Cao S, Li SH, Li M, Xu LN, Ding HY, Xia JL, et al. A thermal self-healing polyurethane thermoset based on phenolic urethane. *Polym J* 2017;49(11):775–81. Available from: <https://doi.org/10.1038/pj.2017.48>.
- [242] Lee D-W, Kim H-N, Lee D-S. Introduction of reversible urethane bonds based on vanillyl alcohol for efficient self-healing of polyurethane elastomers. *Molecules* 2019;24(12):2201. Available from: <https://doi.org/10.3390/molecules24122201>.
- [243] Li M, Ding H, Yang X, Xu L, Xia J, Li S. Preparation and properties of self-healing polyurethane elastomer derived from tung-oil-based polyphenol. *ACS Omega* 2019;5(1):529–36. Available from: <https://doi.org/10.1021/acsomega.9b03082>.
- [244] Cuevas JM, Seoane-Rivero R, Navarro R, Marcos-Fernández Á. Coumarins into polyurethanes for smart and functional materials. *Polymers (Basel)* 2020;12(3):630. Available from: <https://doi.org/10.3390/polym12030630>.
- [245] Bai N, Simon GP, Saito K. Characterisation of the thermal self-healing of a high crosslink density epoxy thermoset. *N J Chem* 2015;39(5):3497–506. Available from: <https://doi.org/10.1039/c5nj00066a>.
- [246] Zolghadr M, Shakeri A, Zohuriaan-Mehr MJ, Salimi A. Self-healing semi-IPN materials from epoxy resin by solvent-free furan-maleimide Diels-Alder polymerization. *J Appl Polym Sci* 2019;136(40):48015. Available from: <https://doi.org/10.1002/App.48015>.
- [247] Li JH, Zhang GP, Deng LB, Jiang K, Zhao SF, Gao YJ, et al. Thermally reversible and self-healing novolac epoxy resins based on Diels-Alder chemistry. *J Appl Polym Sci* 2015;132(26):42167. Available from: <https://doi.org/10.1002/App.42167>.
- [248] Pratama PA, Peterson AM, Palmese GR. Diffusion and reaction phenomena in solution-based healing of polymer coatings using the Diels-Alder reaction. *Macromol Chem Phys* 2012;213(2):173–81. Available from: <https://doi.org/10.1002/macp.201100407>.
- [249] Peterson AM, Jensen RE, Palmese GR. Kinetic considerations for strength recovery at the fiber-matrix interface based on the Diels-Alder reaction. *ACS Appl Mater Interfaces* 2013;5(3):815–21. Available from: <https://doi.org/10.1021/am302383v>.
- [250] Wang XF, Zhao KF, Huang XW, Ma XY, Wei YY. Preparation and properties of self-healing polyether amines based on Diels-Alder reversible covalent bonds. *High Perform Polym* 2019; 31(1):51–62. Available from: <https://doi.org/10.1177/0954008317750727>.
- [251] Scheltjens G, Brancart J, de Graeve I, van Mele B, Terryn H, van Assche G. Self-healing property characterization of reversible thermoset coatings. *J Therm Anal Calorim* 2011; 105(3):805–9. Available from: <https://doi.org/10.1007/s10973-011-1381-4>.
- [252] Turkenburg DH, Fischer HR. Diels-Alder based, thermoreversible cross-linked epoxies for use in self-healing composites. *Polymer* 2015;79:187–94. Available from: <https://doi.org/10.1016/j.polymer.2015.10.031>.
- [253] Mangialetto J, Cuvelier A, Verhelle R, Brancart J, Rahier H, van Assche G, et al. Diffusion- and mobility-controlled self-healing polymer networks with dynamic covalent bonding. *Macromolecules* 2019;52(21):8440–52. Available from: <https://doi.org/10.1021/acs.macromol.9b01453>.
- [254] Guo YK, Zou DL, Zhu WQ, Yang XJ, Zhao PX, Chen CA, et al. Infrared induced repeatable self-healing and removability of mechanically enhanced graphene-epoxy flexible materials. *RSC Adv* 2019;9(25):14024–32. Available from: <https://doi.org/10.1039/c9ra00261h>.
- [255] Khan NI, Halder S, Wang JL. Diels-Alder based epoxy matrix and interfacial healing of bismaleimide grafted GNP infused hybrid nanocomposites. *Polym Test* 2019;74:138–51. Available from: <https://doi.org/10.1016/j.polymertesting.2018.12.021>.
- [256] Lafont U, van Zeijl H, van der Zwaag S. Influence of cross-linkers on the cohesive and adhesive self-healing ability of polysulfide-based thermosets. *ACS Appl Mater Interfaces* 2012; 4(11):6280–8. Available from: <https://doi.org/10.1021/am301879z>.
- [257] Zhou LS, Zhang GC, Feng YJ, Zhang HM, Li JT, Shi XT. Design of a self-healing and flame-retardant cyclotriphosphazene-based epoxy vitrimer. *J Mater Sci* 2018;53(9):7030–47. Available from: <https://doi.org/10.1007/s10853-018-2015-z>.
- [258] Zheng N, Liu J, Li W. TO/TMMP-TMTGE double-healing composite containing a transesterification reversible matrix and tung oil-loaded microcapsules for active self-healing. *Polymer (Basel)* 2019;11(7):1127. Available from: <https://doi.org/10.3390/polym11071127>.
- [259] Mai V-D, Shin S-R, Lee D-S, Kang I. Thermal healing, reshaping and ecofriendly recycling of epoxy resin crosslinked with schiff base of vanillin and hexane-1,6-diamine. *Polymer (Basel)* 2019;11(2):293. Available from: <https://doi.org/10.3390/polym11020293>.
- [260] Hughes T, Simon GP, Saito K. Light-healable epoxy polymer networks via anthracene dimer scission of diamine crosslinker. *ACS Appl Mater Interfaces* 2019;11(21):19429–43. Available from: <https://doi.org/10.1021/acsami.9b02521>.
- [261] Kandelbauer A, Wuzella G, Mahendran A, Taudes I, Widsten P. Model-free kinetic analysis of melamine–formaldehyde resin cure. *Chem Eng J* 2009;152(2-3):556–65. Available from: <https://doi.org/10.1016/j.cej.2009.05.027>.
- [262] Kandelbauer A, Wuzella G, Mahendran A, Taudes I, Widsten P. Using isoconversional kinetic analysis of liquid melamine-formaldehyde resin curing to predict laminate surface properties. *J Appl Polym Sci* 2009;113(4):2649–60. Available from: <https://doi.org/10.1002/app.30294>.

- [263] Urdl K, Weiss S, Karpa A, Perić M, Zikulnig-Rusch E, Brecht M, et al. Furan-functionalised melamine-formaldehyde particles performing Diels-Alder reactions. *Eur Polym J* 2018;108:225–34. Available from: <https://doi.org/10.1016/j.eurpolymj.2018.08.023>.
- [264] Urdl K, Weiss S, Brodbeck B, Kandelbauer A, Zikulnig-Rusch E, Müller U, et al. Homogeneous, monodispersed furan-melamine particles performing reversible binding and forming networks. *Eur Polym J* 2019;116:158–68. Available from: <https://doi.org/10.1016/j.eurpolymj.2019.04.006>.
- [265] Urdl KMU. Monomer auf Melaminbasis: Österreichische Patentanmeldung(AT 50278/2019); 2019.
- [266] Jin K, Wilmot N, Heath WH, Torkelson JM. Phase-separated thiol–epoxy–acrylate hybrid polymer networks with controlled cross-link density synthesized by simultaneous thiol–acrylate and thiol–epoxy click reactions. *Macromolecules* 2016;49(11):4115–23. Available from: <https://doi.org/10.1021/acs.macromol.6b00141>.
- [267] Zhang Y, Broekhuis AA, Picchioni F. Thermally self-healing polymeric materials: the next step to recycling thermoset polymers? *Macromolecules* 2009;42(6):1906–12. Available from: <https://doi.org/10.1021/ma8027672>.
- [268] Liu F, Fang G, Yang H, Yang S, Zhang X, Zhang Z. Carborane-containing aromatic polyimide films with ultrahigh thermo-oxidative stability. *Polymers (Basel)* 2019;11(12):1930. Available from: <https://doi.org/10.3390/polym11121930>.